Sudden Stratospheric Warming and its Influence on the Tropical Atmosphere

Thesis submitted to the
Cochin University of Science and Technology
in partial fulfillment of the requirement for the Degree of

DOCTOR OF PHILOSOPHY
in
ATMOSPHERIC SCIENCE

By

Resmi E A

Department of Atmospheric Sciences
Cochin University of Science and Technology
Cochin - 682 016, India

September 2012

Dedicated
To
My Family

CERTIFICATE

This is to certify that the thesis entitled ***'Sudden Stratospheric Warming and its Influence on the Tropical Atmosphere'*** is an authentic record of the research work done by **Ms. Resmi E A** under my supervision in the Department of Atmospheric Sciences, Cochin University of Science and Technology. I also certify that the subject matter of the thesis has not formed the basis for the award of any Degree or Diploma of any University or Institution.

I also certified that **Ms. Resmi E A** has passed the Ph.D qualifying examination conducted by the Cochin University of Science and Technology in March, 2011.

Cochin-682 016
September, 2012

K. Mohankumar
(Supervising Guide)

DECLARATION

I hereby declare that this thesis entitled ***"Sudden stratospheric warming and its influence on the tropical atmosphere"*** is genuine record of research work carried out by me and no part of this thesis has been submitted to any University or Institution for the award of any Degree or Diploma.

RESMI E A

Cochin-682016
September, 2012

Acknowledgements

I take this opportunity to express my deep gratitude with esteem to my supervising guide Prof. Dr. K. Mohankumar, Professor, Department of Atmospheric Sciences and Dean, Faculty of Environmental Studies, for the guidance, supervision and suggestions. He stands with me through my good and bad times and the timely completion of this thesis is possible with his constant support.

I am indebted to Appu K.S, Manager (Retd.), Meteorological Division, Thumba Equatorial Launching Station (TERLS), Trivandrum who introduced the subject to me, giving timely suggestions and stands constant inspirations for me throughout my research work.

My sincere thanks to Dr. C.A. Babu, Head, Department of Atmospheric Sciences and former head Dr. Santosh K.R for the support provided from the department during the research period.

I express my gratitude to my Doctoral committee member Dr. H. S. Ram Mohan, Professor, Department of Atmospheric Sciences and too Mr. Baby Chakrapani, Dr. Madhu and Dr. Venu G. Nair, faculty members, Department of Atmospheric Sciences for their support and suggestions.

I also acknowledge the staff of the Department of Atmospheric Sciences for the help they gave me during these years of my research and also for Mr. Yashodaran and Dr. Sreedevi. I also take this opportunity to express my gratitude to Dr. Sabin, Dr. Abish, Dr. Rajesh, Jhonson Zaharia, Vijaykumar, Krishna Mohan, Smart, Dr. Lorna R Nayagam and Asha S Philip for their encouragement and help throughout my research period.

I express my gratitude towards my classmates Anila, Jayakrishnan, Sivaprasad and all the research scholars for their co-operations and inspiration.

I thank the Grand commission, Harijan Welfare Department, India for the financial support provided for the research in the form of research fellowship.

My sincere gratitude to Dr. Goswami, Director, IITM, Pune and Dr. Thara Prabhakaran for the time and space provide me to do my last part of my thesis. A word of thanks to Renu, Leena, and Priya for their kind support and suggestions.

The timely completion of this thesis is possible with the patience and support shown by family members father, mother, two brothers and their wives with little ones Arumina and Anushka. I express my whole hearted love and gratitude towards my husband Mr. Manoj Kumar and my in-laws.

RESMI E A

CONTENTS

4. High and Low- Latitude Interaction of Circulation during Early Mid- Winter and Late-Winter Stratwarm Events

PREFACE

Sudden Stratospheric Warmings (SSW) is an important dramatic meteorological event take placed in the northern hemisphere in winter. It plays an important role in the dynamics of the middle atmosphere. The present doctoral thesis deals mainly with the warmings of the northern hemisphere and its associated changes in the mid-latitude and tropical atmosphere.

Warmings are characterized by a sudden increase in the polar stratospheric temperature of the order of 50°C on time scales of few days and distinguished by a strongly disturbed stratospheric vortex. As a result, the temperature gradient reverses its direction from equator to poleward, followed by a reversal of the prevailing zonal mean westerly wind to easterly. SSW events are generated due to the dynamical wave mean-flow interaction in the stratosphere. Planetary waves in the mid-latitudes propagate upward from troposphere to the stratosphere and deposit the westward momentum, resulimg a strong meridional circulation. This interaction produces a large warming in the polar stratosphere due to adiabatic heating.

The stratospheric warming events are categorized into major and minor warming depending on the temperature increase in the polar stratosphere. The warming is called a ‘major’, when the polar temperature increases poleward from 60 degree latitude and followed by a reversal in the zonal wind at 10 hPa (~32 Km). Usually major warming events are associated with the displacement of polar vortex from high to mid latitudes or the splitting of vortices in to two. The warming is called a "Minor", when the polar temperature increases more than 25 degree in a period of a week or less, at any stratospheric level with less intensified easterly wind

anomalies. The stratospheric warmings generated during the transition period of winter to spring are called final warmings. The warming events observed in the early winter period (November to early December) over Canadian region are called Canadian warmings. There is strong interaction between stratosphere and troposphere during SSW period over high and low latitudes regions.

The thesis consists of 7 chapters. Chapter 1 is the introduction on 'middle atmosphere' with special emphasis on Sudden Stratospheric Warming events. A detailed description of the different types of stratwarm events, theory behind the SSW, its interaction with polar vortex, and its effects on the circulation features are also given.

Chapter 2 deals with the data and methodology utilized in the thesis. ECMWF (European Center for Medium Range Weather Forecast) ERA-40, interim and NCEP/NCAR reanalysis datasets from 1980-2010 are utilized to compute the anomaly, to identify the significance of temporal and zonal wind anomalies in recognizing the features of stratospheric warmings. The explanation about the computation of total and transient heat fluxes at mid tropospheric and stratospheric levels is presented. The technique of cross-correlation to analyze the lead and lag correlation between heat fluxes is explained in this chapter.

Classification of sudden stratospheric warming events in the upper and middle stratosphere and its various features are presented in chapter 3. This chapter gives an overview of stratospheric warming events in the upper and mid-stratospheric levels for the last 31 year period (1980-2010). The present study classified the stratwarm events into five different categories like 'intense major', 'major 1', 'major 2', 'intense minor' and 'minor' warmings at 2 hPa and 10 hPa levels. The classification is based on duel criteria of temperature and zonal wind anomalies from the

climatological mean state of the Arctic stratosphere. Usually stratospheric warming events are categorized with the reference level as 10 hPa.

The present thesis work focuses the categorization of stratwarm events considering an additional level of 2 hPa. The chapter gives the general nature of the warming of different groups, decadal and seasonal variability in the occurrence and the properties of the vertical propagation and the location details of the warm and cold vortices. The longitudinal displacement of the cold polar vortex is analyzed at 2 hPa and 10 hPa levels. Study on the decadal variability shows that there is an enhancement in the occurrence of events in the third decadal phase (2000-2010). There is also a clear evidence of downward propagation of the events; from upper to mid-stratosphere. The occurrence of warming is higher during the January (mid-winter) months but the intensity is higher in the warmings of December (early) month.

Analysis of high and low-latitude interactions of circulation during early, mid winter and late winter stratwarm events are carried out and presented in chapter 4. This study addresses the circulation pattern in the Eastern Arctic domain (0-180°E) using composite analysis of two early, mid-winter and late winter stratospheric warming events. An intense northwesterly wind flows from high to mid-latitudes around the peak days of SSWs through the low geopotential area (displaced cold polar vortex from North Pole). Consistent circulation patterns are found between 10 hPa geopotential height contour and 200 hPa circulation features. The above northwesterly wind merges with subtropical westerly jet stream (STJ) at mid-latitudes. As a result there has been a significant amount of variation in the intensity of subtropical jet stream during SSW days. Meridionally advected heat flux over high latitudes (45-75°N) explains the most perturbed wave activity during each stratwarm cases. The total heat flux analysis at 10 hPa and 100 hPa over high latitudes (45-75°N) also shows

the amount of wave activity. The intensity of wave activity is concentrated prior to the peak day and after the day of maximum; the intensity of wave activity is considerably reduced. The total heat flux analysis is also carried out for low latitudes (0-30°N) and cross correlation technique is applied between the heat fluxes to find the lag or lead correlation for high and low latitude regions.

Chapter 5 describes the coupling between tropical and polar stratosphere during major stratospheric warming events mainly over the Indian regions. Polar and equatorial stratosphere undergoes a strong coupling during major and minor warmings. The response of high-latitude stratospheric warming event over Indian region during the years 1984/85, 1987/88, 1998/99 and 2008/09 is analyzed. ECMWF ERA-40 and interim reanalysis data from 1000 hPa to 1 hPa is utilized for the study. Zonal average temperature anomalies explain the intensity of cooling over tropics (30°N-30°S). Six Indian stations are selected to analyze the intensity of upper stratospheric cooling during the above stratwarm events. The analysis shows that equatorial upper stratosphere exhibits almost quick response to the high latitude temperature variations. The annual minimum temperature at the upper stratosphere coincides with the peak phase of the SSWs. This shows the existence of a strong coupling between high and low-latitude upper stratosphere during stratwarm phase.

The circulation features of the troposphere and upper stratosphere over tropics associated with stratwarm events are analyzed and the results are discussed in chapter 6. Tropical upper stratospheric zonal wind anomalies at 2 hPa level show easterly wind anomalies during stratwarm peak days. Tropical (20°N-20°S) upwelling is noticed around the peak days of SSW events and the mass stream function analysis is also used to explain the meridional circulation associated with the events. In addition, surface temperatures over the selected Indian regions show a decrease in

temperature around the peak of high latitude warming events. If the development of the major warmings can be predicted, it is possible to anticipate a cooling over the Indian surface regions.

Major conclusions of the studies are presented in chapter 7. An outline of future scope of research is also mentioned in this chapter. References are given at the end of the thesis in alphabetical order.

List of Tables

List of Figures

Chapter 1

Introduction

1.1. Middle Atmosphere

The middle atmosphere (mainly stratosphere and mesosphere) is the region of the atmosphere between 10 to 100 km altitudes. At its base is the troposphere, where the temperature decreases with height. Above the troposphere is the stratosphere where temperature increases with height and maximum at about 50 km, the stratopause. The increase in temperature with height is due to the absorption of UV energy by the ozone layer and that makes the region very stable. Above the peak (stratopause) the temperature decreases with height in the mesosphere to a minimum near at 85 km, the mesopause. Middle atmosphere includes little portions from troposphere as well as thermosphere.

The mesosphere which lies above the stratosphere is a region where the temperature decreases with height. The atmosphere at this height is both tenuous (there is only 0.01% of the air here compared to the ground) and turbulent. The cold air overlying the warm air makes the atmosphere quite unstable in this region. Studies of dynamical and chemical processes of this region have greatly expanded in recent years.

1.2. Stratosphere

The stratosphere lies above the troposphere and cover the vertical column of 12 to 50 km. Tropopause height varies from 10 km to 16 km from pole to equator respectively. Tropopause is the bottom base of the stratosphere. The stratosphere is characterized by an increase in ozone with maximum ozone concentration at about 26 km of height. Temperature increases with height in stratosphere and reaches around 0°C at about 50 km. This increase is mainly caused as a result of maximum ozone absorbing the UV radiation from the sun. The ozone layer is an essential and important parameter for the life on Earth. The stratosphere is almost without cloud because of the limited of transport of water vapour from the troposphere into the stratosphere. Thus, weather and clouds are rare in this region.

The stratosphere is again divided into a lower stratosphere (15-35 km) with a constant temperature of about -56°C and upper stratosphere above 35 km of height. In the upper stratosphere, temperature reaches maximum of 0°C at about 50 km altitude. Because of the increasing temperature with increasing height (like inversion weather condition) there is only very limited vertical movement. Almost 99% of the mass of the atmosphere is located within the layer below 30 km. Regarding stratosphere it is noteworthy to mention that the ozone concentration is maximum in the lower stratosphere (around 26 km). Recent studies revealed the impact of human activities on the distribution of stratospheric ozone.

1.3. Zonal mean temperature and winds

The latitudinally dependent temperature distribution in the middle atmosphere results from the balance between net radiative drive and the heat transport. The heating distribution is mainly depending on seasonal

temperature variations, with maximum heating in the summer pole and maximum cooling in the winter pole. At equinoxes the maximum heating is at equator and cooling at the poles. The circulation in the meridional plane is balanced by the differential heating. Schematic cross-sections of the longitudinally averaged temperature and zonal winds for the middle atmosphere during solstices and equinoxes months are shown in Fig.1.1.

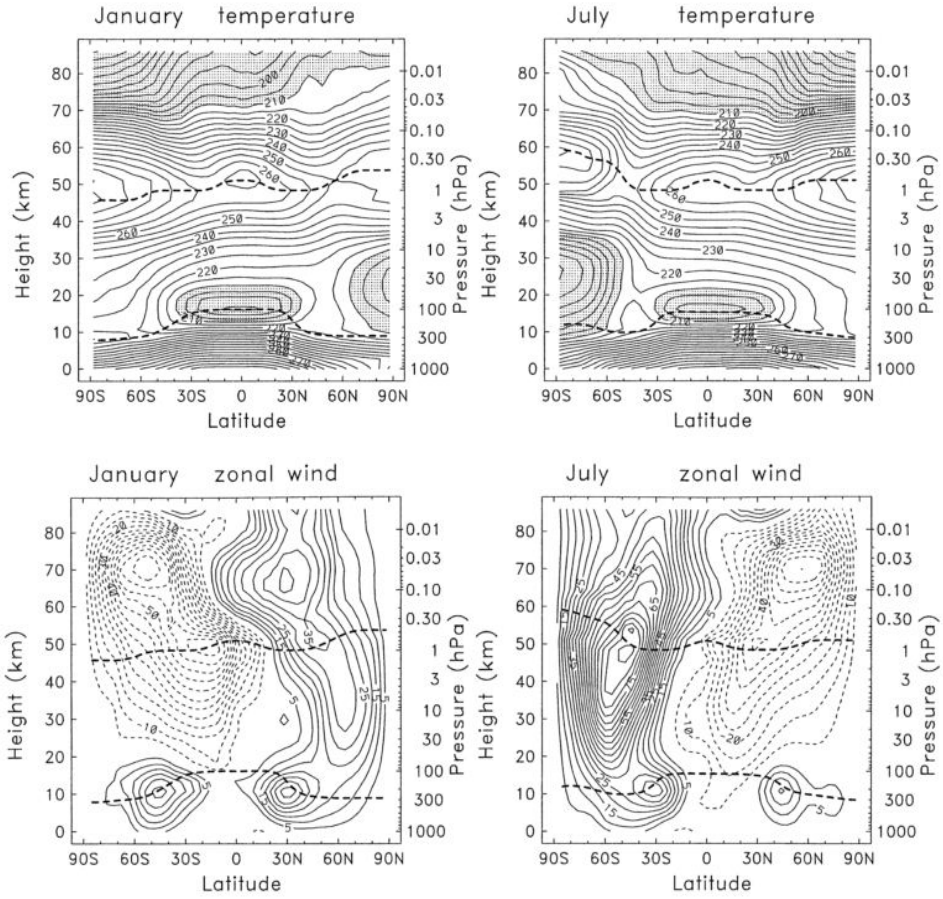

FIG.1.1. Climatological zonal mean zonal temperatures (top) and winds (bottom) for January (left) and July (right). Randel et al. (2004)

Zonal winds are from the URAP dataset (contour interval 5 ms^{-1}, with zero contours omitted). Temperatures are from METO analyses with (1000–1.5 hPa) a combination of HALOE plus MLS data above 1.5 hPa

(see SPARC 2002). The heavy dashed lines denote the tropopause (taken from NCEP) and stratopause (defined by the local temperature maximum near 50 km).

Temperature decreases with latitude in the troposphere. The latitudinal temperature gradient is about twice as steep in the winter hemisphere compared to that in the summer hemisphere. The tropopause is much higher and colder over the tropics than over the Polar regions. The latitudinal distribution of temperature in the lower stratosphere shows that the summer hemisphere had a cold equator and a warm pole. The winter hemisphere is cold at both equator and pole with a warmer region in middle latitudes. The cold pool of stratospheric air over the winter pole is highly variable. It disappears for a period of a few weeks during *sudden stratospheric warming* (SSW) periods. During SSWs the stratospheric temperatures over individual stations rise by as much as 70°C in one week.

At the stratopause, there is a monotonic temperature gradient between the warm summer pole and the cold winter pole. At the mesopause the summer pole is cold and the winter pole warm. Temperatures undergo pronounced diurnal variability in certain regions of the atmosphere. The strongest diurnal variability is observed in the upper thermosphere. In this region, day to night temperature differences are on the order of several hundred degrees.

The mean zonal flow in the winter hemispheres (equatorward of 40° latitude) is westerlies of about 40 ms^{-1} at the 200 hPa level. The maximum wind in the SH situates about 2°-3° latitude nearer the Equator and is about 5 ms^{-1} weaker than that of NH winter. Poleward of 40°S latitude, the zonal winds differ appreciably in winter, with stronger winds in the SH. A westerly maximum in the upper troposphere which extends into the stratosphere is evident between 50° and 60°S in accordance with the

upward-increasing meridional temperature contrast poleward of 45°S. The distribution of wind differs considerably between the summer hemispheres. The upper troposphere westerly maximum is nearly twice as strong as in the SH and is located farther poleward than the peak in the NH. In the middle and upper troposphere the tropical easterlies are much stronger in NH than that in SH. In the subtropics the westerlies are much stronger in SH.

Prominent features are cores of strong westerly winds in middle latitudes at an altitude of 10 km. The strongest zonal winds occur in the mesosphere at an elevation of 60 km. There are two jet cores in middle latitudes, the westerly in winter hemisphere and easterly in the summer hemisphere.

During the equinoxes (Fig.1.1, right) these jets undergo dramatic reversals as the latitudinal temperature gradient reverses. For example, the *sudden stratospheric warming* phenomenon is accompanied by large changes in the longitudinally averaged zonal wind at high latitudes in the winter stratosphere. The midwinter warmings are accompanied by a pronounced weakening of the westerlies at stratospheric levels. Sometimes the westerlies disappear altogether. These changes in the stratosphere have little effect on the wind structure in the troposphere.

The information on the temperature and winds are the required parameters to conduct the launching of the sounding rocket and satellite vehicles. The prevailing wind and thermal conditions may affect the trajectories of the rocket. Understanding of the dynamics of the middle atmosphere is needed in space programme activities.

1.3.1. Zonal mean winds in the equatorial stratosphere

The direction and speed of the zonal mean winds in the tropics is dominated by the equatorial lower stratospheric phenomena known as Quasi Biennial Oscillation (QBO). As a result of QBO zonal winds alter from easterly to westerly at high altitudes above 30 km. Easterly and westerly phases descending downward with height so that the easterly winds will be above the westerly winds and the westerly winds is above the easterly winds. The QBO extends aproximately 10-15 degree latitudes on either sides of the equator. The average period of QBO oscillation is about 28 months. It varies from 20 to 30 months. The strongest easterly winds are about $30ms^{-1}$, while the strongest westerly winds are 20 ms^{-1}.

1.3.2. Semiannual oscillation (SAO)

One of the significant features of the low-latitude upper stratosphere is the semiannual oscillation (SAO) in zonal winds. Amplitude of the SAO of the zonal wind peaks near to the stratopause region with a magnitude of the order of 55 ms^{-1}. The amplitude falls sharply in the middle stratosphere when it attains a value less than 5 ms^{-1} at an altitude of 30 km. The SAO is weak in the troposphere and lower stratosphere.

1.4. Zonally averaged circulation

The annually averaged atmospheric mass circulation in the meridional plane is depicted in Fig.1.2. The total amount of mass circulating around each cell is given by the largest value in that cell, based on the ECMWF ERA - 40 reanalysis data for the period 1979-2001. The rising motion in the tropics is capped from above by the stratosphere where the air warms with height, thus suppressing upward motion. The law of mass continuity requires the air to move away from the tropics, northward and southward as in the diagram. This motion amounts to an upper level

mass divergence, forced by the rising motion. Again, for reasons of mass continuity, the diverging upper-level tropical air must return to the surface poleward of the equator. At the same time, mass continuity at the surface requires low level convergence and the movement of air towards the equator (Mohanakumar, 2008).

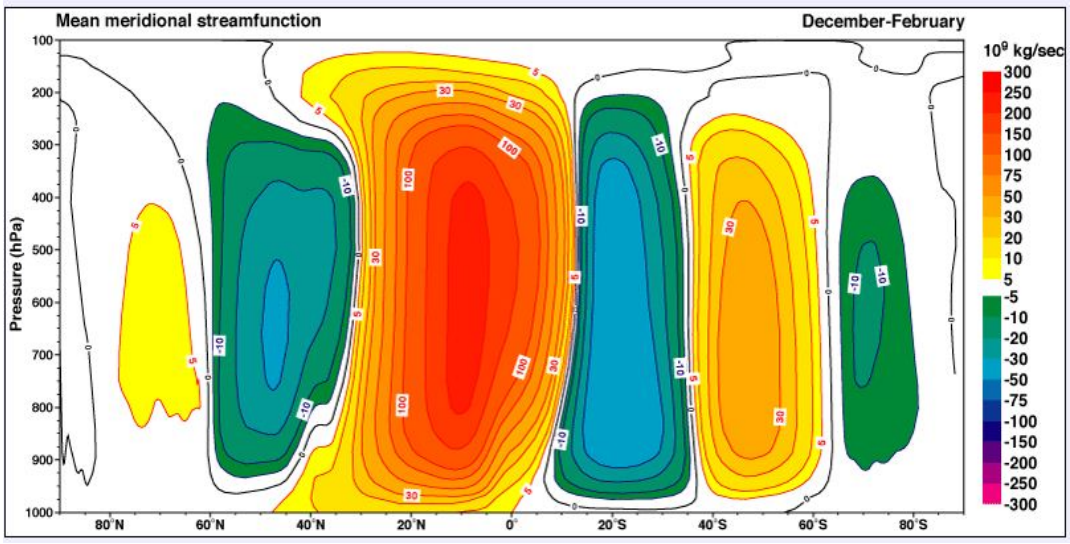

Fig.1.2. The zonally averaged mass circulation.ECMWF ERA-40 Atlas: http://www.ecmwf.int/research/era/ERA40_Atlas/docs/section_D25/parameter_zmmctp.html#

1.5. Brewer-Dobson Circulation

Brewer-Dobson circulation (BDC) model proposed by Alan Brewer in 1949 and Gordon Dobson in 1956 (Brewer, 1949; Dobson, 1956). It is a simple circulation model that speculates the existence of a slow current in the winter hemisphere which redistributes the air. It also explains the meridional atmospheric circulation that transports air poleward and downward from the tropical middle atmosphere (Fig. 1.1). Air is transferred between the equator and poles by this circulation on a time scale of months,

indicating of the strong control by the Coriolis force that deflects the air stream zonally and inhibits meridional motions.

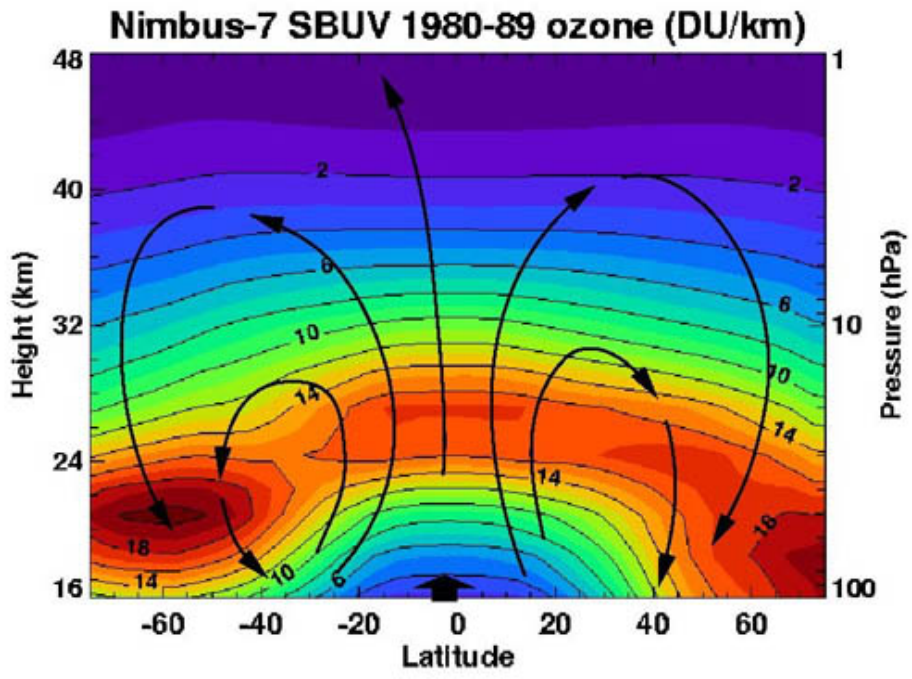

FIG.1.3. The zonally averaged circulation in the middle atmosphere superimposed on top of an annual average ozone density (in Dobson Units per kilometer). The brewer Dobson circulation is depicted by the black arrows. The figure also shows the seasonally averaged ozone density (red denotes a high density of ozone; blue denotes low ozone density). The ozone data is based on 1980-1989 Nimbus-7 SBUV data.

Initially the tropical motion starts from the troposphere into the stratosphere and then it is transported poleward in the stratosphere. The third part is descending motion in the stratospheric middle and polar latitudes. The mid-latitude descending air transported back into the troposphere and at the same time the polar latitude descending air transport into the polar lower stratosphere where it accumulates.

Brewer first proposed this slow circulation pattern to explain the lack of water vapor in the stratosphere. He supposed that water vapor is "freeze

dried" as it moves vertically through the cold equatorial tropopause. Dehydration can occur by condensation and precipitation as a result of cooling of temperatures below -80°C. Dobson later showed the distribution of high ozone concentrations in the lower stratosphere over the Polar regions which are situated far from the photochemical source regions in the tropical middle stratosphere. Dobson also explained the latitudinal (i.e. north-south) distributions of long lived constituents like nitrous oxide and methane is also explained.

The warming of the tropical troposphere through greenhouse gases strengthened the BDC circulation through wave activity (Eichelberger and Hartmann 2005). This circulation also called as residual circulation. The interaction between planetary waves in the extra-tropics disturbs the mean flow which causes a slow meridional drift (Haynes et al. 1991; Rosenlof and Holton, 1993; Newman et al. 2001 and Plumb, 2002).

The convergence of the Eliassen-Palm (EP) flux $\boldsymbol{F}$, i.e. $-\boldsymbol{\Delta}\cdot \boldsymbol{F}$ is usually described the planetary wave activity which drives the Brewer Dobson Circulation. The convergence of the EP flux in the stratosphere is a measure for easterly momentum deposited to decelerate the westerly zonal flow in winter (Newman et al. 2001). Geostrophic balance requires a small meridional flow component that starts the meridional or residual circulation (Andrews et al. 1987). The vertical component of the EP flux vector ($\boldsymbol{F}_z$) is proportional to the eddy heat flux ($\overline{v'T'}$) and is a measure of the vertical propagation of planetary waves from the troposphere. Both EP flux convergence and the eddy heat flux are frequently used to describe variations in the BDC driving.

1.5.1. The Brewer-Dobson Circulation in the Extratropical Latitudes

As far as the stratospheric layer is concerned the Brewer-Dobson circulation carries air from the equator to the poles. Poleward of about 30°N and 30°S belt, the circulation becomes downward as well as poleward. This poleward and downward circulation tend to increase the ozone concentrations in the lower stratosphere of the middle and high (i.e. extratropical) latitudes.

The lifetime of an ozone molecule is more in the lower stratosphere than the extratropical latitudes. In the upper stratosphere ozone is produced more and destroyed as well. In the middle stratosphere the destruction by the photolysis process is limited. Ozone concentration is highest in the lower stratosphere. Ozone is produced by the photolysis (producing two free oxygen atoms) of oxygen molecules and it is destroyed by the catalytic reactions (generally utilizing free molecular oxygen atoms) in the presence of UV radiation. Ozone accumulates as the Brewer-Dobson circulation transports air poleward from the low-latitudes into the high-latitudes and then downward into lower altitudes.

1.6. Sudden Stratospheric Warming (SSW/stratwarms)

During certain winters the zonal mean configuration in the stratospheric temperatures over the NH is dramatically disrupted with rapid increase and lead to a reversal of the zonal mean winds to easterly direction for a period of few days. Such an event is known as *stratospheric sudden warming* (SSW). This high-latitude phenomenon occurs in the winter months of December, January and February in the NH and in June, July and August months in the Southern Hemisphere. Figure 1.1 shows the annual variation of zonal mean of temperature anomalies over the arctic hemisphere from surface to 0.4 hPa level. The figure shows the presence of

a strong SSW in January, 2009. The temperature increase associated with the SSW event and the recovery of the vortex is evident in this figure.

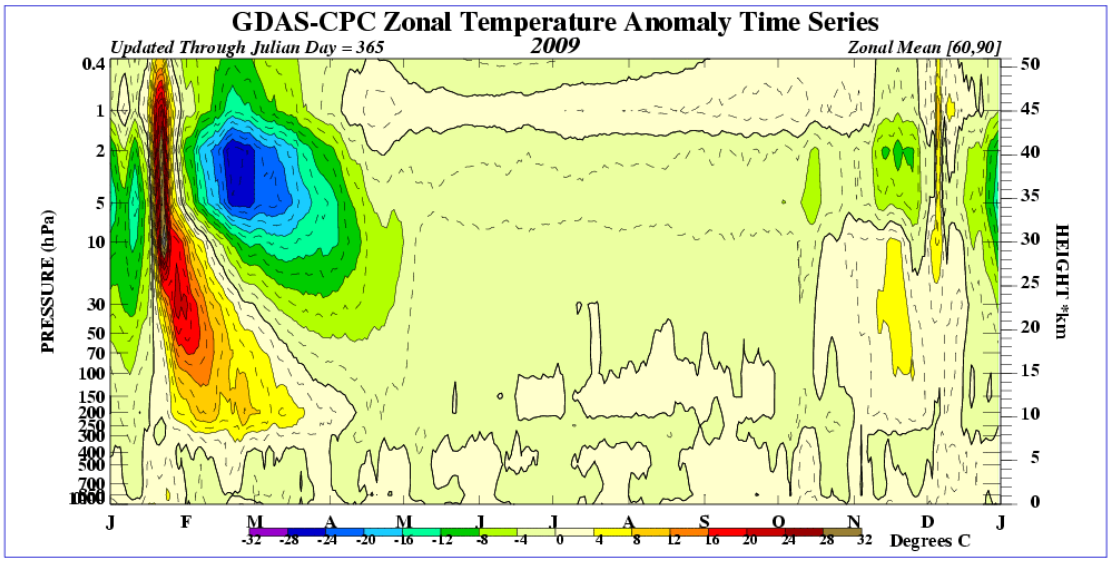

FIG.1.4. Time height cross-section of zonal mean temperature anomaly for the year 2009. http://www.cpc.ncep.noaa.gov/products/stratosphere/strat-trop.

The phenomenon of stratospheric warming was discovered in 1952 by Professor Richard Scherhag (Scherhag 1952, 1960) during high altitude balloon experiments at the Institute of Meteorology, Freie Universität of Berlin. During the first few years, SSWs are known as the "Berlin phenomenon". He was testing the newly developed U S radiosonde which can measure reliable temperatures upto the middle stratosphere. These experiments led him to record the first ever observed stratospheric warming event of the 27th of January 1952. After the discovery, Scherhag created a team of meteorologists specifically to study the winter stratosphere in the university (Free University of Berlin). This group continued to map the northern-hemisphere stratospheric temperatures and geopotential height for many years using balloon radiosonde ascents. These experiments proved that the warming in the winter stratosphere is not a local phenomenon but it extends to the whole polar winter hemisphere. In the late 1960's the satellite

era began and meteorological measurements became more frequent on a global scale. Meteorological satellites like TIROS and NIMBUS series, monitored continues reliable data for the entire stratosphere and later for mesosphere. Today meteorological radiosondes, sounding rockets and various ground based radars are used to monitor the atmospheric regions as a whole.

During the winter months, polar stratospheric temperatures on an average are below minus 70°C. The cold temperatures are combined with strong westerly winds that form the southern boundary of the so-called stratospheric polar vortex. In other words the winter months are dominated by westerly winds with polar night jet attaining the maximum values during February. Before the onset of the SSW, the stratospheric circulation is dominated by cold and eastward polar vortex which lies over the North Pole, covering large part of the Northern Hemisphere outside the tropics. This dominant structure is disrupted in some winters or even reversed. Under these conditions the temperatures in the lower stratosphere rise within a few days by more than 50 degrees. The polar region becomes warmer than southern latitudes. This leads to the reversal in the west winds and collapse of the existing polar vortex (Andrews et al. 1987; Asnani, 1993; Mohanakumar, 2008).

The earliest studies on the synoptic development of the foremost stratospheric warmings are done by Teweles (1958), Craig and Heting (1959), and Lowenthal (1957). The simulation of stratospheric sudden warming using general circulation model is done by Miyakoda et al. (1970). The simulation was able to split the polar vortex without simulating warming. Another successful simulation of the stratospheric sudden warming is presented in terms of quasi-geostrophic numerical model by Matsuno, (1971). This theoretical study proposed the cause of stratospheric warming as the result of the upward propagation of planetary waves from

troposphere to the stratosphere and their interaction with the zonal mean flow. At an initial time, a blocking-type circulation pattern is established in the troposphere. This blocking pattern causes planetary zonal wave number 1 and/or 2 on grow to unusually large amplitudes. The growing wave propagates into the stratosphere. During the propagation the waves encounter with 'critical layers' where the energy is absorbed and thus decelerates the mean zonal winds. The energy absorbed layers undergo warming. The polar night jet weakens and simultaneously distorted by the growing planetary waves. The upward propagation of planetary waves is blocked and leads to a very rapid easterly deceleration. Polar warming occurs at the critical level and it move downward. The warming and zonal wind reversals affect the entire polar stratosphere. Warmings do occur in the SH but with less intensity. This aspect will be discussed in a later session.

1.6.1. Classification of Stratospheric Sudden Warming

Basically SSWs are classified into three categories: major, minor and Canadian warmings. More sub-classes of warmings are introduced by Quiroz, (1975). Further grouping on SSW are done by Labitzke, (1977) including parameters like 11-year solar cycle and QBO phases. The definitions of warmings adopted by World Meteorological Organization (WMO, 1978) are as follows:-

1.6.1.1. Major

A stratospheric warming can be said to be major if 10 hPa or below the latitudinal mean temperature increases poleward from 60 degree latitude and an associated circulation reverses (that is, the prevailing mean westerly winds poleward of 60 latitude are succeeded by mean easterlies in the same area).

1.6.1.2. Minor

A stratospheric warming is called minor if a significant temperature increase is observed (that is, at least 25 degrees) in a period of week or less at any stratospheric level in any area of winter time hemisphere. The polar vortex is not broken down during these warming episodes.

1.6.1.3. Canadian

Canadian warmings occurred in early winter in the stratosphere of the Northern Hemisphere typically from mid-November to early December period. They have no counterpart in the southern hemisphere. Warming is said to be Canadian when it occurs over the Aleutian High regions; in the Canadian region (e.g., Labitzke and van Loon 1999; O'Neill 2003). During Canadian warmings, the warm Aleutian High advect eastward within a few days from its usual position over the International Date Line towards 90°W line of longitude over Canada. In this case, the polar vortex does not breakdown but distorts strongly and displaces from the pole (Andrews et al. 1985; Donfrancesco et al. 1996; Marenco et al. 1997; O'Neill 2003).

Canadian warmings are associated with the intensification of the stratospheric Aleutian high. Aleutian high is linked with the Aleutian low in the troposphere. Wind reversal during Canadian warming happened only six times in the past 50 years (Manney et al. 2001). Theses reversals were short and weak. But these warmings never led to the breakdown of polar vortex (Labitzke and Naujokat, 2000). Juckes and Neill (1988) proposed a tentative connection between the intensification of the tropospheric trough/ridge pattern in the East Asian flow and the establishment of Aleutian high.

Manney et al. (1994) brought out more features of Canadian (South Pacific type) warmings as follows

1. *The cyclonic vortex remains strong; it is being displaced from the pole due to wave number decomposition, and then it appears as a circulation dominated by a wave 1 pattern.*
2. *The flow is affected mainly in the middle and lower stratosphere and the disturbance is nearly equivalent barotropic, i.e., it shows little or no longitudinal phase tilt with height.*
3. *The disturbance moves slowly eastward.*

1.6.1.4. Final

The seasonal cycle of wind in the stratosphere mean flow is westerly (eastward) during winter and easterly during summer (westward). A warming which occurs on this transitional phase so that the polar vortex winds permanently changes the direction during the warming is called as the final warming.

There are sub-classifications of major stratospheric warmings depending the time of occurrences. Major warmings are again sub-classified as early, mid-winter and late winter warmings when they occur in the early December, in January, and in the second half of February respectively. The classifications of the warmings are presented in figure 1.2.

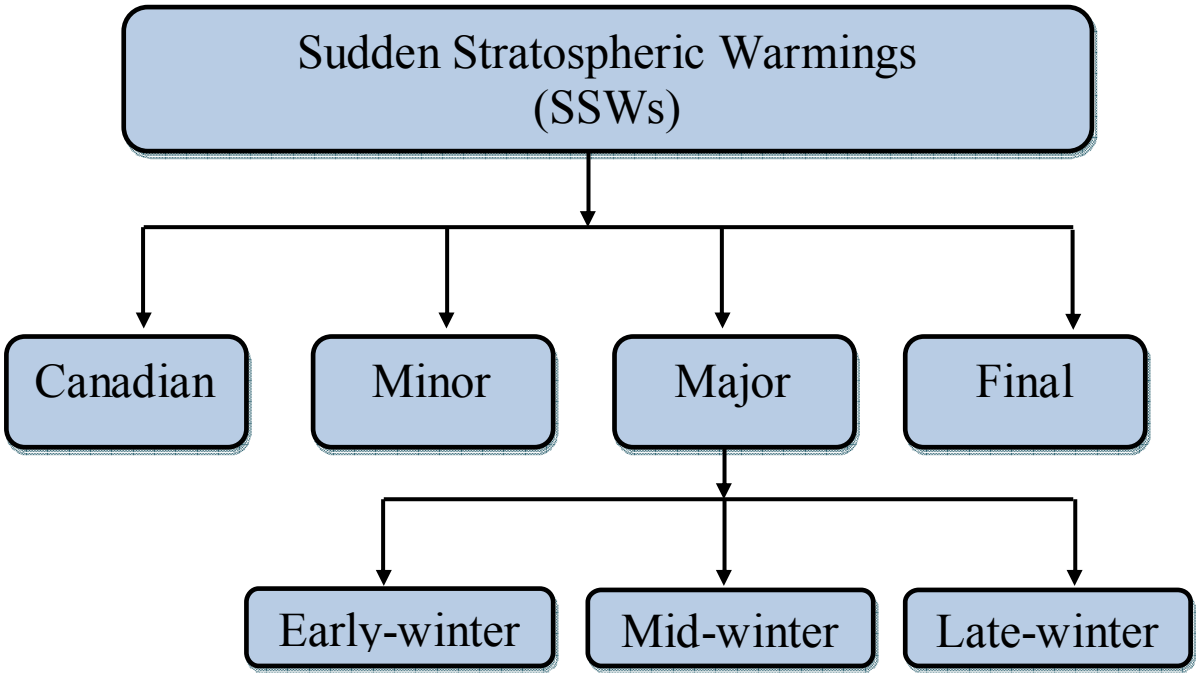

FIG.1. 5. Different types of stratospheric warmings.

1.6.2. Vertical structure of stratospheric warming

One of the well-known characteristics of the sudden warming is its downward propagation from about 45 km into the lower stratosphere. This feature has a non-zonal structure with planetary waves tilting westward with height. Warming in the stratosphereis accompanied by equal and opposite changes in the mesosphere by the way of cooling. Hence the vertical column of SSW system consists of both the stratosphere and mesosphere. Duirng a SSW the thermal perturbation takes place both in the stratosphere and mesosphere but in the opposite directions.

Charney and Drazin (1961) showed that Rossby waves propagate upward only if their horizontal scale is large and if the flow is weakly eastward relative to their phase speed; that is, stationary waves can propagate only through weak westerlies (Andrews et al. 1987). As a result,

the stationary Rossby waves propagate into the stratosphere only in the winter (when westerlies are prevalent) and not in the summer (when easterlies are prevalent). The stratospheric flow is more disturbed in winter than in summer.

1.6.3. Theory of Sudden Stratospheric Warming

Matsuno (1971) was the first to give a generally acceptable theory of SSW. His theory is based on the wave mean flow interactions. Its main features are:-

- A sudden increase in stationary planetary wave amplitude in the troposphere is accompanied by vertical propagation of transient wave energy into the stratosphere.
- The stratosphere is transparent to this wave energy because of this wave energy gets trapped causing convergence of heat and easterly momentum. Due to the lower density of the air in the upper levels, the effect of temperature and wind become extensive. Altogether the pre-warming temperature gradients become weak and get reversed and the westerly jet weakens replaced by easterly winds.
- The appearance of this easterly flow above the westerly flow produces a critical level with zero wind velocity in the mean current. At the same time the horizontal speed of the mean current equals the horizontal phase speed of the stationary wave of the troposphere. The easterly regime descends as the westerly wind gets destroyed; the critical level of the wave energy absorption comes down. The process of energy absorption and sequence of events may be so fast and mixed that the appearance of easterlies may look simultaneous throughout the great depth of the stratosphere.

- The upward rising energy from the troposphere is spread over a band of synoptic-scale and planetary-scale waves but as pointed out by Charney and Drazin (1961), the stratosphere is opaque to synoptic-scale waves and transmissivity increases for the larger wavelengths. As a result, the wave numbers 1 & 2 are dominant in this upward propagation of wave energy from the troposphere into the stratosphere.
- The phenomenon of SSW also shows "hysteresis" development and decay of SSW do not follow the identical paths.

The dynamical explanation of the event through critical level theory is further explained by Schoeberl (1978) and is illustrated in fig.1.6. Within 1 week to l0 days, the sudden increase in the temperatures over the pole leads to the zonal wind reversals (Levoy 1964; Schoeberl and Strobel, 1978) and it can penetrate deep into the troposphere (Taylor and Perry, 1977; Quiroz, 1977; McGuirk, 1978). Julian and Labitzke (1965) draw energy cycles for 1962-1963 warming event and this flow of energy is confirmed by the E.P. fluxes (Palmer 1981).

Clark (1974) used one dimensional two layer model of the polar night jet stream. He obtained a SSW in a time scale of about two weeks. Geisler (1974) also formulated one dimensional model of sudden warming. The vertical structure of the warming and the critical levels are well identified. Holton and Mass (1976) used one dimensional model and explained the interaction of planetary waves with mean flow. The reversed circulations (easterlies) prevent the upward propagation of planetary waves. McIntyre (1982) emphasized the importance of potential vorticity distributions that allows the planetary wave activity to be ducted into the polar stratosphere favorable for the occurrence of SSW.

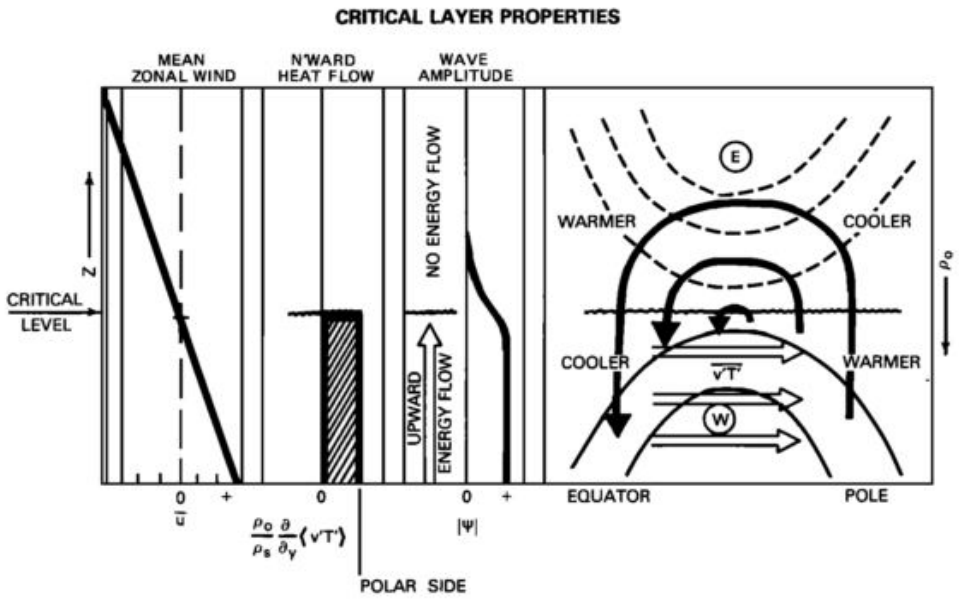

FIG.1.6. Idealized critical layer properties after (Matsuno 1971). From left to right the figure shows the mean zonal wind at mid channel, meridional derivative of the northward flow as function height along the polar side of the flow and the wave amplitude and energy channel at middle latitudes. The diagram on the right shows the two-dimensional idealized structure of a critical layer. Open arrows indicate the direction of eddy heat transport. Solid arrows show cross- channel and vertical flow patterns, the induced secondary circulation. Contours indicate zonal winds: dashed lines are easterly, and solid lines are westerly (Schoeberl, 1978).

Mesospheric cooling at the time of SSWs is shown by (Lindzen, 1981; Holton, 1983; Dunkerton and Butchart, 1984). Chao (1985) considered SSW as a catastrophe; it is a transition from one equilibrium state to another state. Garcia and Boville (1994) studied the mean meridional circulation in the winter polar stratosphere. Gray et al. (2003) utilized stratospheric-mesospheric coupled model, to investigate the stratospheric response to tropospheric wave forcing and equatorial wind. Based on the numerical weather prediction model (NWPM) of the Japan Meteorological Agency (JMA) Mukougawa and Hirooka (2004) examined

the predictability of December, 1998 warming event. They predicted this warming event one month in advance. The remarkable winter in 2003-04 and other recent warm winters in Arctic Stratosphere are analyzed by Manney et al. (2005).The climatological features of the Arctic and Antarctic stratospheric polar vortices are investigated using NCEP/NCAR reanalysis data (Gimeno et al. 2007). The distinctive features of the vortices like average latitude, area, strength and its temperatures are examined using EOF analysis.

Displacement and split type of the polar vortices during stratospheric sudden warming (SSW) events revealed a lot of dynamical aspect. Displacement-type of SSWs are forced by positive anomalies of the energy associated with the first two baroclinic modes of planetary Rossby waves with zonal wavenumber 1. Split-type of SSWs are in turn forced by positive anomalies of the energy associated with the planetary Rossby wave with zonal wavenumber 2, and the barotropic mode appears as the most important component (Liberato et al. 2007).

Bancala et al. (2012) studied about the preconditioning of the major warmings and Blume et al. (2012) made a supervised learning approach to classify the SSW events with temperature anomalies and atmospheric forcing like ENSO, QBO and solar cycle.

1.6.4. The Antarctic stratospheric warming

Stratospheric warmings do occur in the Southern hemisphere during winter months (July, August and September). Temperatures in the SH winter 1975 is raised as large as those in northern hemisphere (Barnett 1975). The lack of strong planetary waves seems to be the cause of non occurrence of major warmings in the SH.

Exceptionally a major SSW event took place in the SH winter of 2002. Kirstin et al. (2005) made a detailed analysis of this warming with a comparison to NH warmings. Manney et al. (2005) and Liu and Roble (2005) simulated this major stratospheric warming event using TIME-GCM. They explored the possible role of the mesosphere in the dynamical processes and found that significant changes in the wind and temperature fields are due to a strong wave number 1. This helped the atmospheric conditions favorable for the upward and poleward propagation of wave energy, not only for wave 1 but also for wave 2 and 3. At the same time, the jet reversal and the planetary wave surf zone also descended from the mesosphere down to the stratosphere. The preconditioning ultimately lead to an extensive breaking of the polar jet and wave 1 in the stratosphere and leads to the major warming.

1.7. Polar Vortex

A polar vortex is a persistent large-scale cyclonic system located on the geographical poles of our planet. The polar vortices are located in the middle and upper troposphere and the stratosphere. Stratospheric polar vortices form and fall when solar heating of Polar regions is cut off. It reaches maximum strength in midwinter, and decay in later winter as sunlight returns to Polar regions. Figure 1.7 shows the polar vortex position over the arctic hemisphere. The air masses are enclosed in this large air vortex as in a pot. The vortex drifts over the northern hemisphere and also regularly reaches areas over Central Europe.

The vortex is most pronounced in the winter hemisphere when the temperature gradient is steepest. It will diminish or disappear in the summer. The Antarctic polar vortex is more powerful and persistent than the Arctic one. This is because of the distribution of the orography in the

southern hemisphere where polar vortex remains undisturbed and strong. The winds at the core may exceed 100 ms^{-1}.

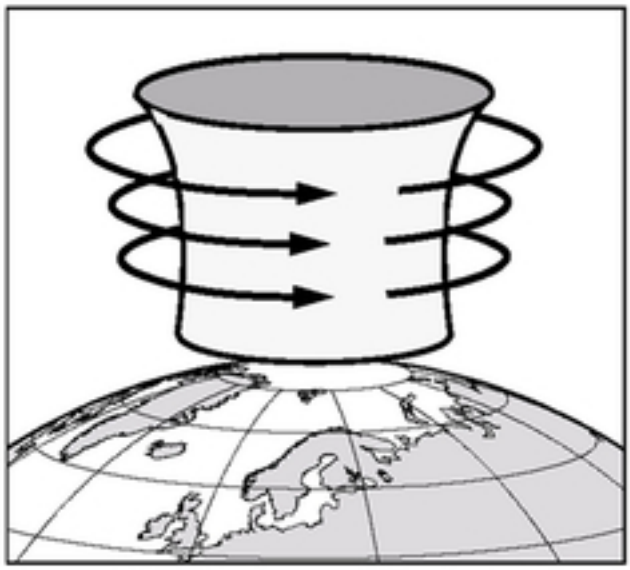

FIG..1.7.Illustration of the polar vortex in the stratosphere over the Arctic. Illustration by: Markus Rex, Alfred-Wegener-Institute.

The walls of the polar vortex act as the boundaries for the extraordinary changes in chemical concentrations and it can be considered a sealed chemical reactor bowl, containing a water vapor hole, a nitrogen oxide hole and an ozone hole, all occurring simultaneously (Labitzke and Kunze 2005). This chemical condition exists only in the short lived Arctic vortex (*Mohanakumar,* 2008). In the last decades various authors (Baldwin and Holton 1988; O' Neil and Pope 1988; Harvey et al., 2002; Limpasuvan et al, 2005; Scott and Dritchell, 2006 and Chen and Wei, 2009) made extensive studies on the behavior of the polar vortices and its relation with SSWs.

There is evidence that the vortex needs to be preconditioned for SSWs to occur (e.g., McIntyre, 1982 and Limpasuvan et al. 2004). While most of the analyses on SSWs are focused on upward propagating Rossby waves, alternate theories also reported incorporating resonant excitation of free modes and vortex interactions between the polar vortex and Aleutian anticyclone (Tung and Lindzen, 1979; Plumb, 1981; O'Neill and Pope, 1988; Esler and Scott, 2005; Esler et al. 2006; and Scott & Dritschel, 2006). Using the upper atmospheric research satellite (UARS) data, Zurek et al. (1996) analyzed the interannual variability of northern hemispheric stratospheric polar vortex with polar stratospheric cloud formation. Martius et al. (2009) observed that major warmings are often preceded by blocking situations in the troposphere over the Atlantic and/or Pacific sector.

During Polar winter, polar vortex forms and the polar air mass in the stratosphere becomes separated from other air masses. The stratospheric air trapped in the vortex become very cold and results in the formation of ice crystals developing clouds. Gas phase HCl dissolves in the surfaces or clings to the surfaces of the clouds. The CFC's react with the HCl ice, converting relatively unreactive chlorine to the more active species; Cl2, ClONO2, and HOCl. At sunrise, in October, the chlorine-bearing compounds are photolyzed, releasing the highly reactive Cl atoms that attack ozone. Ozone densities drop rapidly only to recover when the polar vortex breaks up, mixing warmer air in and releasing the ozone-depleted air to move away from the polar region.

1.8. Jet stream

Jet streams are fast flowing narrow air currents. Jet streams are discovered in 1920s by Meteorologist Wasburo Ooishi, while studying on high elevation wind patterns over Japan using weather balloons (Lewis,

2003). German meteorologist H. Seilkopf was the first to use the term "jet stream" in a published scientific paper in 1939.

The main jet streams are located near the tropopause the transition level between the troposphere and the stratosphere. The major jet streams on Earth are the westerly winds (flowing west to east) and their paths typically have a meandering shape.

1.8.1. Polar jet stream

The polar-night jet stream forms only during the winter months (i.e., polar nights) at around 60° latitudes. Figure 1.8 shows the two westerly jet streams in both the hemispheres encircling the earth. During the dark months the air over the poles becomes much colder than that over the equator. These differences in temperature give rise to extreme air pressure differences in the stratosphere which combined with the Coriolis effect create the polar night jets at an altitude of about 48 km.

FIG.1.8. Typical illustration of westerly jet streams

The polar vortex is situated inside the polar night jet. The warmer air in the mid-latitudes is move along the edge of the polar vortex and the cold polar air becomes cooler inside the vortex. The polar jet is situated at around 7–12 km above sea level and subtropical jets are found around 10–16 km. The Northern and the Southern Hemispheres each have separate polar and subtropical jets. The NH polar jet stream is most commonly found between the latitudes 30°N and 60°N. Jet streams are generally continuous over a long distance. The path of the jet typically is a meandering shape, and these meanders themselves propagate east, at lower speeds than that of the actual wind within the flow. Each large meander, or wave, within the jet stream is known as a Rossby wave. Rossby waves are caused by changes in the Coriolis effect with latitude and propagate westward with respect to the flow in which they are embedded.

1.9. Polar stratospheric clouds

Polar Stratospheric Clouds (PSC) is formed in the stratosphere in altitude layer between 20 and 30 km. It is also known as nacreous clouds (mother of pearl, due to its iridescence). PSCs form at very low temperatures, below −78°C. These temperatures can occur in the lower stratosphere in polar winter. In the Antarctic, temperatures below −88°C frequently cause type II PSCs. Such low temperatures are rarer in the Arctic. In the Northern hemisphere, the generation of lee waves by mountains may locally cool the lower stratosphere and lead to the formation of PSCs. It is frequently appear in winter and mainly over Scandinavia, Scotland, Alaska and Antarctica. In general there are two types of Polar 5tratospheric Clouds:

1.9.1. Type 1: Nitric Acid Trihydrate Clouds (NAT)

Type-1-PSC-particles are a mixture of water and nitric acid (HNO3) and they form just above freezing point (about -78°C). They can appear either solid or liquid as aerosols. The microscopic structure of the particles is contained with each molecule of HNO with 3 molecules of water. Type-1-particles are thus defined chemically as Nitric Acid Trihydrate (NAT). They are about 1 micrometre (one millionth of a metre) in size.

It is supposed that dust in the stratosphere favours the formation of mother-of-pearl clouds because small dust particles are very good sublimation nuclei for water molecules. In Scandinavia, mother-of-pearl clouds are observed almost in every winter. At lower temperatures they can include small amounts of chloric acid (HC1) and sulphuric acid (H2SO4). The appearance of NAT-clouds is described as very delicate (similar to NLC) and they widely spread over a large area.

1.9.2. Type 2: Mother-of-pearl clouds

Type-2-PSC consists of pure crystals of frozen water. They form at even lower temperatures between -95°C and -90°C and less (188 K at an altitude of 25 km). An example of type 11 PSC clouds is shown in figure1.6.

FIG.1.9. A type II (water) PSC showing iridescence. http://remus.jpl.nasa.gov/kiruna/a015z.htm.

These particles are about 10 micrometres small. Due to this the ice crystals are so heavy, PSC tend to sink down into the troposphere. The less amount of water in stratospheric air becomes dehydrated over the poles. PSC of this type, which are also called mother-of-pearl clouds, have mostly lenticular appearance and appear only over a small area.

1.10. Sudden Stratospheric Warming & Arctic Oscillation

The Arctic oscillation (AO) or Northern Annular Mode/Northern Hemisphere Annular Mode (NAM) is an index of non-seasonal sea-level pressure variations north of 20N latitude. It is characterized by pressure anomalies of one sign in the Arctic with the opposite anomalies centered about 37–45°N. Moreover, the Arctic Oscillation is an opposite atmospheric pressure patterns in northern middle and high-latitudes. The polar stratospheric vortex splitted or displaced from the pole during stratwarm days and this leads to the mixing of polar air to middle latitudes.

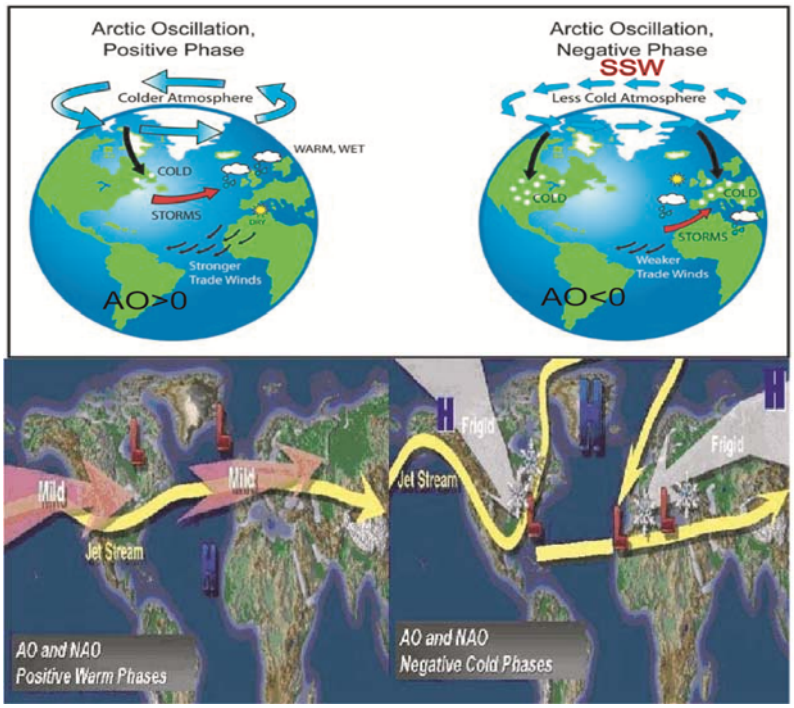

FIG.1.10. Schematic representation of SSW and Arctic Oscillation.

Certain features of the relation between SSW and Arctic oscillation (Fig.1.10) are given below:-

- *Strongly negative AO indices are found in association with strong SSW events, concurrently with severe cold weather and rain/snowfall in the mid-latitudes.*
- *The impact of SSW can reach the surface (& change AO sign) in a few days (Kim & Flatau 2010), much faster than what was previously reported and believed.*
- *AO is linked to tropics (Kim & Flatau 2010).*
- *AO Index values have been strongly negative in winter over the last few years, with unprecedented frequency and strength.*

There has been a direct link between stratospheric polar vortex variability and the Arctic oscillation (eg., Thompson and Wallace 1998; Baldwin and Dunkerton, 1999; Ambaum et al. 2001; Black 2002; Lin et al. 2002;Wang and Chen 2010; Hinssen et al. 2010 and Cohen 2011).

1.11. Atmospheric waves

A wave is defined as form or a state of disturbance advancing with a finite velocity through a medium. The energy is transmitted in the media through propagation. The wave is considered as perturbation on the steady slowing changing back ground. Waves in fluids result from the action of restoring forces on fluid parcels, which have been displaced from their equilibrium positions. The restoring forces may be due to compressibility, gravity, rotation, etc.

Atmospheric waves can be classified according to their physical or geometrical properties according to their restoring mechanisms: thus buoyancy or gravity waves owe their existence to stratification, while

inertio-gravity waves result from a combination of stratification and Coriolis effects. Planetary or Rossby waves result from the effect or from the northward potential vorticity gradients (Mohanakumar, 2008).

1.11.1. Rossby and Gravity waves

Rossby waves are planetary scale waves that are most important for stratospheric transport. Rossby waves are developed due to the large scale variations in potential vorticity. The restoring force of these waves is the variation in Coriolis effect with latitude. The Rossby wave is nearly spherical in shape and the stationary planetary waves that are forced by orography or traveling free waves. The wave forcing is seen through the isentropic gradient of potential vorticity (i.e., the change of the Coriolis parameter f with latitude). The Steady planetary waves conserve potential vorticity, just as steady buoyancy waves conserve potential temperature. The gravity wave, also known as a buoyancy wave, results from the stability or buoyancy of air in a stably stratified atmosphere.

Rossby waves induced by topography, known as the stationary planetary waves, that propagate vertically and break in the stratosphere, causing the wintertime stratospheric sudden warmings in the polar regions that lead to the Brewer-Dobson circulation.

The main causes of wave dissipation are

Thermal dissipation: Thermal dissipation refers to the process of wave dissipation in which radiative heating and cooling reduced the temperature differences that are associated with Rossby wave formation. These Rossby waves are associated large scale areas of warm and cold temperature perturbations. The warm regions will radiatively cool to space at greater rates than the colder regions and restore the atmosphere to a more

uniform temperature field. This thermal damping process becomes more significant with increasing altitude in the stratosphere.

Wave breaking: Wave dissipation or damping is occurd by a process wave breaking. Atmospheric waves grow to large amplitudes and break, thereby causing rapid meridional mixing. This process is evident in the winter middle latitudes. Waves propagate vertically from the troposphere into the stratosphere, and then equatorward into the subtropics. As the wave moves upward, the density of the atmosphere decreases, and the strength of the wave consequently grows. This eventually leads to wave "breaking," in which air parcels undergo large and rapid latitudinal excursions causing them to undergo strong, irreversible, meridional mixing. As a result, material (i.e., long-lived tracers) becomes thoroughly mixed throughout the subtropics and lower middle latitudes.

Chapter 2

Data and Methodology

2.1. General

Data obtained from the European Center for Medium Range Weather Forecast (ECMWF) ERA-40, interim, and National Center for Environmental Prediction/National Centers of Atmospheric Research (NCEP/NCAR) reanalysis projects are used for the study. One of the main advantages of this data is the vertical resolution. The NCEP/NCAR reanalysis provide data from 1000 hPa to 10 hPa levels and ECMWF reanalysis data from 1000 hPa to 1 hPa levels. The sudden stratospheric warmings and its coupling effects are explained using these reanalysis data sets. The details of the data taken are described in relevant sections.

The doctoral thesis mainly consists of the daily data of temperature, zonal and meridional components of the wind, vertical velocity and geo-potential height at different pressure levels. Earlier times ECMWF ERA-40 Reanalysis server data is available for the period 1958-2002 and later on they make available ECMWF interim reanalysis data for the rest of the years (1979-present). These two data set combined gives a vertical structure of various parameters of the atmosphere for the period from 1958 to present with different grid scales. ECMWF ERA-40 and interim reanalysis provide 2.5°×2.5° and 1.5°×1.5° latitude and longitude grids respectively.

Climatology is defined as the long-term average of a given variable over time periods of 20-30 years. A monthly climatology will provide a mean value for each month and a daily climatology will provide a mean

value for each day. Deviations in a particular data are computed by subtracting the same from climatological mean. The daily anomalies in temperature, zonal and meridional components of winds are calculated from a long term and seasonal means at different pressure levels. A positive anomaly indicates warming while a negative anomaly indicates cooling.

In chapter 3 the temperature and zonal wind anomalies in the daily data are calculated from the long term mean of 1980-2010 period for 2 hPa and 10 hPa levels. Stratospheric warming events are identified based on the deviations from 10 hPa level. For this purpose ECMWF interim data for the period of 1980-2010 are used. The nature of temperature anomaly at this level during the winter (December through February) gives the presence/absence of stratospheric warming pulses. Vertical wind shear is computed using zonal and meridional components of wind during stratwarm days in chapter 4. The data is taken from NCEP/NCAR reanalysis data server. The stratospheric transient and total heat fluxes are also computed using temperature and meridional wind from the above data server. To analyze various features of the tropical response of sudden stratospheric warming temperature anomalies in the daily data are computed from (a) long term mean (b) seasonal mean (December-January-February) and (c) normalized temperature anomalies. This computation is carried out for different Indian stations as well as high latitude regions and is discussed in chapter 5.

2.2. Computation of transient and total heat fluxes

The zonally averaged flux of heat ($v'T'$) is the important diagnostics of atmospheric wave behavior and large-scale transport. Their calculation is based on co-variances of eddy winds and temperatures (in longitude) and the flux provide sensitive diagnostics of planetary wave behavior and

coupling with the mean flow (in both observations and models). The eddy heat and momentum fluxes are most important quantities involved in the calculation of the Eliassen-Palm (EP) flux and its divergence (Andrews et al. 1987). Of primary importance is the poleward eddy heat flux ($v'T$) in the extratropical lower stratosphere, which is proportional to the vertical wave activity flux (EP flux) from the troposphere into the stratosphere (e.g., Andrews et al. 1987). The fluxes considered here are calculated from daily data.

The transient heat fluxes at 10 hPa level are computed for the stratwarm events occurred during the years of 1984/85, 1987/88, 1998/99 and 2008/09 for the domain 0-180°E using NCEP/NCAR reanalysis data (chapter 4). The product of the meridional wind and temperature anomaly (v't') is calculated for a period of 20 days (before and after the peak dayof the six SSW events). The difference in transient heat flux between two adjacent grid points is divided by the distance between them and is given as $\partial / \partial y(v't')$. The unit of meridional flow of transient heat flux is degree Kelvin per second.

The zonal mean (0-180°E) total heat fluxes $\left[\overline{v't'}\right]$ are computed using meridional wind and temperature fields at 10 hPa and 100 hPa pressure levels. The heat fluxes are calculated for high latitudes (45°-75°N) and low latitudes (0-30°N) regions for the above two levels, with brackets denoting a zonal mean and asterisks a deviation from the zonal mean. The departure from the zonal mean are calculated for each latitude between 45°-75°N around 20days before and after the peak day of each SSW and the zonal averaged value is weighted by the cosine of the latitude. The unit of the total heat flux is °K ms^{-1}.

2.3. Cross correlation technique

Correlation coefficient (R) between 10 hPa and 100 hPa heat flux at high and low-latitudes are computed in chapter 4. Cross correlation technique is adopted to analyze the lead-lag correlation between 10 hPa and 100 hPa heat flux at high latitudes (45-75°N) and for low-latitudes (0-30°N) respectively.

Cross correlation is a standard method of estimating the degree to which two series are correlated. Consider two series x (i) and y (i) where i=0, 1, 2...N-1. The cross correlation r at delay d is defined as

$$r = \frac{\sum_i [\,(x(i) - mx) * (y(i-d) - my)\,]}{\sqrt{\sum_i (x(i) - mx)^2}\sqrt{\sum_i (y(i-d) - my)^2}} \qquad \ldots 2.1$$

Where *mx* and *my* are the means of the corresponding series. If the above is computed for all delays d=0, 1, 2,... N-1 then it results in a cross correlation series of twice the length as the original series.

$$r(d) = \frac{\sum_i [\,(x(i) - mx) * (y(i-d) - my)\,]}{\sqrt{\sum_i (x(i) - mx)^2}\sqrt{\sum_i (y(i-d) - my)^2}} \qquad \ldots 2.2$$

There is the issue of what to do when the index in the series is less than 0 or greater than or equal to the number of points (i-d < 0 or i-d >= N). The most common approaches are either to ignore these points or assume the series *x* and *y* are zero for $i < 0$ and $i >= N$. In many signal processing applications the series is assumed to be circular in which case the out of

range indexes are "wrapped" back within range, ie: *x(-1) = x(N-1), x(N+5) = x(5)* etc

The range of delays d and thus the length of the cross correlation series can be less than *N*, for example the aim may be to test correlation at short delays only. The denominator in the expression above serves to normalize the correlation coefficients such that *-1 <= r(d) <= 1*, the bounds indicating maximum correlation and 0 indicating no correlation. A high negative correlation indicates a high correlation but of the inverse of one of the series.

2.4. Mean meridional mass stream function

The strength of the mean meridional overturning of mass can be derived from meridioanl velocity from 1000 hPa to 100 hPa heights (Oort and Yienger 1996). The mass transport is computed using observed zonal mean meridional winds.

Zonally averaged mass continuity equation is computed in the form

$$\frac{\partial[\bar{v}]\cos\phi}{R\cos\phi} + \frac{\partial[\bar{w}]}{\partial p} = 0 \qquad \ldots 2.3$$

Where *[v]* is temporal and zonal averaged meridional velocity, ω is vertical velocity in pressure co ordinates, *R* is mean radius of earth and p is pressure.

Introducing a Stokes stream function ψ, given by equation

$$[\bar{v}] = g\frac{\partial\psi}{2\pi R\cos\phi\,\partial p} \qquad \ldots 2.4$$

We can calculate the ψ field, assuming $\psi=0$ at the top of the atmosphere and integrating the equation downward to the surface.

$$\psi = \frac{2\pi R \cos\phi}{g} \int_{p}^{p_0} [\bar{v}] dp \qquad \ldots 2.5$$

Using this Stokes stream function, meridional circulation features before, during and after the SSW events are analysed. We used positive sign for ψ in the case of clockwise rotation and negative sign for anticlockwise rotation as represented by Oort and Yienger (1996). According to this sign convention, strengthening of two tropical Hadley cells would mean larger positive values of ψ in the Northern Hemisphere (NH) tropics and more negative values of ψ in the Southern Hemisphere (SH) tropics. The difference of mass stream function between two points on a cross section is equal to the amount of mass flowing across a line joining the two points.

2.5. Reanalysis data

Reanalysis is a scientific method for developing a comprehensive record of weather and climate for a period of long time. Observations and a numerical model that simulates one or more aspects of the Earth system are combined objectively to generate a synthesized estimate of the state of the system. A reanalysis typically extends over several decades or longer, and covers the entire globe from the Earth's surface to well above the stratosphere. Reanalysis products are used extensively in climate research and services, including for monitoring and comparing current climate conditions with those of the past, identifying the causes of climate variations and change, and preparing climate predictions. Information derived from reanalysis is also being used increasingly in commercial and business applications in sectors such as energy, agriculture, water resources, and insurance.

2.5.1. ECMWF ERA-40

ERA-40 is a global atmospheric reanalysis (Uppala et al. 2005) of the 45-year period from 1 September 1957 to 31 August 2002. It is produced using a June 2001 version of the ECMWF Integrated Forecast Model (IFS Cy28r3). The spectral resolution is T159 (about 125 km) and there are 60 vertical levels, with the model top at 0.1 hPa (about 64 km). Observations are assimilated using a 6-hourly 3D variational analysis (3D-Var). Satellite data used include Vertical Temperature Profile Radiometer radiances starting in 1972, followed by TOVS, SSM/I, ERS and ATOVS data. Cloud Motion Winds are used from 1979 onwards. Various data from past field experiments are also used, such as the 1974 Atlantic Tropical Experiment (GATE) of the Global Atmospheric Research Program (GARP), 1979 FGGE, 1982 Alpine Experiment, ALPEX and 1992-1993 TOGA-COARE.

2.5.1.1. The excellence of ERA-40 data with an emphasis on stratosphere

The eruption of Mt. Pinatubo caused problems in the assimilation of HIRS infrared radiances that affect the humidity analysis in the tropical troposphere. The ERA-40 analyses appear to capture well the stratospheric warming that is caused by the increased solar heating due to the aerosols. The subsequent cooling is also well captured. 100hPa temperature time series show a temperature maximum in 1992 and cooling thereafter. The ERA-40 analyses thus accurately match the low-frequency variability in these data, which are representative of layer-mean lower stratospheric temperatures.

The ERA-40 reanalysis provides a good representation of the QBO and the assimilating model in ERA-40 tends to exhibit significant biases in

upper-stratospheric temperatures. The analyzed temperatures are sensitive to the availability and the use of satellite measurements in the upper stratosphere, supplied first by the SSU instrument and subsequently by AMSU-A over the period since 1979. Questions concerning the temperature climatology of the upper stratosphere in general and of the whole stratosphere over Antarctica are under investigation. Stratospheric humidity evolves in the assimilating ERA-40 model, but no observations are assimilated. Its distribution is clearly a major improvement on the simple prescription of a uniform specific humidity of 2.5x10-6 in ERA-15, but analyses are generally drier than seen in UARS data for the 1990s and the tropical stratospheric "tape recorder" runs much too fast.

2.5.2. ERA-interim

ERA-Interim is originally planned as an 'interim' reanalysis in preparation for the next-generation extended reanalysis to replace ERA-40. It uses a December 2006 version of the ECMWF Integrated Forecast Model (IFS Cy31r2). It originally covered dates from 1 January 1989 but an additional decade, from 1 January 1979, is added later. ERA-Interim is being continued in real time. The spectral resolution is T255 (about 80 km). There are 60 vertical levels, with the model top at 0.1 hPa (about 64 km). The data assimilation is based on a 12-hourly four-dimensional variational analysis (4D-Var) with adaptive estimation of biases in satellite radiance data (VarBC). With some exceptions, ERA-Interim uses input observations prepared for ERA-40 until 2002, and data from ECMWF's operational archive thereafter. A full description of the ERA-Interim system is given by Dee et al. (2009); Kobayashi et al. (2009); Simmons et al. (2010) and Dee et al. (2011).

ERA-Interim analysis daily products are available from 1 January 1979 onward by MARS users (expver=1, class=ei). It is also available for

twice daily ten-day forecasts and monthly means. The ERA-Interim archive is more extensive than that for ERA-40 e.g. the number of pressure levels is increased from ERA-40's 23 to 37 levels and additional cloud parameters also included. ERA-Interim products are publicly available on the ECMWF Data Server, at a 1.5° resolution, including several other products that are not available in ERA-40.

Progress of Era-interim relative to ERA-40 is made in the following areas:

- *The reanalysis continues in near-real time*
- *Low-frequency variability is much better*
- *Analysis accuracy has improved*
- *The hydrological cycle has improved*
- *The quality of the stratospheric circulation is better*

2.5.2.1 Exact problems in ERA-Interim

A list of known quality issues with ERA-Interim is maintained by the producers at the site of http://www.ecmwf .int/research/era/do/get/index /QualityIssues. It includes the following spurious shifts in ERA-Interim time series related to changes in the observing system:

- Shifts in precipitation (especially over tropical oceans) during the period January 1992 - December 2009, due to the assimilation of rain-affected radiances from SSM/I (Dee et al. 2011).
- A discontinuity in upper-stratospheric temperatures (at levels 5 hPa and above) associated with the introduction of radiance data from AMSU-A in August 1998 (Dee and Uppala 2008).
- Warming of the lower stratosphere by approximately 0.2 K in December 2006, with the introduction of GPS radio occultation data

from the COSMIC constellation, which partly corrects an otherwise unconstrained cold bias in the assimilating model (Poli et al. 2010).

- Slight excess warming of upper-tropospheric temperatures due to the assimilation of growing numbers of warm-biased temperature measurements from aircraft, beginning in 1999 (Dee and Uppala 2009). After December 2006, this drift is somewhat reduced with the introduction of GPS radio occultation data from the COSMIC constellation (Poli et al. 2010).
- The homogeneity of the ozone time series is affected by the availability of observations from different satellite ozone instruments, which fluctuates over time (Dee et al. 2011).

The main advances in the ERA-Interim data assimilation are:

- *12 hour 4D-Var*
- *T255 horizontal resolution*
- *Better formulation of background error constraint*
- *New humidity analysis*
- *Improved model physics*
- *Data quality control that draws on experience from ERA-40 and JRA-25*
- *Variation bias correction of satellite radiance data, and other improvements in bias handling*
- *More extensive use of radiances, and improved fast radiative transfer model*

2.5.3. NCEP/NCAR reanalysis

This reanalysis is the first kind for NOAA. NCEP used the same climate model that is initialized with a wide variety of weather observations: ships, planes, RAOBS, station data, satellite observations and

many more. By using the same model, scientists can examine climate/weather statistics and dynamic processes without the complication that model changes can cause. The dataset is kept current using near real-time observations. On October 1, 2005, the Climate Diagnostics Center, the Environmental Technology Laboratory, and the Aeronomy Laboratory's Tropical Dynamics & Climate Division merged into the Physical Sciences Division (PSD) of the Earth System Research Laboratory (ESRL). As part of the transition, the ETL Optical Remote Sensing Division moved to the ESRL Chemical Sciences Division. This merger brings together a combined expertise in:

1. weather and climate dynamics, diagnostic and modeling analyses,
2. physical observations, monitoring and related technology development,
3. Physical process understanding and research that will help ESRL meet critical NOAA objectives in climate and weather research.

The Physical Sciences Division will carry out research on climate and weather processes, diagnostics, modeling, empirical analyses, focused field observations and supporting technology development. The model (Kalnay et al. 1996) used in the NCEP reanalysis has 28 vertical levels extending from the surface to ~40 km, and analyses of winds, temperatures and geopotential height are output on stratospheric pressure levels of 100, 70, 50, 30, 20 and 10 hPa.

Four times daily, daily, monthly values are present from 1948 to present at 17 pressure levels and 28 sigma levels on a global domain with 2.5°×2.5° latitude and longitude.

2.5.4. Comparison of reanalysis data set

In meteorological model forecasts the reanalysis data sets are often used as a reference to study atmospheric processes such as stratospheric ozone depletion or troposphere-stratosphere exchanges etc. Studies are conducted on the comparison of different types of reanalysis data set. Over Antarctic region the accuracy of the reanalysis data set (ECMWF and NCEP/NCAR) is carried out by Boccara et al. (2008). The ERA-40 residual heating in the tropics is found to be stronger than NCEP's (and ERA-15), especially in July when its zonal–vertical average is twice as large (Chan and Nigam 2008). The bias is strongest over the Maritime Continent in January and over the eastern basins and Africa in July. Comparisons with precipitation indicate ERA-40 heating to be much more realistic over the eastern Pacific but excessive over the Maritime Continent, by at least 20% in January.

In another study (Zhao and Fu 2009) an intercomparison of summertime (JJA) subtropical geopotential heights from the ERA-40 and NCEP/NCAR reanalysis is specifically conducted over East Eurasia and the western North Pacific. The NCEP/NCAR is lower than the ERA-40 in the mid-to-lower troposphere in most regions of East Eurasia before the mid-1970s, but becomes higher than the ERA-40 after the mid-1970s. Thus it demonstrates increased trends during the period of 1958–2001. Both reanalysis are lower than the observations in most regions of China. The NCEP/NCAR especially shows tremendously systematic lower values before the mid-1960s and displays abrupt changes before the 1970s.

Yu et al. (2010) validated the ECMWF ERA-40 and the NCEP/NCAR Re-Analysis data and compared with the Antarctic station observations, including surface-layer and upper-layer atmospheric observations, on intraseasonal and interannual timescales. At the

interannual timescale, atmospheric pressure at different height levels in the ERA-40 data is in better agreement with observed pressure than that in the NCEP–NCAR reanalysis data. ERA-40 reanalysis also outperforms NCEP–NCAR reanalysis in atmospheric temperature, except in the surface layer where the biases are somewhat larger.

Spatiotemporal patterns of (1979–2008) air temperature trends are evaluated using three reanalysis datasets and radiosonde data over Arctic regions (Alexeev et al. 2012). ERA-40 Arctic atmospheric temperatures are closer to the observed ones in terms of root mean square error compared to other reanalysis products. The changes in the ERA-40 data assimilation procedure produce unphysical jumps in atmospheric temperatures, which may be the reason for the elevated tropospheric warming trend in 1979–2002. NCEP/NCAR Reanalysis data show that the near-surface upward temperature trend over the same period is greater than the tropospheric trend and which is consistent with direct radiosonde observations and inconsistent with ERA-40 results.

TABLE 2.1. Details of the reanalysis data.

Name	Source	Time Range	Dataset Resolution	Dataset Output Times and Time Averaging
ECMWF 40 year Reanalysis (ERA-40)	ECMWF	1958-2001	2.5x2.5 / 1.125x1.125	3-hourly for most surface fields; 6-hourly for upper-air fields Monthly averages of daily means, 6-hourly fields
ECMWF Interim Reanalysis (ERA Interim)	ECMWF	1979-present	1.5x1.5	3-hourly for most surface fields; 6-hourly for upper-air fields Monthly averages of daily means, 6-hourly fields
NCEP/NCAR Reanalysis I (R1)	NCEP/ NCAR	1948-present	2.5x2.5 2x2 gaussian	4 times daily/daily/monthly also LTMs

A multi data set is used (Brönnimann et al. 2012) to compare the daily, interannual, and decadal variability and trends in the thermal structure of the Arctic troposphere using eight observation-based, vertically resolved data sets, four of which had data prior to 1948. Table 2.1 shows the details of the three reanalysis data set used in our study.

2.6. Research groups

2.6.1. Climate Prediction Center (CPC)

The **Climate Prediction Center** (CPC) is one of the National Centers for Environmental Prediction, and is a part of NOAA's National Weather Service http://www.cpc.ncep.noaa.gov/. The CPC's products are operational predictions of climate variability, real-time monitoring of global climate, and attribution of the origins of major climate anomalies. The products cover time scales from a week to seasons, and cover the land, the ocean, and the atmosphere, extending into the stratosphere.

2.6.1.1. Stratosphere Home

Stratosphere home in CPC provides forecast reports on stratospheric temperatures and ultra violet indexes. They issued assessments reports of winter bulletins and ozone depletions. The research groups also make available constant stratosphere –troposphere monitoring analysis for the time period 1979 to the present. It includes annual time series of temperature, zonal wind, normalized geopotential height anomalies and amplitude of the height fields of Wave 1, Wave 2 and Wave 3, meteorological conditions and ozone in the polar stratosphere. The CPC stratospheric analyses are based on a successive-correction objective analysis (Finger et al. 1965) for pressure levels 70, 50, 30, 10, 5, 2, 1 and 0.4 hPa, incorporating TOVS and ATOVS satellite data and radiosonde

measurements (in the lower stratosphere of the NH). This analysis system is nearly constant over time (October 1978- April 2001).

Stratospheric temperatures at standard levels are derived by interpolation between the TOVS layer mean temperatures (Randel et al. 2004). The fields are produced each day for a nominal time of 1200 UTC, using 12 hours of TOVS data (0600-1800 UTC). The NCEP operationally analyzed tropospheric fields over 1000- 100 hPa but CPC analyses cover 1000-0.4 hPa. As a note, the CPC analyses are changed beginning in May 2001, with the data up to 10 hPa based on the NCEP operational analyses, and fields above 10 hPa based solely on ATOVS.

2.6.1.2. Global temperature time series

The CPC global temperature analyses are derived each day at 8 stratospheric levels, 70, 50, 30, 10, 5, 2, 1, and 0.4 hPa (approximately 18-55 km). Graphical aids for monitoring temperature anomalies in the stratosphere for 70 hPa and 50 hPa (approx. 20 km), representative of the lower stratosphere, 30 hPa and 10 hPa (approx. 30 km) representing the middle stratosphere, and 5 hPa, 2 hPa (approx. 42 km), and 1 hPa representing the upper stratosphere are given. Daily temperature values averaged over each latitude region (90-60°N, 65-25°N, 25°N-25°S, 25-65°S, and 65-90°S) are shown. The values for the current year are compared to the average values for each day and the extreme maximum and minimum values for the entire temperature analysis record from 1979 to current.

2.6.2. Stratospheric Research group, Berlin

‘The physics of the middle atmosphere’ is a division under the institute of meteorology (http://www.geo.fu-berlin.de/en/met/index.html) in Freie University of Berlin (FUB). The division is mainly focused on the

analysis of the climatology and variability of the stratosphere and mesosphere in measurements and model, stratospheric winter diagnostics, radiative, chemical and dynamical processes and their interactions with Chemistry-Climate-Model, the effect of solar cycle on climate, model simulations of early earth conditions to study the evolution of life and the application of advanced methods of time series analysis to the climate research. Stratospheric analysis in the Berlin University gives a wide range of forecast products, including stratospheric diagnostics, stratospheric warmings, stratospheric analysis and North Pole temperatures, QBO and balloon campaign support.

2.6.2.1. ECMWF stratospheric diagnostics

Based on ECMWF analyses and forecasts for stratospheric levels, they provide maps of geopotential height and temperature, potential vorticity on isentropic levels, and zonal sections for the northern hemisphere. In addition to they also provide time series of derived quantities during the Arctic winter from 01 November - 30 April.

The aim of this group is to inform all researchers, engaged in various studies connected with stratospheric circulation modeling and analysis, tropospheric/stratospheric interactions, stratospheric ozone and climate studies, about the current state of the northern hemisphere stratospheric circulation.

Data links available are given below:

US National Centers for Environmental Prediction (CPC/NCEP):
http://www.cpc.ncep.noaa.gov/products/stratosphere/
Japan Meteorological Agency (JMA):
http://ds.data.jma.go.jp/tcc/tcc/products/clisys/STRAT/
Deutsches Zentrum für Luft- und Raumfahrt (DLR), Institut für

Physik der Atmosphäre:
http://www.pa.op.dlr.de/arctic/index.html

2.6.2.2. ECMWF stratospheric analysis

The Berlin dataset consists of 35 years of daily (every two days in summer**)** geopotential height and temperature fields at 50, 30 and 10 hPa in the northern hemisphere**.** The hemispheric analyses are produced in real time by a subjective analysis technique, using the 00UT radiosonde reports from the observational network, by a team of experienced meteorologists. Both geostrophic and hydrostatic balances are assumed in the analysis procedure, and the wind observations are given a high priority**.** The Berlin analyses represent the synoptic-scale structure of the lower and middle stratosphere

The data are available in regular northern hemispheric latitude-longitude grids:

- *Geopotential height from November 1964 to June 2001*
- *Temperatures from July 1965 to June 2001*

2.6.2.3. Monthly mean North Pole temperatures at 30 hPa

Muench and Borden (1962) analysed monthly mean stratospheric charts from 1955-1959. From these data, B. Naujokat extrapolated the 30 hPa North Pole temperatures for the period July 1955 till June 1957 which enlarges the data set of the Freie Universität Berlin analyses (FUB-analyses) for the North Pole. The other temperature data are extrapolated from our daily maps until 1965 when the temperature analyses on published together with the maps and digitized accordingly, like the height maps. The FUB-analyses end in June 2001. All later data are taken from the operational analyses of ECMWF.

The FUB data is used in a large number of studies of the climatology of the middle atmosphere, including trends and low-frequency variability (e.g., Labitzke and Naujokat, 1983; Pawson et al. 1993). Daily data is extensively exploited to understand the occurrence of very cold regions which are associated with polar stratospheric cloud formation and ozone loss (Pawson and Naujokat, 1999). It should be noted that these analyses do not include wind as a product; while their utility is restricted by this, they are a valuable record of the stratosphere between about 1957 and 2001, analysed in a consistent and uniform manner throughout this period. Full details of the FUB analysis, together with the entire data set, are available in compact disk (CD) format (Labitzke et al. 2002).

2.6.3. SPARC

Stratospheric processes and their Role in climate (SPARC) is a core project of the World Climate Research Programme which coordinates international efforts to bring knowledge of the stratosphere to bear on relevant issues in climate variability and prediction. The main theme of sparc activities are listed below

- Climate-chemistry interactions
- Detection, attribution and prediction of stratospheric change
- Stratosphere-troposphere dynamical coupling

2.6.3.1. SPARC Data center

The SPARC data center is established in June 1999, and the number of data sets is growing rapidly. Several data sets are now available on online. High-resolution temperature and wind data from radiosondes, which are purchased from NOAA and are currently available for 1998-2008. Solar forcing and historic ozone data and the data from the GRIPS model

intercomparisons are also available. The Water Vapor Assessment (WAVAS) archives, includes H_2O data from ground-based, airborne and satellite instruments.

The SPARC data center provides public access to data related to SPARC´s contribution to the International Polar Year 2007-2008. The SPARC data center's aim is to provide data to the SPARC scientific communities through the listed links below:

(http://www.sparc.sunysb.edu/html/RefData.html)

- SPARC International Polar Year 2007-2008
- Small Organic Peroxy Radicals Data
- SPARC Reference Climatology Project
    - *CIRA-86*
    - *FUB Obervations*
    - *UKTOVS*
    - *URAP T,winds*
    - *Randel's Climatologies*

The available data sets are:

- *Monthly Meteorological Data*
- *UARS*
- *Ozone trends for 1979-1996*
- *Tropopause Heights*
- *Temperature and Zonal Wind Climatology*
- *Updated Ozone Data*
- *Updated Temperature Trends*

The data sets used in this doctoral thesis are retrieved from the above discussed reanalysis servers and the results are analyzed in the subsequent chapters.

Chapter 3

Classification of Sudden Stratospheric Warming Events in the Upper and Mid-Stratospheric Levels and its Various Features

3.1. Introduction

Sudden stratospheric winter warmings in the Northern Hemisphere (NH) exhibit significant variability in interannual timescales. The stratosphere as a whole is highly disturbed during each winter. The disturbances originated in the troposphere penetrate into middle stratosphere and culminate into warmings with varying intensities (Quiroz et al. 1975). Disturbed winters are primarily associated with the increase in polar temperature by 50°C or more in just a few days (Andrews et al. 1987). Mainly there are two types of warmings; major and minor. A minor warming is defined as a thermal pulse in any part of the winter stratosphere with a temperature increase of 25°C with in a period of one week. A major warming is one where the temperature increases poleward of 60 degree latitude and results in reversing the prevailing westerly winds. Temperature disturbances below these intensities are explained as thermal pulses. During any winter period either one major or at least one minor warmings do occur. Both the major and minor SSWs are evolved in the upper stratosphere and then propagate downward to the middle and lower stratosphere (see Quiroz, 1969; 1971 and Scott, 1972).

Stratospheric warmings are studied extensively in the last several decades since its discovery by Scherhag in 1952, (eg: Matsuno, 1971; Van loon, 1975; Labitzke, 1977; 1982; 1987; Schoeberl, 1978; Holton and Tan, 1980; Baldwin and Dunkerton, 1999; 2001; Mukougawa et al. 2005; Nakagawa and Yamazaki, 2006; Hirooka et al. 2007; Kuroda, 2008; Schimanke et al. 2011, etc). Labitzke (1977) and Labitzke and Naujokat (2000) made distinctive studies on grouping the events incorporating more parameters such as, phase of Quasi biennial oscillation (QBO) and sunspot number. In another classification study by Manney et al. (2005), an area averaged stratospheric zonal mean zonal wind at 60-80°N for 10 hPa levels is considered as a parameter. They used NCEP/NCAR reanalysis data corresponding to 26 arctic winters from 1978 to 2004. Ryoo and Chun (2005) analyzed the NCEP/NCAR reanalysis data and classified stratospheric warmings from 41 arctic winters during 1958-1999. Their categorization includes the Type 1 and Type 2 warmings associated with the phase of QBO. In another study (Hoffman, 2002) showed mesospheric wind reversals were observed in 65% of the 12 arctic winters (1989-2000) in relation with enhanced planetary wave activity at 10 hPa level.

A detailed study related with the climatology of SSW is reported by Charlton and Polvani, (2007). They tabulated the events from late 1950s to 2002 using NCEP-NCAR and ERA-40 reanalysis daily data. Their categorization is mainly based on vortex displacement or splitting of the polar vortex. The peak days are important to assess various features of warmings during the development, peak and decay phases of SSWs. Schimanke et al. (2011) analysed the multi-century variability in the number of occurrence of major SSWs using atmosphere-ocean general circulation model simulation (AOGCM) and showed that the interaction between ocean-troposphere-stratosphere systems.

During 1960's when WMO formulated the classification of warmings, the upper limit of then available data was around 10 hPa levels. That may be the reason to fix the 10 hPa level as the reference level to categorize the warming events. Later studies (Schoeberl 1978) clearly showed that warmings do occur in further higher altitudes of the upper stratosphere (2 hPa). There are cases where the peak intensity of minor warming is higher than that of major warmings. Such events could not be considered as major events because of the absence of wind reversals at 10 hPa levels. While studies on the tropical response of SSW, the tropical cooling is found to occur in association with the SSWs of the upper stratospheric levels (Labitzke et al. 1972, Appu, 1984; Mukherjee, 1985). In this context, it may be appropriate to have another type of classification of SSW, incorporating both temperature and winds pertaining to the upper and middle stratospheric layers. We made an attempt in this direction. For the purpose of our study we selected 2 hPa (45 km) and 10 hPa (32 km) as reference levels to classify the warmings. Accordingly we categorized the SSWs into five groups based on both the temperature and zonal wind at the above two levels. Our analysis is carried out using 31 years of ECMWF interim data from 1980 to 2010.The following dynamical features of the warmings (a) decadal variability (b) interannual variability (c) intra seasonal variability (d) nature of vertical propagation of warming system and (e) variation of warm and cold centers are also presented.

3. 2. Data and methodology

The daily temperature and zonal wind data from the ECMWF (European Center for Medium Range Weather Forecast) interim reanalysis for the middle and upper stratospheric heights: viz 10 hPa (~32 km) and 2 hPa (~45 km) for the period 1980-2010 are used in this study. The temperature and zonal wind anomalies are calculated in the latitudinal range

(60-90°N) and the entire longitudinal belt (0-360°) with a horizontal spatial resolution of 1.5° ×1.5° grid. The anomalies in the daily temperature (ΔT) and zonal winds (ΔU) are computed based on the deviations from the long term climatological means (T and U) derived from the 31 years of data. The day where maximum deviations take palace is considered as the peak day of the warming event. For the purpose of analyzing the decadal variability, the 31 year period of data is grouped into 3 decades as decade (1) 1980-89, (2) 1990-99 and (3) 2000-2010. To study the vertical propagation of the warming events, we considered composited zonal mean temperature and zonal wind anomalies for the time period of 20 days before and after the peak day for the altitude layer from upper to lower stratosphere (1 hPa to 20 hPa). To analyze the position and intensity of the warm and cold vortices, composite of major and minor stratwarm peak days are calculated on decadal timescale at 2 hPa and 10 hPa levels.

3. 3. Results and Discussion

3.3.1. Definition of the five groups based on temperature and zonal wind at Upper and Middle Stratosphere

The different criteria adopted in defining the five groups are illustrated in Tables 3.1 and 3.2 for 10 hPa and 2 hPa levels respectively. The day in which maximum temperature anomaly over the winter polar stratosphere coincides with the zonal wind anomaly is considered as the peak day of the event. We classified the stratwarm events events as (1) '***intense major***', (2) '***major 1***', (3) '***major 2***', and (4) '***intense minor***' and (5) '***minor***' warmings. The criteria for the five groups are (1) $\Delta T \geq 15°C$, $\Delta U > -40$ ms^{-1} (2) $\Delta T \geq 15°C$, $\Delta U \geq -25$ ms^{-1} and < -40 ms^{-1} (3) $\Delta T \geq 10°C$ and $< 15°C$, $\Delta U > -40$ ms^{-1}, and (4) $\Delta T \geq 10°C$ but $< 15°C$, $\Delta U \geq -25$ ms^{-1} and < -40 ms^{-1}, (5) $\Delta T \leq 9$ and $\Delta U \leq 24$ respectively; where ΔT and ΔU

represent the deviations in the daily anomalies of temperature and zonal wind respectively.

Since the atmospheric conditions in the upper stratosphere are quite different from that of the middle stratosphere, the criteria for the classification of SSWs at 2 hPa level is slightly modified considering the temperature and zonal wind state at this altitude. The conditions for the five groups are : (1) $\Delta T \geq 20°C$ & $\Delta U \geq -50$ ms^{-1} 'intense major'; (2) $\Delta T \geq 20°C$ & $\Delta U \geq -35$ ms^{-1} but < -50 ms^{-1} 'major 1'; (3) $\Delta T \geq 15°C$ and $< 20°C$ & $\Delta U \geq -50$ ms^{-1} 'major 2'; and (4) $\Delta T \geq 15°C$ and $< 20°C$ & $\Delta U \geq -35$ $ms^{-1} < -50$ ms^{-1} 'intense minor' (5) $\Delta T \leq 14$ and $\Delta U \leq 34$.

TABLE 3.1. Magnitude of temperature and winds variations in classifying the five groups for 10 hPa level.

Serial No	Classified Group	Deviations in temp ($\Delta T°C$)	Deviations in wind ($\Delta U ms^{-1}$)
1	'Intense major'	≥ 15	> -40
2	'Major 1'	≥ 15	≥ -25 to < -40
3	'Major 2'	≥ 10 to < 15	> -40
4	'Intense minor'	≥ 10 to < 15	≥ -25 to < -40
5	'Minor'	≤ 9	≤ 24

TABLE 3.2. Same as Table 1 but for for 2 hPa level.

Serial No	Classified Group	Deviations in temp ($\Delta T°C$)	Deviations in wind ($\Delta U ms^{-1}$)
1	'Intense major'	≥ 20	> -50
2	'Major 1'	≥ 20	≥ -35 to < -50
3	'Major 2'	≥ 15 to < 20	> -50
4	'Intense minor'	≥ 15 to < 20	≥ -35 and < -50
5	'Minor'	≤ 14	≤ 34

Accordingly all the events in the 31 year period are classified and summarized in Table 3.3 and 3.4. Major and minor warmings are marked as bold and italics respectively in tables. Double pulse stratwarm events in a single winter are also included in the Tables. References on the earlier studies conducted on the concerned warming events are shown in Table 3.3.

TABLE 3.3. Summary of the distribution of stratospheric warming events at 10 hPa level during 1980-2010 period.

	Temperature		Zonal wind			
Year	Peak day	ΔT (°C)	Peak day	ΔU (ms^{-1})	Type of warming	References
1980/81	05/02/81	22.74	16/02/81	-22.40	*Minor*	Baldwin et al. 1988
1981/82	27/01/82	20.07	26/01/82	-15.78	*Minor*	Hamilton K. 1995
1982/83	27/02/83	17.28	28/02/83	-15.03	*Minor*	Hamilton K. 1995
1983/84	25/02/84	19.64	26/02/84	-34.94	**Major 1**	Petzoldt K. 1987
1984/85	02/01/85	30.49	02/01/85	-56.32	**Inte. major**	Fairlie et al. 1988, Mukerjee et al. 1987
1985/86	18/02/86	10.39	18/02/86	-13.77	*Minor*	Naujokat et al. 1993
1986/87	24/01/87	14.84	25/01/87	-43.97	*Minor*	Naujokat et al. 1987
1987/88	11/12/87	25.21	13/12/87	-52.96	**Inte. major**	Baldwin, 1989
1988/89	20/02/89	19.28	23/02/89	-32.22	**Major 1**	Fairlie. 1990
1989/90	11/2/90	20.09	12/02/90	-14.32	*Minor*	Naujokat et al. 1989
1990/91	28/01/91	17.49	04/02/91	-32.95	**Major 1**	Ryoo and Chun 2005
1991/92	19/01/92	23.44	19/01/92	-21.64	*Minor*	Degorska et al. 1996
1992/93	24/02/93	10.67	17/02/93	-13.89	*Minor*	Degorska et al. 1996
1992/93	06/03/93	11.68	06/03/93	-26.02	*Inte. minor*	Hamilton *K* 1995

Table 3.3continued

	Temperature		Zonal wind			
Year	Peak day	ΔT (°C)	Peak day	ΔU (ms^{-1})	Type of warming	References
1993/94	02/01/94	13.55	02/01/94	-31.86	*Inte. minor*	Naujokat et al. 1994
1994/95	30/01/95	21.13	24/01/95	-30.87	**Major 1**	Ryoo and Chun 2005
1995/96			No event			
1996/97			No event			Labitzke, 2000
1997/98	27/12/97	17.43	28/12/97	-32.60	**Major 1**	THESO. 1997/98
1998/99	17/12/98	29.33	18/12/98	-52.69	**Inte. major**	Manney et al. 1999; 2005.
1998/99	28/02/99	21.70	02/03/99	-35.74	**Major 1**	Sridharan et al. 2008
1999/00			No event			
2000/01	20/12/00	17.71	20/12/00	-20.90	*Minor*	EORCU, reports
2000/01	02/02/01	12.83	13/02/01	-31.40	*Inte. Minor*	EORCU, reports
2001/02	29/12/01	26.86	01/01/02	-33.39	**Major 1**	Hirooka. 2007
2001/02	19/02/02	12.89	18/02/02	-26.72	*Inte. Minor*	EORCU, reports
2002/03	30/12/02	21.51	01/01/03	-13.10	*Minor*	Najoukat. 2003
2002/03	17/01/03	19.39	18/01/03	-34.98	**Major 1**	Peters et al. 2003
2003/04	28/12/03	22.73	12/01/04	-46.09	**Inte. Major**	Hirooka. 2007, Manney et al. 2005, Pancheva. 2008
2004/05	01/03/05	08.60	28/02/05	-13.22	*Minor*	Peters et al. 2003
2005/06	23/01/06	18.87	25/01/06	-55.63	**Inte. Major**	Hoffman. 2007
2006/07	27/02/07	8.89	25/02/07	-37.97	*Minor*	Alexander and Shepherd. 2010
2007/08	23/02/08	17.85	25/02/08	-36.53	**Major 1**	Alexander and Shepherd. 2010
2008/09	23/01/09	34.78	01/02/09	-45.19	**Inte. Major**	Labitzke and Kunze 2009, Manney et al. 2009, Harada et al. 2010
2009/10	31/01/10	17.75	11/02/10	-34.30	**Major 1**	Kuttipurath et al. 2012

TABLE 3.4. Summary of the distribution of stratospheric warming events at 2 hPa during 1980-2010 periods.

	Temperature		Zonal wind		
Year	Peak day	ΔT (°C)	Peak day	ΔU (ms^{-1})	Type of warming
1980/81	01/02/81	24.38	01/02/81	-28.84	*Minor*
1981/82	25/01/82	13.51	26/01/82	-35.23	*Minor*
1982/83	28/01/83	21.05	29/01/83	-28.70	*Minor*
1982/83	06/02/83	16.04	06/02/83	-30.74	*Minor*
1982/83	26/02/83	18.55	26/02/83	-42.46	*Inte. Minor*
1983/84	22/02/84	22.27	25/02/84	-42.36	**Major 1**
1984/85	01/01/85	34.19	01/01/85	-88.65	**Inte. Major**
1985/86	20/01/86	19.17	23/01/86	-23.79	*Minor*
1985/86	18/02/86	18.26	18/02/86	-40.01	*Inte. Minor*
1986/87	24/01/87	17.39	24/01/87	-69.11	**Major 2**
1987/88	08/12/87	27.94	11/12/87	-78.68	**Inte. Major**
1988/89	12/02/89	22.93	20/02/89	-17.62	*Minor*
1989/90	10/02/90	25.06	10/02/90	-43.35	**Major 1**
1990/91	27/01/91	21.25	27/01/91	-36.01	**Major 1**
1991/92	14/01/92	30.06	15/01/92	-46.72	**Major 1**
1992/93	23/02/93	24.15	20/02/93	-19.68	*Minor*
1993/94	05/01/94	9.02	03/01/94	-50.51	*Minor*
1994/95	27/01/95	19.84	28/01/95	-42.67	*Inte. Minor*
1995/96			No event		
1996/97			No event		
1997/98	26/12/97	24.47	27/12/97	-47.35	**Major 1**
1998/99	15/12/98	16.52	18/12/98	-76.82	**Major 2**
1998/99	24/02/99	21.63	28/02/99	-52.34	**Inte. Major**
1999/00	09/02/00	15.40	09/02/00	-20.48	*Minor*
2000/01	12/12/00	39.27	12/12/00	-40.86	**Major 1**
2001/02	24/12/01	35.83	25/12/01	-62.04	**Inte. Major**
2001/02	17/02/02	18.86	17/02/02	-52.22	**Major 2**
2002/03	30/12/02	29.61	31/12/02	-38.50	**Major 1**
2002/03	17/01/03	12.93	17/01/03	-67.63	*Minor*
2003/04	24/12/03	33.87	24/12/03	-54.24	**Inte. Major**
2004/05			No event		
2005/06	12/01/06	33.99	23/01/06	-80.49	**Inte. Major**
2006/07	26/02/07	12.06	25/02/07	-40.75	*Minor*
2007/08	25/01/08	15.86	25/01/08	-34.94	*Inte.minor*
2007/08	06/02/08	25.06	07/02/08	-31.42	*Minor*
2007/08	23/02/08	9.26	24/02/08	-53.85	*Minor*
2008/09	21/01/09	28.53	25/01/09	-57.23	**Inte. Major**
2009/10	25/01/10	21.59	30/01/10	-47.66	**Major 1**

3.3.1.1. Summary of the different groups

During the 31 year period there are 32 cases of stratwarm events reported at 10 hPa level in which 50% of the cases showed an enhancement of temperature more than 15°C. Regarding these 16 cases, the wind anomalies exceed 40 ms^{-1} in 6 cases only. This comes under 'intense major' group. In the remaining 10 cases, the easterly anomalies were weaker and fall in the category of 'Major 1'. Four stratwarm events are grouped as 'intense minor' were temperature in between 10 and 15°C and wind speed anomalies falls between 25 and 40 ms^{-1}. No major 2 category formed during the entire period of study. The remaining 12 cases included in the fifth group.

At 2 hPa level, a total number of 35 events are noted. There are 15 cases where temperature exceeds 50°C. Considering the wind criteria, 7 events included under 'intense major' warming group and remaining 8 events under the 'major 1' group. Moderate temperature increase of 15-20°C occurred in 7 cases, out of which 3 reported large anomaly in zonal wind 'major 2' and 4 cases where the wind speed lies between 35 and 50 ms^{-1} ('intense minor'). Hence about 50% of the cases come under the 'minor' warming group.

The percentage of different stratwarm events identified at 2 hPa and 10 hPa levels are illustrated in figure 3.1. The data period is 31 years from 1980-2010. The 'intense major' warming accounts for 20% and 19% (red) at the two levels respectively. The 'major 1' type stratwarms are account for 23 and 31 percentage (yellow). 'Major 2' type warmings are 9% at upper stratosphere (green) while at mid- stratosphere this category is absent. 'Intense minor' warmings are noted 11% and 12% respectively. The percentage of occurrence of 'minor' warmings is 37 at 2 hPa and 38 at 10 hPa level.

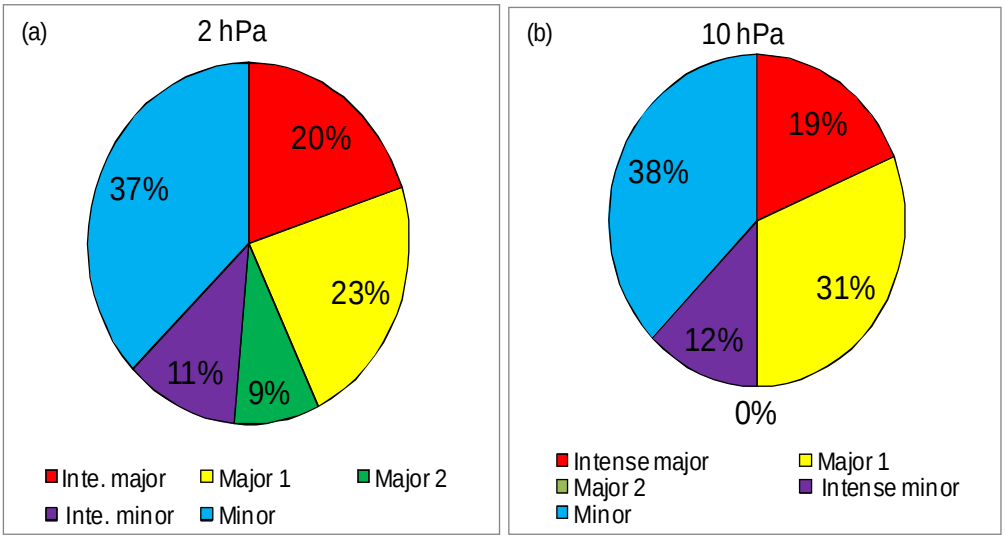

FIG.3 1. Percentage values for five categories of stratwarms (a) at 2 hPa and (b) at 10 hPa during 1980-2010 period.

As part of the seasonal characteristics the winter stratosphere is generally unstable and undergoes continuous perturbations with varying intensities. The disturbed condition is generated due to the interaction between stratospheric-tropospheric couplings through wave actives (Baldwin and Dunkerton 2001; Gerber and Polvani 2009). It also indicates that while propagating from upper to mid-stratosphere major 2 type stratwarms in the upper stratosphere are characterized by decreases in zonal wind intensity as a result it does not satisfy the major 2 type criteria at 10 hPa. In addition, at upper and mid-stratosphere each 50% of perturbations are major and minor events for the last three decade. The degree of perturbations in the stratosphere can influence tropospheric dynamical structure. Thus about 50% of the stratospheric perturbations at both the levels can directly propagate downward. But the minor warming can decelerate westerly wind in the stratospheric levels and its downward propagation is limited to stratospheric levels.

1.3.2. Scatter diagram to represent the frequency distribution of warming groups

The scatter diagram exhibits nature of occurrence of the five different categories of SSWs at 2 hPa (Fig. 3.2a) and at 10 hPa (Fig. 3.2b) levels. Vertical and horizontal dashed lines represent the criteria for temperature and zonal wind anomalies respectively. The stratwarm events which follow the condition are given in the colored regions.

The filled diamonds in the red colored region represent the 'intense major' warming events in the upper stratosphere. Those warming winters are 1984/85, 1987/88, 1998/99, 2001/02, 2003/04, 2005/06 and 2008/09. Mostly these intense events are associated with zonal wave number 1 and 2. The zonal wind anomalies are propagated downward due to the interaction between planetary waves and mean flow. The number of 'major 1' type SSWs at 2 hPa is 8 and represent in spheres in yellow region (Fig. 3.2a). They corresponds the years 1983/84, 1989/90, 1990/91, 1991/92, 1997/98, 2000/01, 2002/03 and 2009/10. There are three major 2 types (star sign) and four 'intense minor' warming events (multiple sign). In addition, 13 'minor' warmings (plus sign in non-shaded area) are also observed with less intensified easterly wind anomalies. The above statistical distribution of stratwarm events explains the nature of different type of perturbation occurring in the upper stratosphere. In a similar way the event at 10 hPa level is presented in fig. 3.2b.

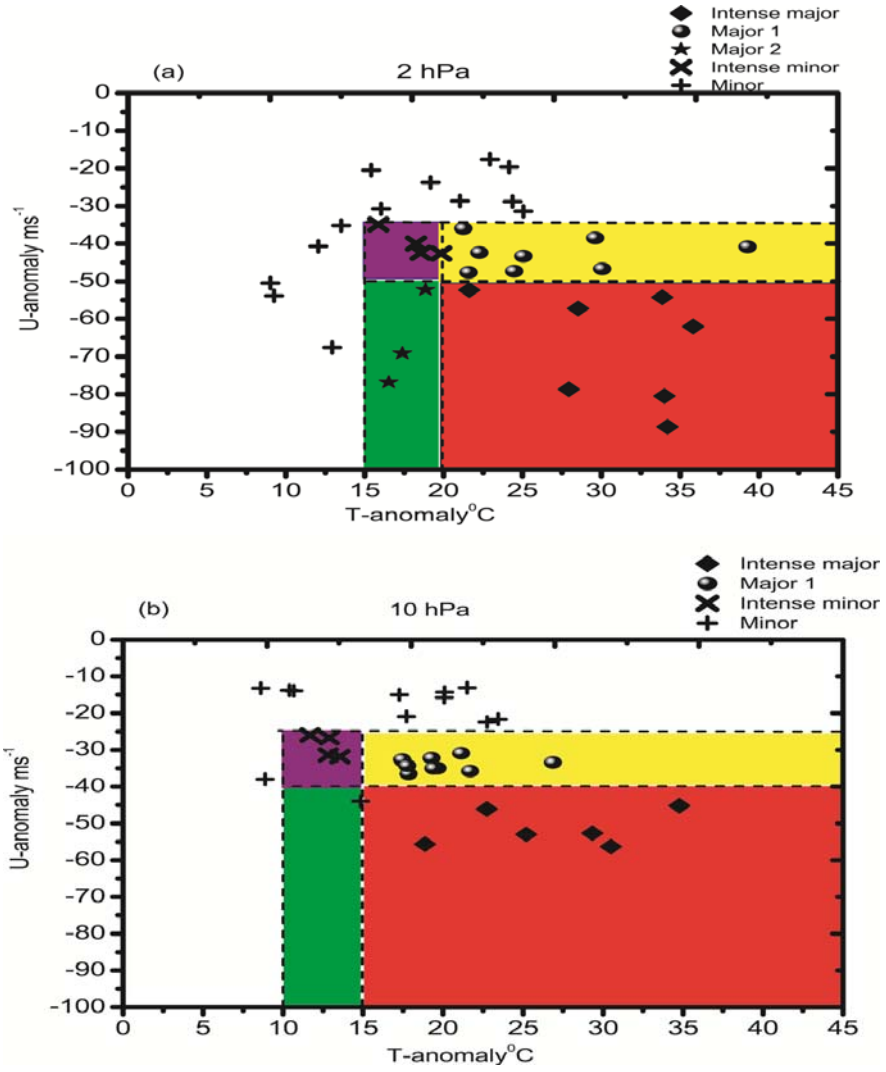

FIG.3.2. Scatter diagram explain the five categories of SSW events identified during the period 1980-2010 at (a) 2 hPa and (b) 10 hPa levels. Temperature and zonal wind anomalies of the SSW peak days are shown. The four categories of stratwarms are expressed in colored regions and the 'minor' warmings in non shaded regions.

Upper stratosphere is characterized with more number of perturbations when compared with 10 hPa level. The intensity of the easterly wind anomaly (Fig. 3.2a) varies from -50 ms^{-1} to -90 ms^{-1} during 'intense major' warming events. At the same time, over mid-stratosphere,

wind anomalies vary from -40 ms^{-1} to -60 ms^{-1} for the same stratwarm events. It reveals that easterly wind anomalies are comparatively stronger at 2 hPa levels.

3.3.3. Time series of stratospheric warming events

The intensity of peak day of all the events for (a) 2 hPa and (b) 10 hPa levels are illustrated in figure 3.3. The five category of stratwarm events are represented different colored vertical and downward bars. The 'intense major', 'major 1', 'major 2', 'intense minor' and 'minor' warming events are represented as red, yellow, green, blue and white bars respectively.

In few cases warming is confined to both the levels indicating the larger vertical extension. The 'intense major' warming events are confined to the whole stratospheric layers with an exception of the event during 2001/02, where no prominent temperature increase took place at 10 hPa level. During this year, the event is confined only at 2hPa. Minor warmings mostly happens at higher levels (2 hPa). The propagation of zonal mean zonal wind anomalies from stratosphere to tropospheric levels (Kodera et al. 2000; Nagakava and Yamazaki 2006 and Zhou et al. 2002) reflects the intensity of stratwarms. The intensity and vertical propagation of the warming systems are interlinked as the dynamical aspects to generate the intensity of the warming systems.

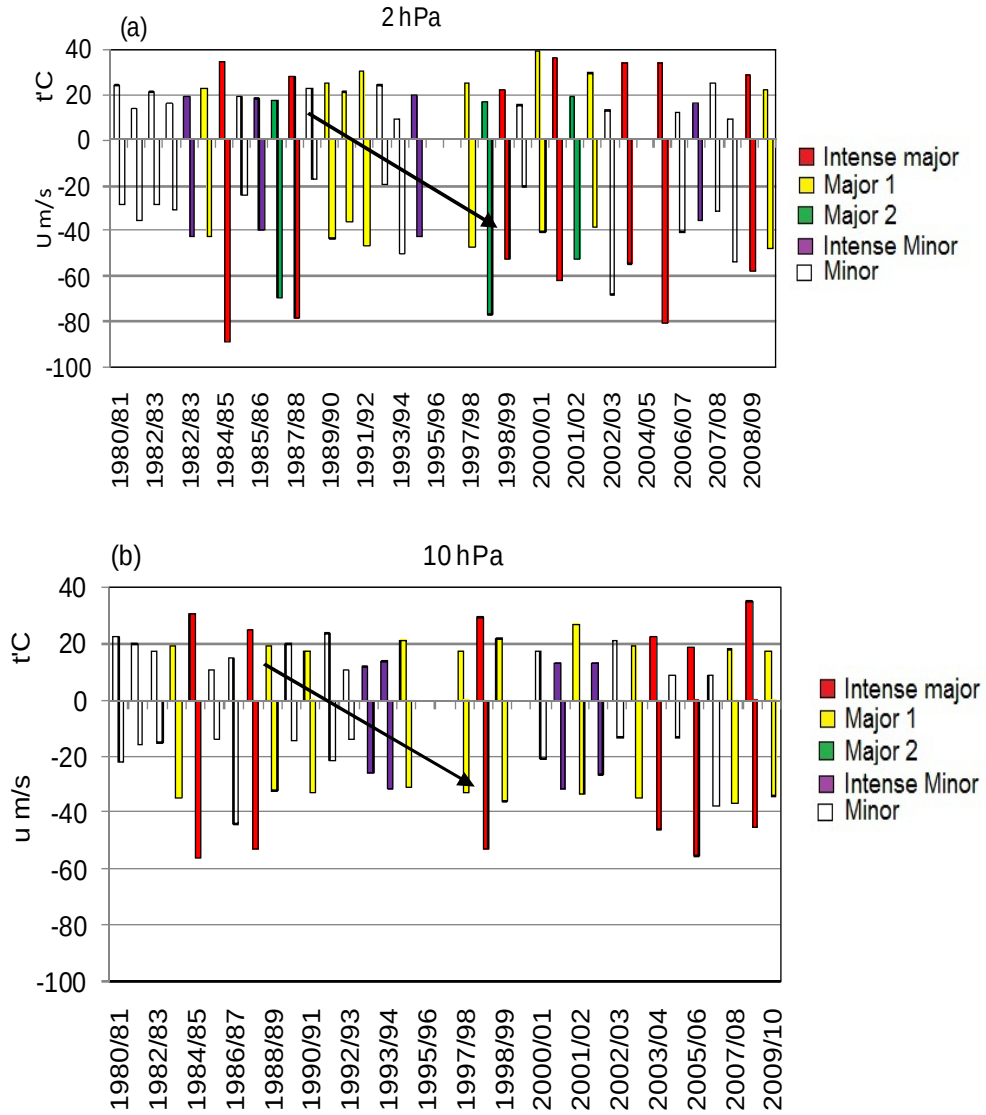

FIG. 3.3. Temperature and zonal wind anomalies occurred during the peak day of each event from 1980 to 2010 period at (a) 2hPa and at (b) 10 hPa levels. The five different types of stratwarm are represented in special colors. The vertical and downward bars represent the temperature and zonal wind anomaly of an event. The arrow denotes the absence of 'intense major' event in the upper and mid-stratosphere.

As per the WMO definition an event to classify as major, wind reversal at 10 hPa level is required parameter. The event during 2001/02 exhibit high level intensity and wind reversal at 2 hPa level but not at 10

hPa levels. The temperature increase was 62°C at 2 hPa level, a very strong rise. In our classification this event comes under 'intense major' warming whereas it comes under minor warming as per WMO definition. The 'intense major' stratwarms classified in the study are comparable with the previous study done by Fairlie et al. 1988; Baldwin 1989; Manney et al. 2005; Hirooka 2007; Hoffman 2007 and Manney et al. 2009. Mainly stratwarm events are originated in the upper stratospheric levels and propagate towards the lower layers even reaching to tropospheric levels. The strength of the warming is directly linked to the intensity of the wave activity.

Before 1990, major warming occurred almost once in every two years (e.g Labitzke, 1982; Naujokat and Labitzke, 1993; Labitzke et al. 2002, and references therein). It is to be noted that no major warming occurred in nine consecutive winters from 1989-90 winter to 1997-98. We also found the non occurrence of 'intense major' warmings during the same period (Fig. 3, arrow). Even though the stratosphere warmed in those winters with a change in the direction of zonal wind, the intensity of the reversed easterly wind is less of the order of 10 ms^{-1}.

The upper stratospheric thermal structure experienced four 'intense minor' warmings at both the levels (Fig.3.3a). Three of the 'major 2' type warmings (1986/87 (Jan), 1998/99 (Dec) and 2001/02 (Feb)) in the upper stratosphere weakened during the downward propagation and reduced its intensity. Hence there is no 'major 2' type warming in the mid-stratosphere. Limpasuvan et al (2004) showed the relation between the vertical propagation of the warming systems and its intensity. While SSWs undergo downward propagation its intensity is reduced. During the course of propagation major warmings at upper stratosphere turned to the intensity of minor warmings at lower altitude.

3.3.3.1. Decadal variability of the warmings

Figure 3.4 depicts the occurrences of major, minor and no stratwarm events at 2 hPa and 10 hPa levels. The nature of the decadal variability is studied by grouping the events into three decades (1) 1980/81 to 1989/90, (2) 1991/92 to 1999/00 and (3) 2000/01-2009/10. The 'intense major', 'major 1', 'major 2' type events at both the levels are commonly termed as 'major' SSWs and the 'minor' warming events combining of 'intense minor' and 'minor' warmings (Table 3.3 and 3.4). Major and minor warmings with double pulse are also included to quantify the number of warmings. The first set of bar in fig. 3.4a and 3.4b represents the number of major warming from 1980/81 to 1989/90 winter periods at both the levels. The second bar (horizontal dotted) shows minor and the third bar, the quantity of non-stratwarm winters for the same time periods at both the levels. The next set of bar represents the 1990/91-1999/00 and then after the decade 2000/01-2009/10.

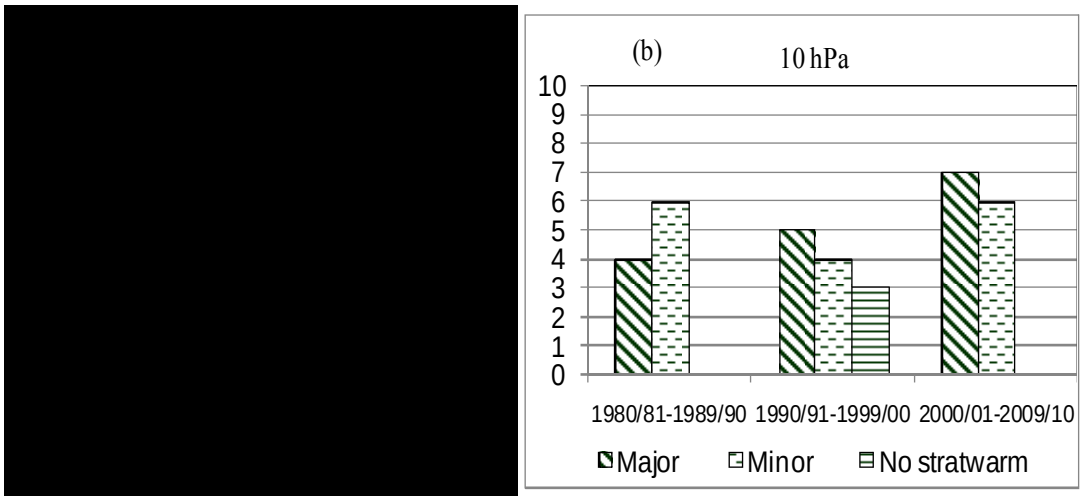

FIG.3.4 Occurrence of major, minor and no stratwarm winters are represented at (a) 2 hPa and (b) 10 hPa levels on decadal scales.

In each decade, major and minor warmings do occur with varying frequency at both the levels. In the first decade (1980/81-1989/90) the occurrence of minor warming shows a slight increase than major warmings. All the winters in the above decade is associated with major and minor warmings. In the second decade 2 hPa levels experienced major and minor except in the winters 1995/96, 1996/97. The winter of 1999/2000 and 2004/05 are also years of non-stratwarm winters at 10 hPa and 2 hPa level. During the third decade, number of major warmings shows slight increase (Fig. 3.4a and 3.4b).

Hence it is found that the maximum major events occurred in the third decade and minimum during the first decade. Regarding the minor warmings, maximum is in first decade and minimum in the last decade. The magnitude of variations is almost same in the second decade. Lu et al. (2008) analysed the decadal scale changes using the Holton–Tan relationship with QBO and NH polar vortex. They reported that the extra-topical QBO changes sign in late winter which results in the occurrence of major stratospheric warming under westerly phase of QBO. Latest study (Schimanke et al. 2011) reported the heat flux is driven from the North Atlantic Ocean and it interacts with the troposphere and stratosphere system, thereby increasing the occurrence of warming events in the stratosphere. The incidence of minor warming events in last decade is also an important point to note. These active perturbations continuously happened in the upper and mid-stratospheric levels.

3.3.3.2. Intra-seasonal variability of stratospheric warming events

The intra seasonal variability of warming events is analyzed. The time of occurrence of SSW is listed into 3 phases of the winter season as December (early winter), January (mid-winter) and February (late winter). Figure 3.5 explains the intensity and occurrence of stratwarms in the above

category at 2 hPa and 10 hPa levels. We included all categories of stratwarm events. The two warming episodes which occurred in the month of March 1992/93 and 2004/05are not included in this analysis as it occurred in the early spring. Intra seasonal variability of the warmings are given below:-

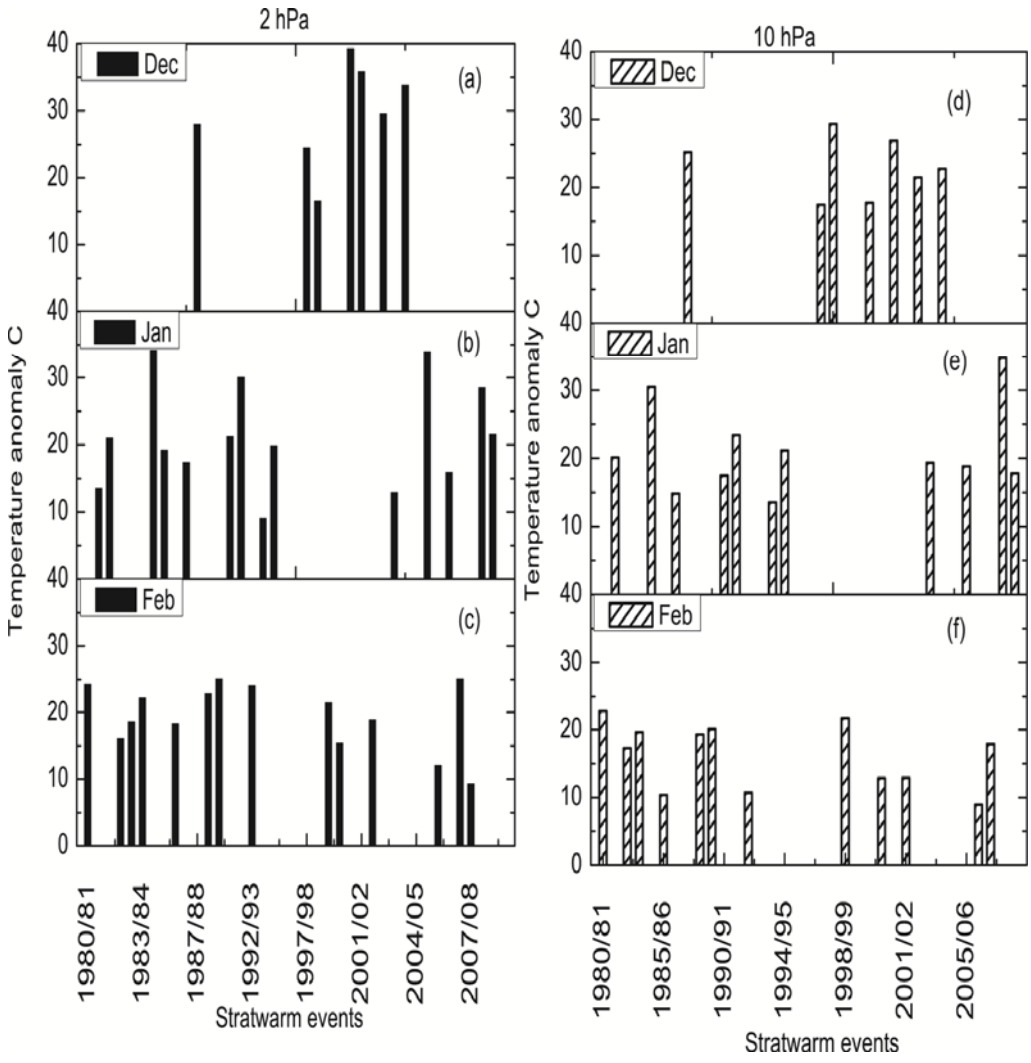

FIG.3.5. Temperature anomalies for the peak day of stratospheric warming events during December, January and February months at 2 hPa (left) and 10 hPa (right) levels for the 30 winter months.

3.3.3.2.1. December (Early winter)

We have plotted the temperature anomalies of the peak days for the December month at 2 hPa (left) and 10 hPa (right) levels (Fig. 3.5a-f). In the first decade only one major stratwarm event is noticed during the early winter period (Fig. 3.5a and 3.5d) and that event observed in 1987/88. The next set of early (December) perturbation is noticed after nine years. An occurrence of early winter warming is noticed in the beginning of the last decade in few winters till 2003/04. They are totally six cases and the corresponding winters are 1997/98, 1998/99, 2000/01, 2001/02, 2002/03 and 2003/04. It is important to note that the intensity of these early warming events is high compared to other winter events of January and February months at both the levels.

On an average, temperature anomaly for the early winter warmings at 2 hPa and 10 hPa levels are 29°C and 22°C respectively. The early stratwarm event of 2000/01 has the highest temperature anomaly of 39°C and it falls in the category of 'Major 1' event at 2 hPa level. The absence of early winter warming event is continued for both the levels after 2003/04 stratospheric warming episode. Hu and Pan (2009) explain that the warming trends in early winter Arctic stratosphere are forced by observed SSTs through changes in atmospheric wave activity.

3.3.3.2.2. Mid- winter (January)

Earlier studies showed the occurrence of stratospheric warming events is more during January and February months (Schoeberl, 1978; Charlton et al. 2007). The same reflects in our study also. Stratospheric perturbations in January had an average temperature anomaly (ΔT) of 20°C (Fig. 3.5b and 3.5e). The intensity distribution of 2 hPa January temperature anomalies is strong with peak values exceed 20°C for 1984/85 and 2005/06

warming events. These two events are 'intense major' warmings at both the levels. The mid-winter stratospheric warming events also show an absence of SSWs during 1994/95 to 2002/03 period. The absence of mid- winter warmings continued for a long period of 8 consecutive winters.

3.3.3.2.3. Late winter (February)

From the distribution of late winter warmings the frequency of warming is once in every three winters. The intensity of the late winter cases is comparatively less at both the levels. The average intensity of late winter warming pulse is 20°C (Fig.3.5c) and 15°C (Fig.3.5d) for upper and mid-stratospheric levels. The absence of warming events is noticed during 1993/94 to 1998/99 period (Fig. 3.5c and 3.5f) at both the levels. Two consecutive late winter warmings are noticed during 1988/89&1989/90 and 1998/99&1999/00 winter periods. The winter 2007/08 also experienced 'intense minor' and 'minor' warming perturbations. But the number of perturbation is almost regular irrespective of small gaps.

Thus it can be concluded the intensity of warmings are high for the events occurring during the early winter period where as the frequency of occurrence is maximum during the mid- winter periods.

1.3.3. Propagation of stratospheric warming systems from upper mid-stratospheric levels

Figure 3.6 explains the composite of temperature (ΔT) and zonal wind anomalies (ΔU) for all the events in the five groups. For the composite analysis we averaged zonal mean temperature and zonal wind anomalies over the region 60-90°N. The time period taken for the composite analysis is 20 days, before and after the peak day from upper to mid-stratospheric levels. The peak days for the temperature and zonal wind anomalies are selected from the Table 3.4.

For ‘intense major’ warmings, we have composited seven events (Table 3.4). The temperature and zonal wind anomalies are greater than 20°C and -50 ms^{-1} in all the cases. In figure 3.6a the temperature anomalies ranges above 25°C along the closed contour from upper to mid-stratosphere around the peak day. This shows that warm anomalies propagate downward with a constant intensity from upper to mid-stratospheric levels. In other words its intensity is not reduced while propagating through different altitude levels. Due to this strong temperature gradient, the mean westerly winds are reversed and thereby easterly wind appeared at upper stratospheric levels. The zonal wind anomalies propagated downward from P-4 day to P+15 day with an intensity of -70 ms^{-1} to -50 ms^{-1}. Even though the temperature gradient is almost equal at both the levels, easterly wind anomaly is higher over upper stratosphere than that the mid-stratosphere. The time evolution of the temperature and easterly wind anomalies shows that it is very intense irrespective of the downward propagation from upper to mid-stratospheric levels.

‘Major 1’ stratwarm cases (composite of 8 events from Table 3.4), the distribution of temperature gradient is almost similar to that of the ‘intense major’ warmings. Though the intensity of temperature perturbations is same they differ in the strength of the wind circulation. The upper stratospheric temperature deceleration is noticed almost five days prior to the onset day (day 0) and it continued after the peak day. The categorization of ‘major 1’ event is such a way that temperature anomaly greater than 20°C and easterly wind anomalies greater than 35 ms^{-1} but less than 50 ms^{-1}. In this case, the intensity and the downward movement of easterly wind anomaly are limited to upper levels (Fig. 3.6b) only. The discrepancy between ‘major 1’ stratwarm cases in Table 3.3 and Table 3.4

depends up on the downward deceleration of temperature and zonal wind from upper to mid-stratospheric levels.

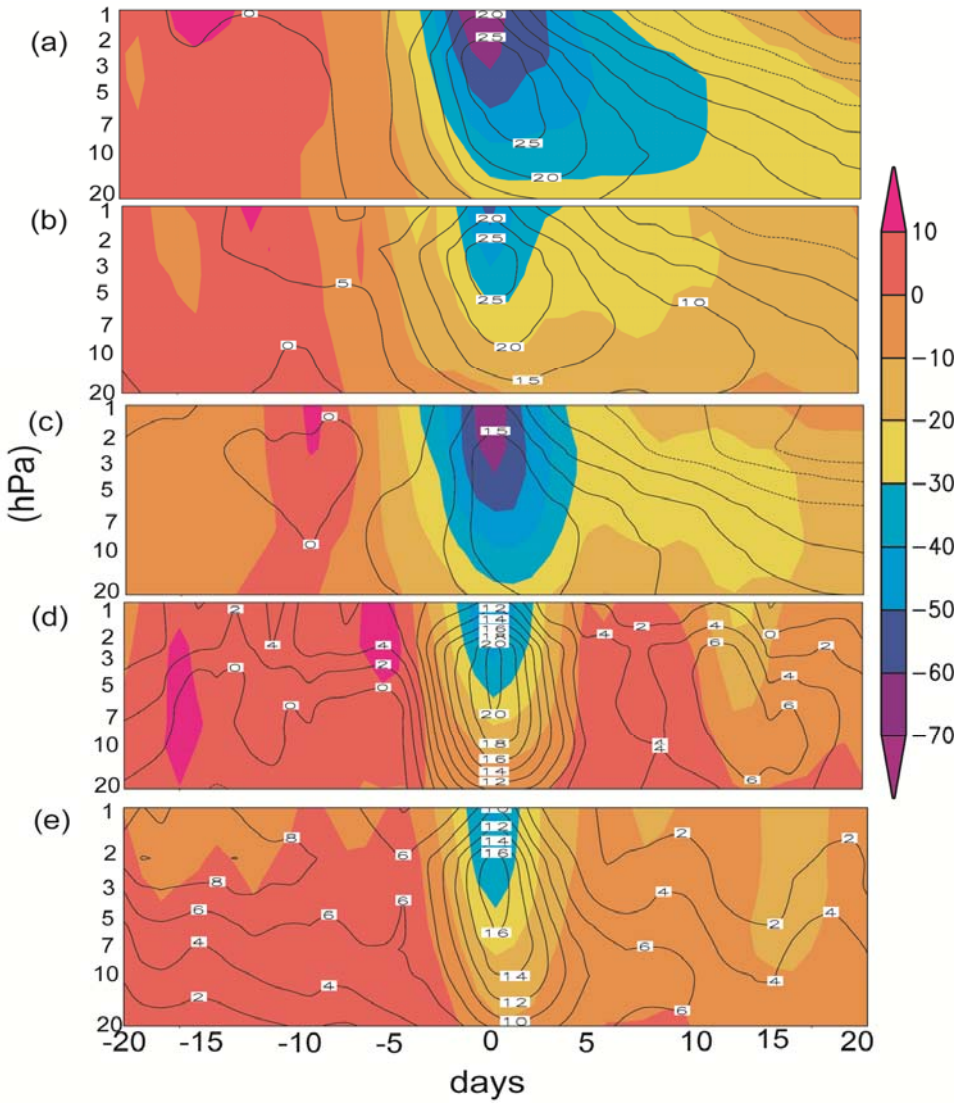

FIG.3.6. Pressure - time cross section of zonal mean temperature (ΔT, contours) and zonal wind anomalies (ΔU, shaded) averaged over 60-90°N during (a) 'Intense major' (b) 'Major 1' (c) 'Major 2' (d) 'intense minor' and (e) 'Minor' warming. The composite analysis is made for the period 20 days before and after the peak of each event.

'Major 2' type stratwarm events show different features than the above two type of events. Figure 3.6c explains the composite anomalies of zonal mean high-latitude (60-90°N) temperature and zonal wind anomalies from the day -20 to day +20 for 'major 2' stratwarm cases. We have composited three 'major 2' type events (Table 3.4). Even though the wind strength is as strong as the 'intense major' warmings (Fig. 3.6a) but the positive temperature anomalies limited 15°C from upper to mid-stratospheric levels. Because of these dual criteria the intensity of warming events differed from upper to mid-stratospheric levels. The easterly wind intensity (ΔU) associated with the 'major 2' event is maxima around the peak day (day 0) of -70 ms^{-1} and above. The strength of easterly anomaly decreased at mid stratosphere with -40 ms^{-1} to -30 ms^{-1} and furthermore its anomalies extends up to P_{+15} days with -30 ms^{-1} to -20 ms^{-1}.

The time evolutions of the 'intense minor' and 'minor' warming events are characterized with less intensified temperature and easterly wind anomalies around the peak days. For the composite analysis, 4 'intense minor'; warmings and 13 'minor' warmings events are used (Table 3.4). The warm anomalies are propagated through the stratospheric levels of 12°C to 15°C for both the cases of stratwarm events and also the easterly wind anomalies are symmetric about the peak day for both the cases. The easterly wind anomalies associated with the 'intense minor' warmigs which generated in the upper stratospheric levels propagate downward (Fig. 3.6d, shaded) after 5 days, these wind anomalies turned as westerlies. A sudden recovery of positive wind anomalies are observed with 'intense minor' warmings. In the case of 'minor' warming events wind anomalies are tend to be in the easterly phase up to around P+20 days.

In each case (Fig.3.6a-e) an intensified easterly wind anomalies are observed at upper stratospheric levels than at the mid-stratospheric levels and the maximum positive temperature gradients are concentrated along the peak days. This section details the reason for the discrepancy between the categorized stratwarm cases in Table 3.3 and 3.4. There are cases where intensity of the warming gains and losses while propagating to downward.

The analysis reveals the presence and nature of downward propagation of warming systems from upper to mid-stratospheric levels.

3.3.5. Variation of warm and cold vortices

The position and intensity of the warm and cold polar vortices during major and minor warming events at 2 hPa and 10 hPa levels are studied. Figure 3.7 illustrates the composite of major and minor stratwarm peak days at 2 hPa (upper panel) and 10 hPa (lower panel) respectively. Here major warming stands for the total of the three groups- 'intense major', 'major 1', and 'major 2'events and similarly the minor warming stands for both the 'intense minor' and 'minor' events.

During the peak of major SSW at 2 hPa the warm core area is characterized by positive temperature anomaly of 0-15°C (Fig.3.7a) over the Polar regions: Northern parts of Siberia and Greenland, covering the eastern and western hemispheres. At the same time, during the minor SSW peak days, the North Pole region is of negative temperature gradient by -15°C to 0°C (Fig.3.7b). The position of the stratospheric warm core area is same for the major and minor warmings. Throughout the stratospheric warming days the large circumpolar vortex moved to middle latitudes. Large cold air transported from vortex into middle latitudes and the number of cold days becomes more intensified especially over Europe, northern Eurasian continent and North America (kolstad et al. 2010).

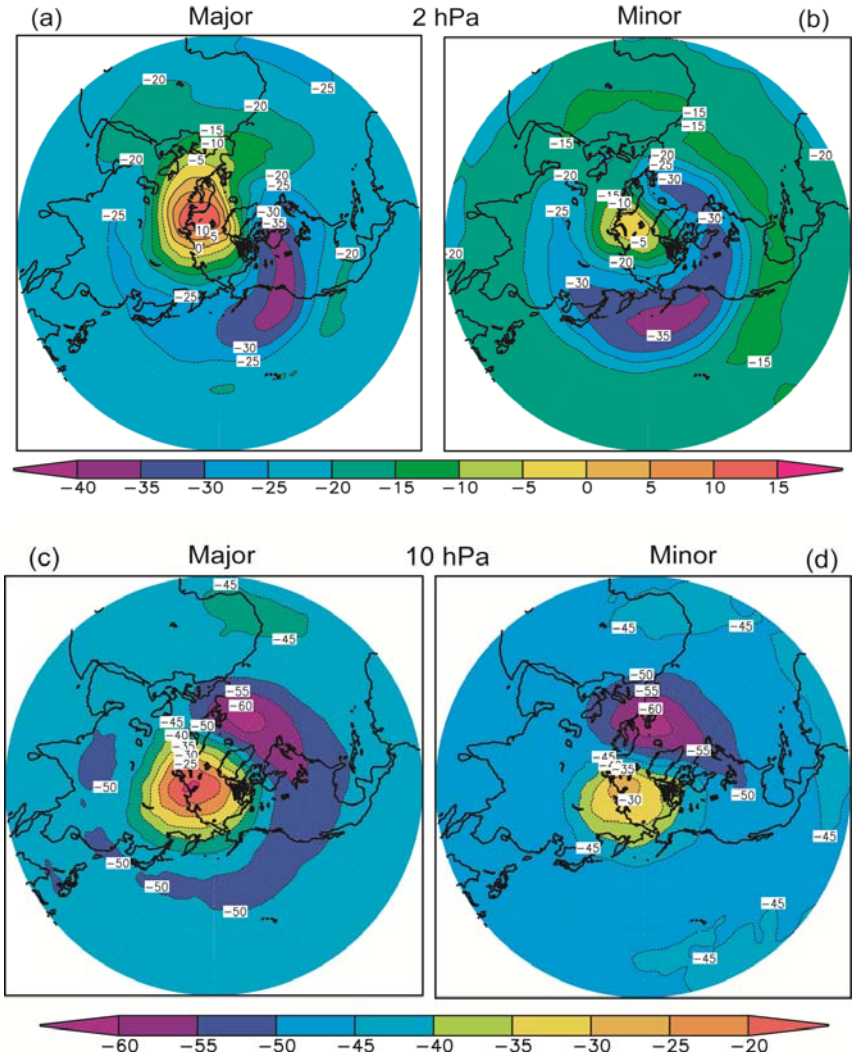

FIG. 3.7. The composite of major and minor stratwarm events during the peak days (a & b) at 2 hPa and (c & d) 10 hPa level.

Warming events are also associated with Negative Arctic oscillation indices. Consequently severe cold polar air reaches into the middle latitudes associated with the displacement of polar vortex from high to mid-latitudes. The mechanism for the coupling between polar vortex and NAO is analyzed by Ambaum and Hoskin (2002). The NAO life cycle is mainly depends on the behavior of the stratospheric polar vortex.

The displaced vortex has temperatures of -30°C to -40°C (Fig. 3.7a) over the longitudinal area 190°W-270°W at 2hPa. For the minor warmings (Fig.3.7b) the intensity of the cold polar vortex is same but the cold vortex position slightly extends more to middle latitudes, covering the eastern and western arctic hemispheres with in a longitudinal extension of 80°E to 360°W.

At mid-stratospheric levels the cold vortex position is slightly different from 2 hPa level. During major and minor warming events the polar vortex at 10 hPa level is dislocated more towards the mid- latitude western hemisphere especially in between 300°W to 360°W. The longitudinal extension area of the dislocated cold vortex is large (Fig.3.7c) during major warming events. Associated with minor warming events the longitudinal area of the vortex extends from 280°W to 360°W. The strength of the cold vortex at 10 hPa level ranges from -50°C to -60°C. But the position of the stratospheric warm area is the same for major and minor warmings at 10 hPa level.

Thus the study reveals that there is uniformity in the location of warm centers during major and minor warmings. But longitudinal extension of cold polar vortices varies.

3.4. Summary and Conclusion

Chapter 3 provides a categorization of the stratospheric warming events into five groups considering 2 hPa and 10 hPa levels as reference altitudes. The ‘intense major’ events at 2 hPa are almost consistent with the warming event at 10 hPa level in almost all cases. The analysis reveals that the major perturbations increased during the 2000-2010 at both the levels. Percentage analysis also shows that almost fifty percentages of the warmings are of major types and other 50% are of minor types. Early

winter warmings are observed regularly during 1997/98 to 2003/04 period. The average temperature anomaly (ΔT) is 30°C for the early winter warming at 2 hPa levels and this is high compared to mid and late-winter warmings. The study brings out the presence of intra-seasonal variability in the intensity as well as frequency of warming events. Stratwarms are not observed during a continuous period of seven years in mid-winter (January) month. The average maximum intensity of late winter warming events is 20°C and 15°C. Downward propagation of temperature and zonal wind anomalies are intense around the peak day irrespective of the groups. Warming systems shows the behavior of downward propagation from upper to mid- stratospheric levels. Composite analysis explains the position and the intensity of the warm vortex at both the levels. It also shows the position of the displaced polar vortex during major and minor stratospheric warming events. There is a shift in the longitudinal location of the cold centers from 180°W-360°W during minor and major warmings at 2 hPa and 10 hPa levels.

Chapter 4

High and Low-Latitude Interaction of Circulation Systems during Early Mid-Winter and Late Winter Stratwarm Events

4.1. Introduction

Sudden stratospheric warming events (SSWs) are observed over the Northern Hemisphere winter stratosphere. Usually major warming events are associated with the displacement of polar vortex from high to mid-latitudes or the splitting of vortices. The displacement or breakup of the polar vortex leads to large volume of polar air being transported from the vortex as narrow tongues (Manney et al. 1994) to mid and low-latitudes (Bencherif et al. 2007). The lower stratospheric winter circulation is also dominated by cold low centered near the pole which becomes more pronounced with increasing altitudes and is surrounded by a band of strong west winds. These winds are distinct from the strong tropospheric westerlies of the lower latitudes.

The sub-tropical westerly jet stream (STJ) is an integral part of the upper-tropospheric circulation over the winter hemisphere. The jet-stream core situated close to 200 hPa surface and has a maximum speed of 70 ms^{-1} as an average (Krishnamurthy, 1960). In its equatorward meanderings the polar night jet sometimes merges with the subtropical jet stream (Louis. 1979). The

maximum intensity of STJ is noted during the late winter month (February). Gerbert et al. (2009) found persistent equatorward shift of STJ during stratospheric warming days while using model experiment over NH. Spatial and temporal variability of fast upper tropospheric wind is analysed by Strong and Davis (2006) and they reported that Arctic Oscillation (AO) and El nino/Southern Oscillation (ENSO) are the leading contributors to surface of maximum wind (SMW) and pressure variability over NH.

Earlier studies (Charney and Drazin, 1961; Holton and Mass, 1976 and Andrews et al., 1987) have shown that sudden warmings are forced from below, possibly due to the upward propagation of planetary wave's activity troposphere to stratosphere. The studies carried out by Fusco and Salby (1999); Newman et al. (2001) and Hu and Tung (2002) have shown the relationship between polar cap temperatures and meridional heat flux. Kim and Choi (2006) found significant correlation between lower stratospheric polar temperatures in March with stationary component of the eddy heat flux on an interannual time scales.

The meridional heat flux analysis is used as a measure of the wave forcing from troposphere to stratosphere (e.g.,Waugh et al. 1999; Newman and Nash 2000; Polvani and Waugh 2004 and Charlton et al. 2007). Most of the planetary wave activity crosses the 100 hPa level between 40 and 80°N (see. e.g., Charlton and Polvani 2007). The increased occurrence of SSWs can thus be related to the poleward eddy heat flux in the lower stratosphere of high latitudes (45-75°N) as shown by Yoden et al. (1999) and Polvani and Waugh (2004). The heat flux is proportional to the vertical component of the quasi geostrophic EP flux. Polvani and Waugh (2004) also showed that the time series of eddy heat flux at 100 hPa exhibits a high anti-correlation with Arctic

Oscillation (AO) index at 10 hPa. According to Karpetchko and Nikulin (2004), November–December averaged stratospheric total eddy heat flux is strongly anti-correlated with the January–February averaged total eddy heat flux in the midlatitude of the stratosphere and troposphere.

In the present study consider two cases each for early (1987/88 and 1998/99), mid-winter (1984/85 and 2008/09) and late-winter (1983/84 and 2007/08) warming events. The composites of the two cases of early, mid and late winter SSWs are analysed separately to understand the atmospheric circulation in the Eastern Arctic domain (0-90°N & 0-180°E). In addition, the intensity of subtropical westerly jet stream and the northward advection of heat flux for high latitudes ranging 45-75°N and low latitudes 0-30°N at mid-stratospheric (10 hPa) and mid-tropospheric (100 hPa) levels are also examined.

4.2. Data and methodology

The NCEP/NCAR reanalysis data (Kalnay et al. 1996) with a horizontal grid spacing of 2.5°×2.5° at 17 levels from 1000 hPa to 10 hPa examine the entire troposphere and lower and middle stratosphere are used in the present study. The variables used are temperature, zonal and meridional winds and geopotentail height. The anomalies are calculated by subtracting the 31 yr averaging of daily values from the geopotential height data at 10 hPa so that the mean annual cycle is filtered out.

Six stratwarm events are selected. These stratwarm events are (1) 1987/88 and (2) 1998/99 (early winter), (3) 1984/85 and (4) 2008/09 (mid-winter), and (5) 1983/84 and (6) 2007/08 (late-winter). Instead of analysing each SSW cases individually we have taken the composite of two cases each

for early, mid and late-winter SSW events. To analyse the intensity of the STJ during stratwarm days, normalized vertical wind shear is computed for the composite of stratospheric warming events. The vertical wind shear is calculated as

$$\frac{\partial V}{\partial Z} = \sqrt{\left[\left(\frac{\partial u}{\partial z}\right)^2 + \left(\frac{\partial v}{\partial z}\right)^2\right]} \quad \text{....4.1}$$

Where, $$\frac{\partial u}{\partial z} = \frac{(u'^{100} - u'^{200})}{dz} \quad \text{....4.2}$$

and $$\frac{\partial v}{\partial z} = \frac{v'^{100} - v'^{200}}{\partial z} \quad \text{....4.3}$$

The notation u' and v' denote the zonal and meridional wind anomaly at 100 hPa and 200 hPa level for ± 20 days around the peak date of each stratospheric warming event. And the anomalies are calculated for latitudinal and longitudinal belt of 25°N-35°N to 100°-180°E. The distance between the two levels dz is metres. The anomalies are normalized by dividing its standard deviation (SD).

Meridional flow of transient heat flux is computed for the domain 0-180°E from equator to pole. The product of meridional wind and temperature anomaly (v't') is calculated during 20 days before and after for each of the six SSW events. The difference in transient heat flux between two adjacent grid points divided by the distance between them is given as $\partial / \partial y(v't')$. The unit of meridional flow of transient heat flux is degree Kelvin per second.

The meridional wind and temperature fields on 10 hPa and 100 hPa pressure levels are used to determine the zonal mean heat flux $[\overline{vT}]$ over high latitudes (45°-75°N) and low latitudes (0-30°N), with brackets denoting a

zonal mean and asterisks a deviation from the zonal mean. Zonal mean values are computed for the longitudinal belt of 0-180°E. The departure from the zonal mean are calculated for each latitude between 45°-75°N around 20days before and after the peak day of each SSWs and the zonal averaged value is weighted by the cosine of the latitude. The unit of total heat flux is °K ms^{-1}. The methodology is assigned in NH low latitudes extending from equator. Correlation coefficient (R) between 10 hPa and 100 hPa heat flux at high and low latitudes are computed. Cross correlation technique is adopted to analyze the lead-lag correlation between 10 hPa and 100 hPa heat flux at high latitudes (45-75°N) and for low latitudes (0-30°N) and respectively.

4.3. Results and Discussion

4.3.1 Circulation and heat flux: Early SSWs

4.3.1.1Geopotential height anomaly for 1987 and 1998 SSWs

Figure 4.1 shows the 10 hPa geopotential height anomalies on the peak day of the two early winter stratwarm events of the year 1987 and 1998. The anomalies are calculated from the period of 1980-2010. An anomalously high geopotential height is observed above North Pole with values greater than 1800 m associated with early winter warmings. The cold polar vortex distorted and substantially displaced from the pole. This warming occurs due to the amplification of zonal wave number 1 planetary wave emanating from troposphere (Baldwin and Dunkerton, 1989). The centre of the shifted polar vortex lies along Date Line (180°E) for December 1987 warming (Fig. 4.1a).

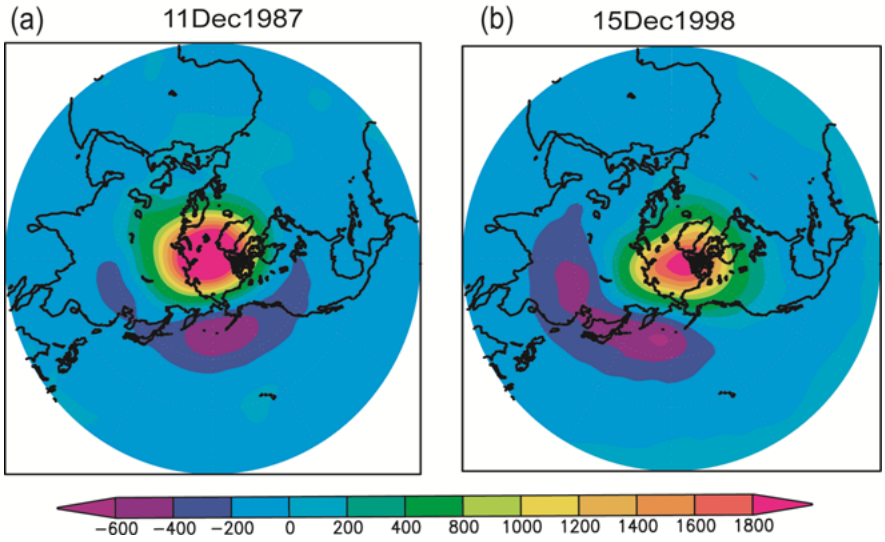

FIG.4.1. Polar stereographic projections of the geopotential height anomalies from the mean period 1980-2010 over North Pole at 10 hPa level on the peak day of two early winter SSW events in (a) 1987/88 and (b) 1998/99.

The winter of 1998/99 is experienced by two pulses of warmings. The first pulse of warming is noticed in the first week of December 1998 and the second in February 1999. It has reported that the evolution of December 1998 stratospheric warming had similarity with that of 1987/88 (Manney et al. 1999).

On 15 December 1998 an elongated shifted polar vortex is noticed in the longitude between 100-180°E (Fig. 4.1b). As the warming intensified geopotential heights are anomalously intensified over the polar region and anomalously low geopotentail height anomalies are observed middle latitudes.

4.3.1.2. Circulation pattern at 200 hPa level and 10hPa geopotential height: Composite of Early SSWs

Figure 4.2 explains the composite fields of circulation pattern at 200 hPa level and 10 hPa geopotential heights (white contour) during stratwarm days. Circulation patterns are illustrated with reference to peak day (P_0). The stratwarm days before the peak day are denoted as P_{-3}, P_{-2}, and P_{-1} day. The days after the peak are denoted as P_{+1} and P_{+2}. The figure illustrates the qualitative relation between upper-tropospheric circulation pattern and mid-stratospheric geopotentail height.

Closed contour loop or low geopotentail values explain the position of displaced polar vortex. The high geopotentail values stand for the stratwarm area. The 200 hPa circulation pattern is dominated by STJ in lower latitudes. At higher latitudes strong downward propagation of wind flow is noticed before, during and after the stratwarm days. A northerly component of wind flows from high latitudes (Fig.4.2b, P_{-3} to P_0) around the longitudes 60-100°E that is coherent with the closed contour of low geopotential at 10 hPa. The intensification of SSW accompanies the descending motion of northerly wind with 20-40 ms^{-1} at 200 hPa. This northerly flow merges with the subtropical westerly flow. During these stratwarm days the path of STJ exhibits a meandering pattern.

The upper tropospheric circulation system shows large amplitude variations associated with the strength of the northern hemispheric stratospheric polar vortex. Baldwin and Dunkerton (1999) reported different features of the propagation of arctic oscillation from stratosphere to

troposphere. The strength of the mid-stratospheric polar vortex followed by coherent changes in the circulation pattern and in turn affects the intensity of subtropical westerly jet stream.

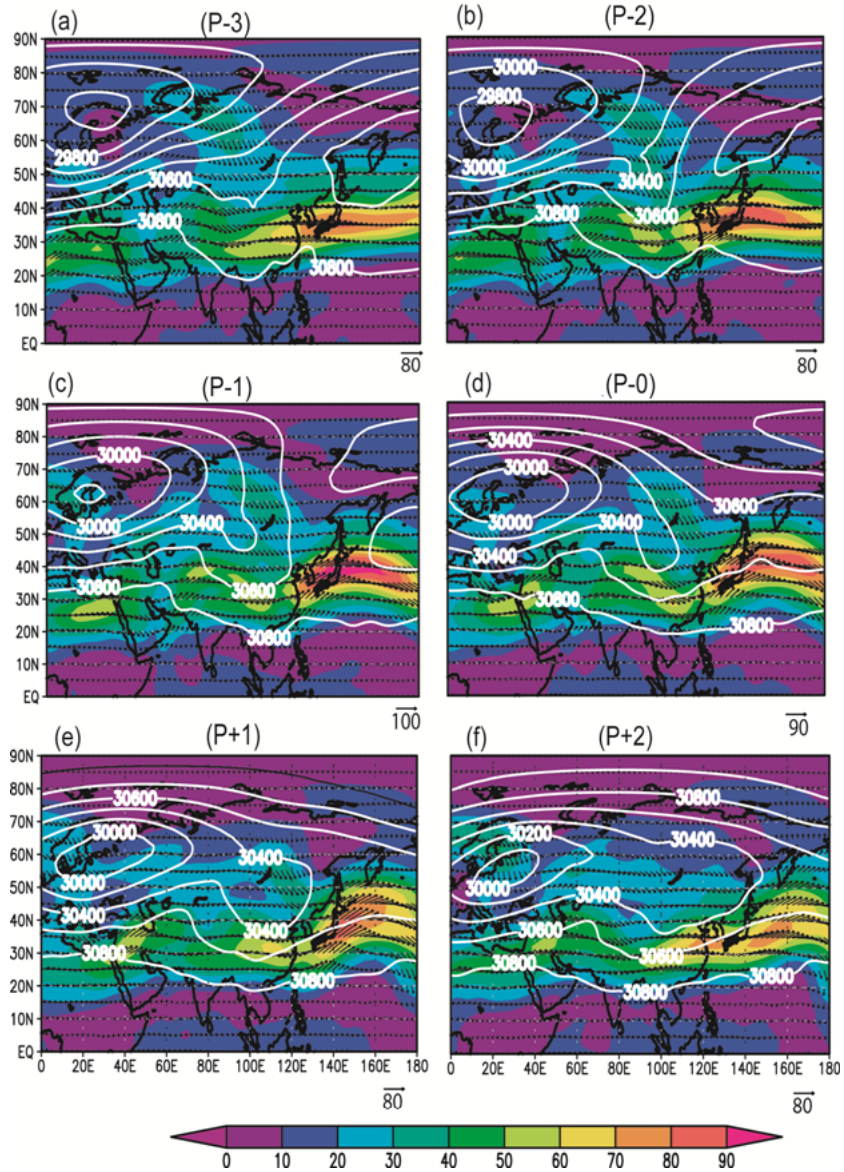

FIG. 4.2a-f. Composite of both the wind vector at 200 hPa level and 10 hPa geopotentail heights (white contour) during two early winter SSWs. The contour interval is 200 m.

Based on this qualitative analysis, during stratwarm days STJ shift its position slightly northward. This shift of STJ is noticed due to the downward movement of northerly flow from high latitudes along the closed contour loop of 3000 m, along cold polar vortex area. The northerly component of the zonal wind component lies in the longitude 60-100°E before the peak day of this December SSW. In these SSWs STJ strengthens and slightly shifts poleward probably due to the northward flow.

4.3.1.3. Vertical wind shear

In this section, the normalized vertical wind shear associated with subtropical westerly jet stream is analyzed. Figure 4.3 shows the composite time series of shear during early (December) SSW in 1987 and 1998 respectively. The time period ranges 20 day before and after the peak day of each SSW.

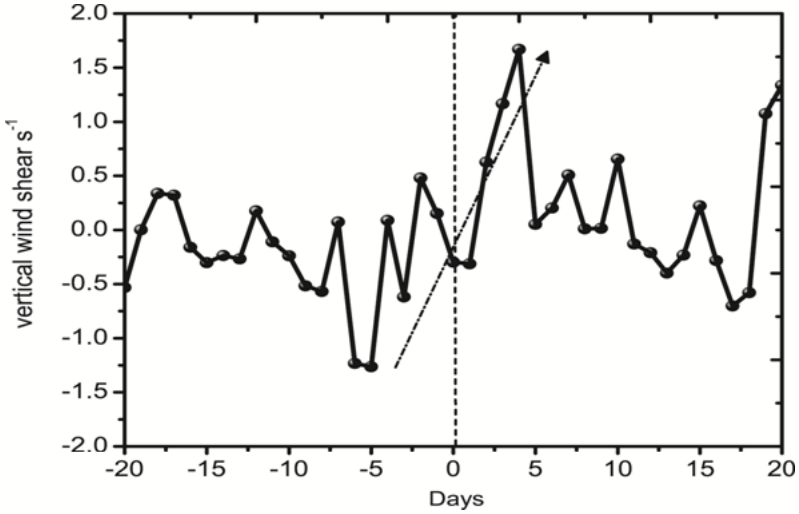

FIG.4.3. Composite of normalized vertical wind shear of the STJ between 100 hPa and 200 hPa level over the area 25-35°N and 100-180°E. The dashed vertical line denote the peak day.

The total shear variations are from -1.5 to 2 standard deviations with highest values on P_{+5} day, which means after the peak day the vertical wind shear is above 1.5 (Fig. 4.3) standard deviations and this shows occurring of large variations in shear during stratwarm days.

The total shear variations are from -1.5 to 2 standard deviations with highest values are noted after the peak day (P_{+5}) and vertical wind shear is above 1.5 standard deviations (See Fig.4.3). Before 5 days of the occurrence of SSW events, the vertical wind shear became the lowest but steeply increased to the peak values on P_{+4} day. The steep rise in vertical wind shear within 10 days is indicated by a dashed arrow in the figure. Zhou et al. (2002) analyzed the response of STJ during propagating and non-propagating stratwarm events and they found the largest fluctuations to occur in North Atlantic region with wind speed maximum over the south side of the jet stream and minimum on the north side of the jet stream. Thus the STJ is disturbed by the intrusion of high latitude air during early winter stratwarm days.

4.3.1.4. Meridional flow of transient heat flux

The latitude- time cross section of transient heat flux at 10 hPa for 1987 and 1998 stratwarm days are illustrated in Fig. 4.4a and Fig. 4.4b respectively. The unit of heat flux is degree Kelvin/second. The duration of this heat flux ranges 10 Days (1-10 December 1987). The significant amount of positive and negative transient heat flux (Fig.4.4a) is observed before the peak day over the latitudes 45°-90°N. This meridional heat flux is originated due to the wave activity prior to the warming and it induces changes in circulation pattern from stratosphere to tropospheric levels. Negligible amount of heat flux variation is observed in the tropics for the entire period.

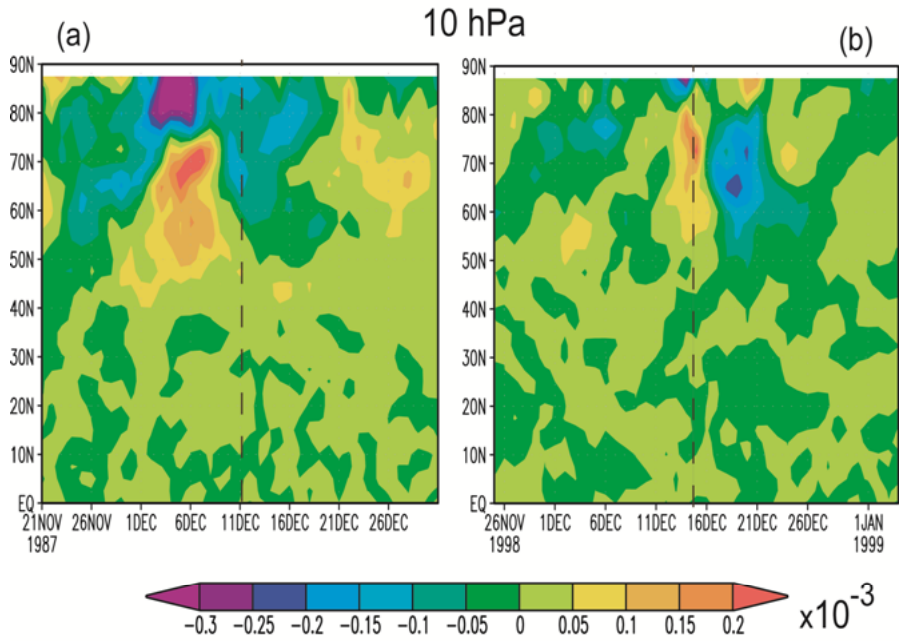

FIG.4.4. Meridional flow of transient heat flux at 10 hPa level during (a) 1987 and (b) 1998 stratwarm event. The dashed vertical line denote the peak day of each event.

Mid-stratospheric transient heat flux is pertinant to the peak day for the December 1998 warming event. The heat flux in December 1998 is comparatively lower than that in December 1987. The poleward advected heat flux shows that high-latitude region (60°-80°N) accompany the highest gradient during stratwarm days.

4.3.1.5. Total eddy heat flux

Figure 4.5 illustrates the composite fields of northward advection of total heat flux during December 1987 and 1998 stratwarm cases at high and low-latitudes. The dashed vertical line denotes the peak days of each SSWs. Prior to the peak day of early winter SSWs the total heat flux steeply increased

from 100-225 °K ms^{-1} (Fig.4.5a, red line) on P_{-15} to P_{-10} days at 10 hPa level and at 100 hPa level heat flux varies 0-40 °K ms^{-1}(Fig.4.5a, black line) for the same time period. After the peak day there is a significant decrease in the amount of northward advected heat flux at both the levels. All these sudden variations in heat flux are noticed from P_{-5} to P_{+15} days (dotted arrow). After the stratwarm event this large amount of heat flux reduced to below the normal values.

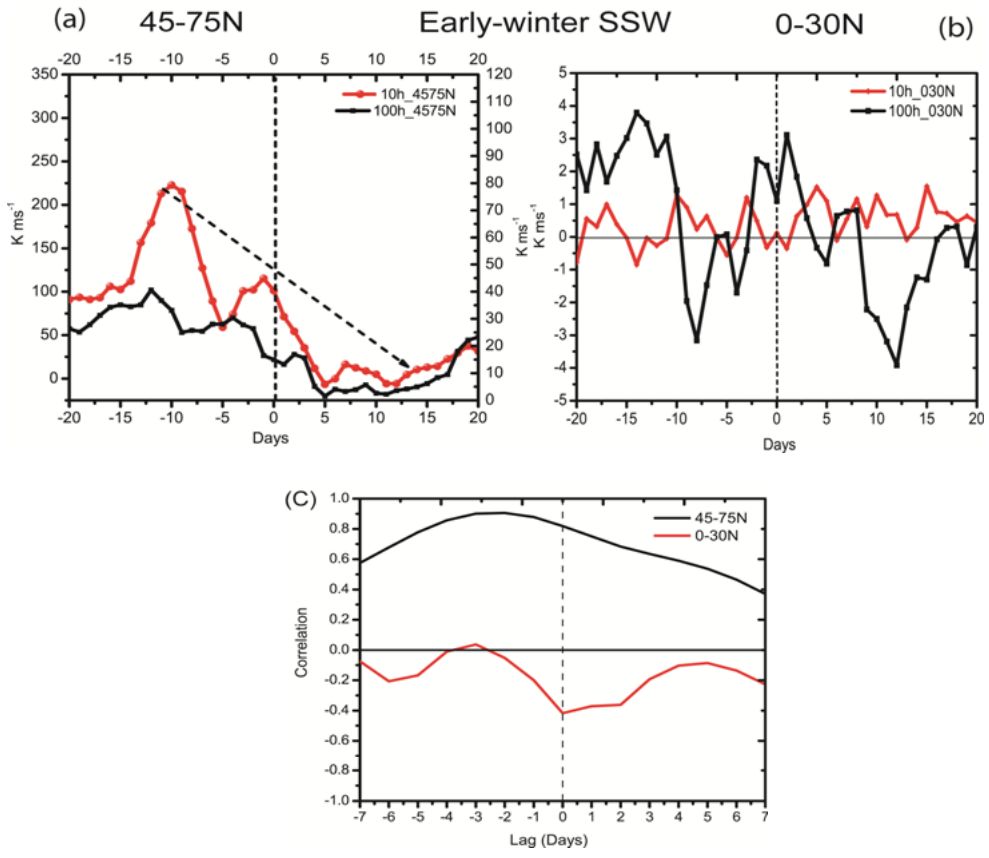

FIG.4.5. Time series of northward advection of heat flux at 10 hPa (red) and 100 hPa (black) for (a) 45-75°N and (b) 0-30°N. The dashed vertical line denote the peak day of each cases.(c) Cross correlation of 10 hPa and 100 hPa heat flux for 45-75°N (black) and0-30°N (red).

Both the time series given in Fig.4.5a are positively correlated with R=0.81 suggesting the variability of 10 hPa and 100 hPa heat flux over 45°-75°N tends to be in phase during stratwarm days. The 100 hPa heat flux has lag correlation of 3-days with that 10 hPa, i.e., it takes three days to reach at 10 hPa (Fig.4.5c, black). The reduced heat flux at 10 hPa level is due to the cut off upward propagating planetary waves from troposphere to stratosphere (Charlton and Polvani, 2007). After the peak day of SSWs easterly circulation prevails in the stratospheric levels. According to Charney and Drazin theorem upward propagating waves cannot propagate through easterly circulation. Hence wave activity is prominent only observed before the peak day of SSWs.

While comparing the mid-stratospheric (10 hPa) and tropospheric (100 hPa) heat flux (Fig.4.4b) over low latitudes, large amount of tropospheric forcing is visible at 100 hPa. Hence both the series shows an out of phase relation throughout the days and it explains negatively correlation (-0.42) with zero lag. The 100 hPa zonal mean heat flux is an input of upward propagating planetary wave energy.

4.3.2. Circulation and heat flux: Mid-winter SSWs

4.3.2.1. Geopotential height anomaly

Figure.4.6 shows the fields of geopotentail height anomaly at 10 hPa level on 2 January 1985 and 23 January 2009 respectively. The stratospheric warming characteristics of both the events and its peak days are mentioned in the previous chapter of the thesis. In both the case the polar vortex is splitted into two (Randel and Boville., 1987 and Harada et al. 2010). The positive geopotentail anomaly is noticed over North Pole covering Greenland and

northern part of Siberia and the displaced polar vortex lies in the longitudinal belt between 180-270°W (Fig. 4.6a).

The stratospheric warming occurred on January 2009 is the strongest and most prolonged event (Manney et al. 2009). On 23 January 2009, the stratwarm area has an elongated shape and cold polar vortex displaced toward the middle latitudes.

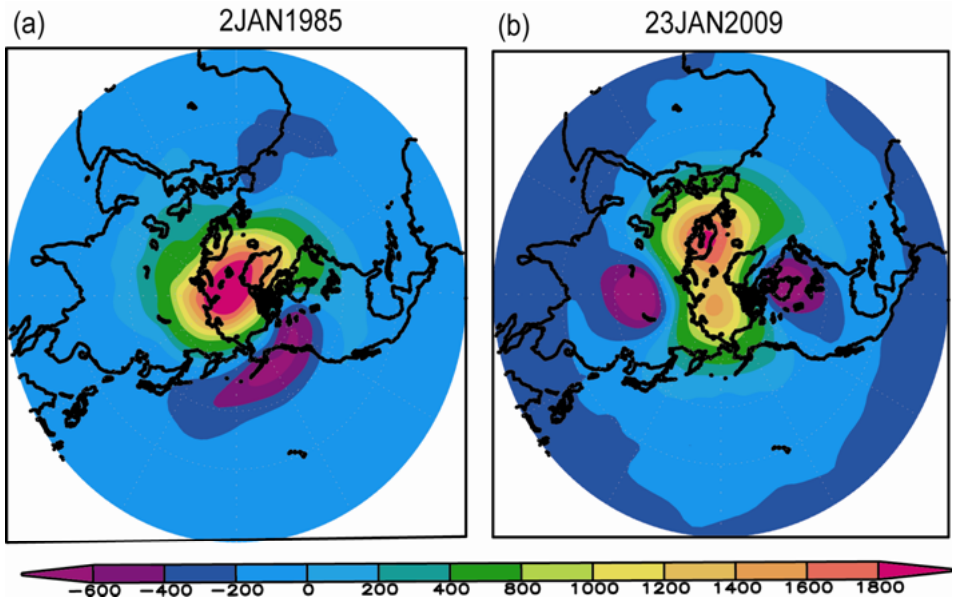

FIG. 4.6. North polar stereographic projections of geopotentail height anomaly at 10 hPa level on the peak day of two mid-winter stratwarm events. (a) 1984/85 and (b) 2008/09.

The location of the displaced or splitted polar vortex is covered large areas of both the eastern and western northern hemisphere (Fig. 4.6b), that mainly covered central Siberia and Canada. These positive and negative geopotential height anomalies have a direct influence on the tropospheric weather and climate.

4.3.2.2. The 200 hPa winds over Eastern Arctic domain and 10 hPa Geopotentail height

Figure. 4.7 reveals the composite flow fields at 200 hPa and 10 hPa geopotentail height during above two mid-winter stratwarm days (2 January 1985 and 23 January 2009). Circulation pattern is represented three day before (P_{-3}, P_{-2}, and P_{-1}) and two day after (P_{+1} and P_{+2}) the peak day. The low latitude regions at 200 hPa are dominated by subtropical westerly flow. The STJ core is located in between 30°-35°N and 120°-160°E which are influenced by the strong north-westerly flow from high latitudes (80°-40°N) during stratwarm days. The descending motion of the northerly wind is negligible along the low geopotentail areas (polar vortex).

The strong gradient between high and low geopotentail can influence the circulation pattern from stratosphere to tropospheric levels. In particular, intrusion of high-latitude circulation to low latitude is not visible in the composite analysis. Waugh and Polvani (2009) simulated the polar vortex disturbed by the Rossby wave 1 breaking, which shows the filaments of vortex air striped from the vortex and stirred in to mid-latitudes. This transport of air can influence the distribution of trace gases in the stratosphere (Plumb, 2002; Shepherd 2007). Stratospheric warming on 2008/09 induces circulation change due to the displacement of the cold vortex. The geopotentail field on P_{+1} and P_{+2} day shows cold polar vortex area (low geopotentail) in the longitude 20°-100°E. The stratwarm core is splitted into two distinct areas along Greenwich meridian and Date line. After the peak day the displaced cold vortex area and stratwarm regions again intensified (Fig. 4.7f). The easterly circulation at low latitudes (equator to 20°N) is unaffected by the high-latitude circulation changes during stratwarm days.

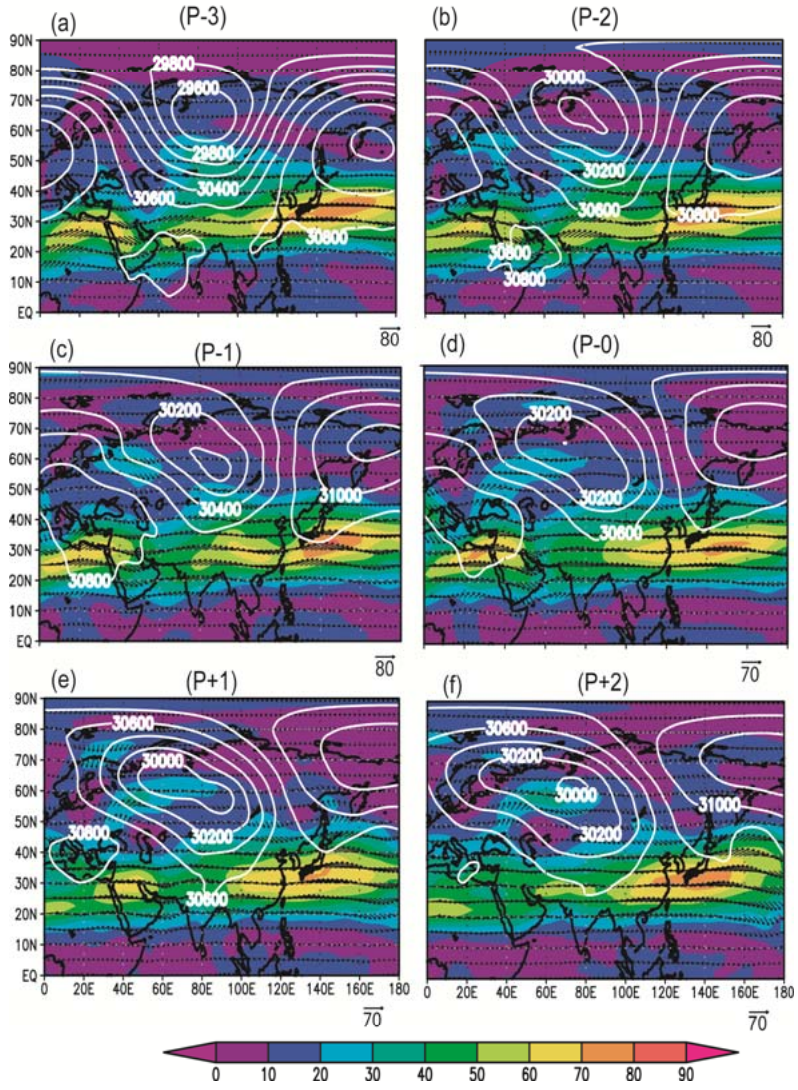

FIG.4.7. Spatial distribution of 200hPa winds during mid-winter stratwarm days and the white contour line indicates 10 hPa geopotential heights. The contour interval is 200 m.

4.3.2.3. Vertical wind shear

Two mid-winter stratwarm events and its influence on subtropical westerly jet stream are studied in this section. The zonal and meridional wind anomalies are calculated 20 days before and after each SSW. We have made the composite of vertical wind shear for the above time period on mid winter SSWs (January 1985 and 2009) is taken for the grid for the grid 25-35°N and 100-180°E. Results showed that during both the mid-winter events STJ appears to be fluctuated with reference to peak days. The normalized total shear on P_0 day is found to be -1.25 standard deviation.

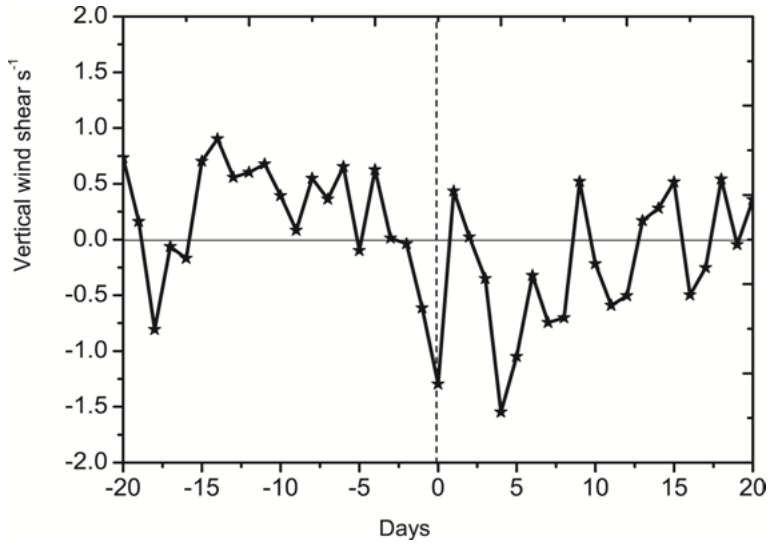

FIG.4.8. Normalized vertical wind shear between 100 hPa and 200 hPa during mid-winter stratwarm events. The dashed vertical lines denote the peak day of each SSW.

This sudden variation in the amplitude is due to the influence of high latitude north westerly winds, originated from the displaced middle latitude polar vortices. The intrusion of cold air during these two events are found to be

less prior to the peak day of warming (Fig. 4.8). In the case of 2008/09 SSW events the zone of maximum amplitude in wind shear is noticed from 17 to 23 January 2009. It indicates that the vertical wind shear become stronger before the peak day of SSW.

4.3.2.4. Meridional flow of transient heat flux: 1984/85

To examine the meridionally advected heat flux in the longitudinal sector of 0°-180°E, we considered the product of meridional wind and temperature anomaly at 10 hPa level (Fig.4.9).

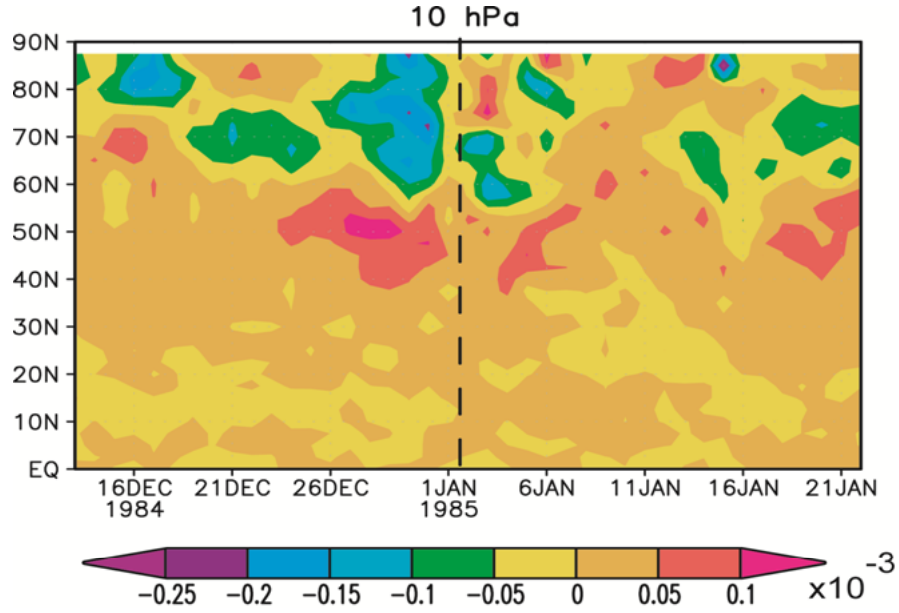

FIG.4.9. Latitude-time cross section of meridionally advected heat flux at 10 hPa for the period of 13December 1984-22 January 1985. The dashed line indicates the (2 January 1985) peak day.

In the eastern arctic domain it can be seen that negative heat flux of -0.1 to -0.2 °Ks^{-1} (polar vortex) in the latitudinal belt of 60°N-90°N. And mid-

latitude region has the positive heat flux of 0.1 °Ks^{-1}. The dominant pattern of heat flux is noticed from 40°N to 90°N. This gradient in heat flux is due to the enhancement of planetary wave activity during stratwarm days.

4.3.2.5. Meridional flow of transient heat flux: 2008/09

The mid-stratospheric meridional transient heat flux is computed for the eastern arctic domain (0°-180°E) during 2008/09 stratwarm days and is shown in Fig 4.10.

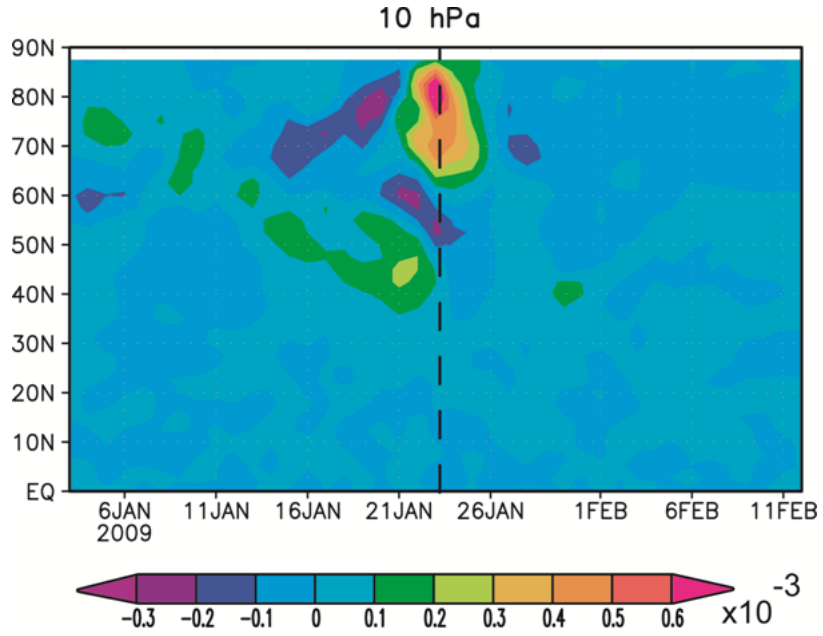

FIG.4.10. Latitude-time cross- section of meridionally advected heat flux at 10 hPa for the period of 03January -12 February 2009.

Magnitude of heat flux varies from minimum (-0.3×10^{-3} °Ks^{-1}) to the maximum is (0.6×10^{-3} °Ks^{-1}). These variations take place around the peak days. Significant amount of high and low heat flux is observed at high-latitudes with in a period of 10 days. The Positive heat flux is extended from 90°-60°N. This

gradient in heat flux at high latitudes indicates the wave activity. Before the onset of stratwarm, the westerly vortex interacts with the flux of planetary wave activity in the stratosphere. Due to this stratospheric vortex is preconditioned and sufficiently strong (e.g., Labitzke 1981; Butchart et al. 1982; McIntyre 1982; Baldwin and Dunkerton 1999, 2001 and Limpasuvan et al. 2004). This factor induces meridionally driven circulation in accordance with the onset of mid-winter warming. The transient heat flux anomalies are negligible after the occurrence of warming over high latitudes.

4.3.2.6. Total eddy heat flux: Mid-winter SSWs

The northward advected total heat flux at 10 hPa and 100 hPa around ± 20 days at high and low-latitudes are shown in Figure. 4.11a and 4.11b. The dashed vertical line represents the peak day. Figure 4.11c show the cross correlation results between 10 hPa and 100 hPa heat flux at high latitudes (45-75°N) and the same for low-latitudes. Over high-latitudes large amount of heat flux about -50 to 250 °K ms^{-1} is noted prior to the peak day at 10 hPa (Fig.4.11a, red) and it is a coherent pattern with 100 hPa heat flux (Fig.4.11a, black). The mid- tropospheric (100 hPa) flux ranges 0- 65 °K ms^{-1} and it had a lead correlation of five days with that 10 hPa. It shows that the signatures of wave activity five days before the onset of stratwarm at 100 hPa level. This large increase in heat flux begins on P-5 day and reaches its normal value on P_{+10} day (Fig.4.11a dotted arrow). So the pattern explains that it takes a period of 15days for the strengthening and reduction of heat flux during stratwarm days.

Both the heat flux at 10 hPa and 100 hPa had a positive correlation with a moderate correlation coefficient of 0.038. The heat flux is directly

proportional to the planetary wave activity. Hu and Tung (2002) found the vertically coherent pattern of wave number 1 amplitude at different lower stratospheric levels on inter annual time scales over high latitudes. The climatological mean of eddy heat flux at lower stratosphere (Hood and Soukharev. 2003) is very negligible in summer hemisphere due to easterly circulation and amplitude of eddy heat flux is found to be more in January in NH and in September- October in the SH.

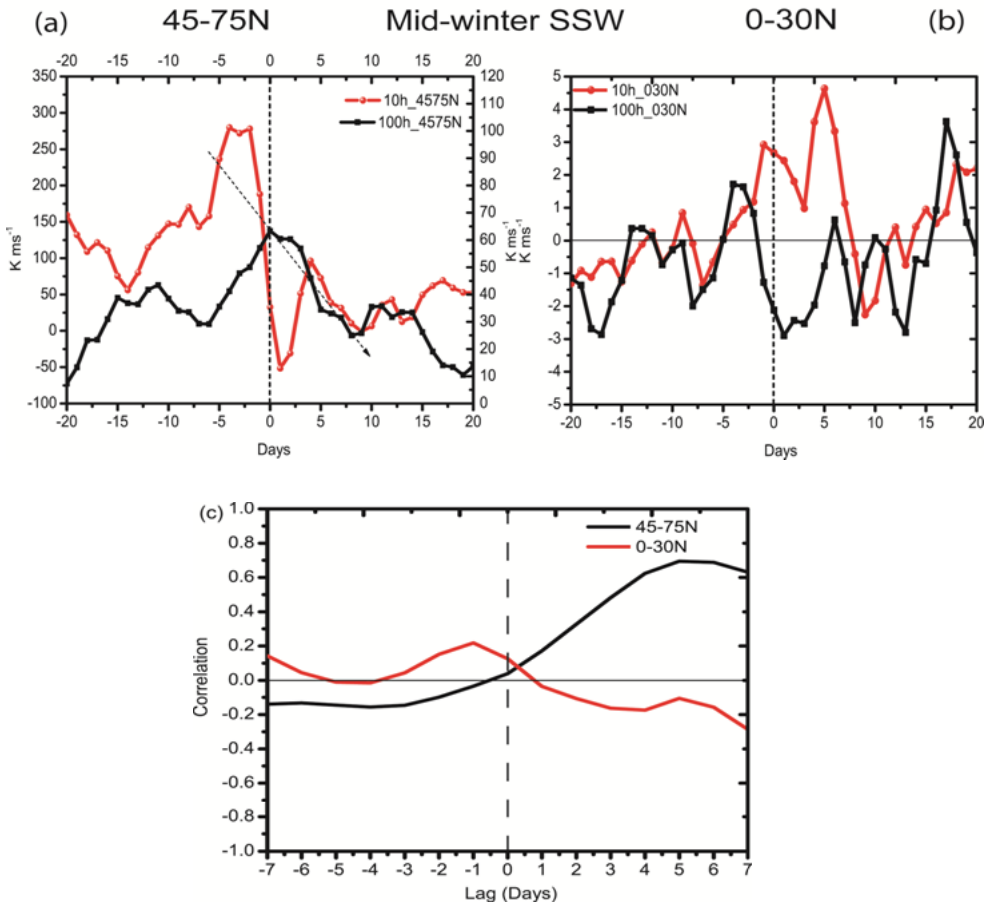

FIG.4.11. Time series of northward advection of heat flux at 10 hPa and 100 hPa for high (left) and low latitudes (right). The dashed vertical line denote the peak day. (c) Cross correlation of time series in fig 4.11a (black) and in fig.4.11b (red). Days with negative sign indicates 100 hPa heat flux lags with 10 hPa and positive indicate lead.

The low-latitude heat flux (Fig.4.11b) at 10 hPa and 100 hPa shows an out of phase relation after the establishment of SSW over high-latitudes. The in phase relation between heat fluxes for the above two levels, leads to an out of phase relation during the peak day. And it starts from P_{-1} day to P_{+10} day. For the high and low-latitudes on P_{-5} to P_{+10} day is very crucial. The total heat flux over low latitude varies from -3 to 4.5 °K ms^{-1}. Here both the heat fluxes are positively correlated (0.12) with maximum lag of one day.

4.3.3. Circulation and heat flux: Late-winter SSWs

In this section we are focused on two late winter stratospheric warming events and its influence on circulation pattern at 200hPa level, intensity of STJ and total heat flux over high and low latitudes. The composite analysis is carried out for the events in February 1884 and 2008.

4.3.3.1. Geopotential height anomaly

Figure 4.12.explains the geopotentail height anomaly on 24 February 1984 and 23 February 2008. Stratwarm areas are represented interms of geopotential height anomaly. The amplitude of geopotential height over North Pole varies in the range 1000- 1400 m during the peak day of both the event. The stratwarm core is concentrated above North American region and Greenland on 24 February 1984 (Williams. 1988). The displaced cold vortex is moved to mid-latitudes covering Siberia and North Atlantic Ocean. The time evolution of 2007/08 stratospheric warming is described by Alexander and Shepherd (2010). This late winter warming on 24 February 2008 is preceded by few minor warmings like in late January 2008, and followed by warmings in February 2008.

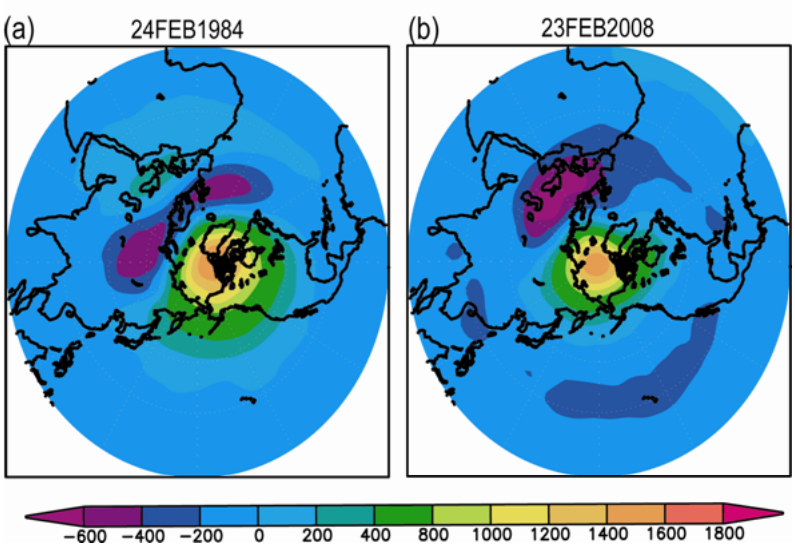

FIG.4.12. Geopotentail height anomaly at 10hPa on the peak day of Late-winter stratwarm events. (a) 1983/84 and (b) 2007/08.

4.3.3.2. Circulation pattern over Eastern Arctic domain at 200 hPa Level

Figure 4.13 shows the qualitative relation between 200 hPa zonal wind and 10 hPa geopotential heights for the period of late-winter warmings. The composite fields of geopotential height explain the position of cold vortex at high latitudes and the longitudinal extension of the low geopotential area remains 0-120°E. The intensification of the stratwarm leads to widening of the cold vortex area in to low-latitudes. The composite field of circulation shows northerly flow from high latitudes. This northerly flow composed with cold polar air from high latitudes. During stratwarm days these air flows are from high to low-latitudes, then merges with STJ in midlatitudes. The intrusion of

cold polar air is coherent with the low geopotential area and it is visible on P-3 day. After the peak day this coherent pattern is evident on P_{+1} and P_{+2} days.

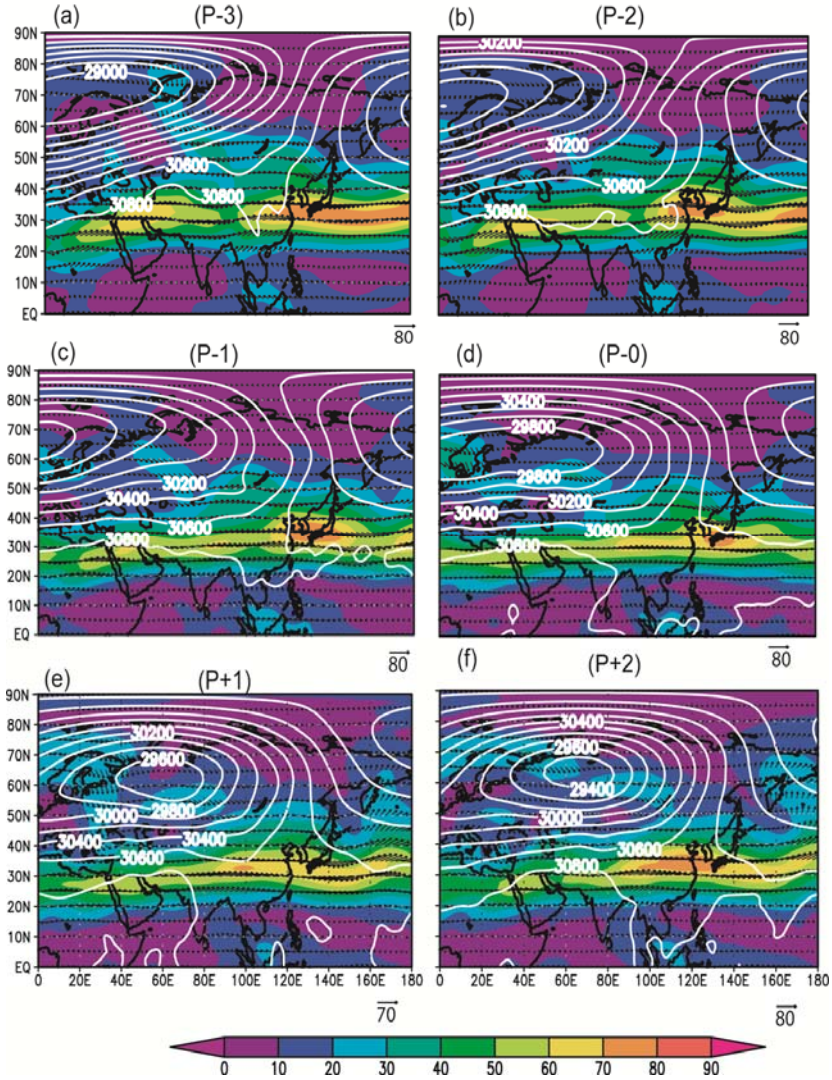

FIG.4.13. Temporal evolution of the average of two late winter SSW events. The circulation pattern at 200 hPa and 10 hPa (white contour) geopotentail height. The contour interval is 200 m.

4.3.3.3. Vertical wind shear

Figure 4.14 illustrates the vertical wind shear calculated between 25°-35°N and between pressure levels 100 hPa and 200 hPa in the longitudinal belt of 100°-180°E. The time period taken for the calculation is ±20 days before and after the SSWs in late winter. Composite of total wind shear shows that the strength of STJ is fluctuated about 1.5 to -1.4 s.d prior to and after the SSW. During these days, the amplified wind strength is observed with 1.5 s.d on P-5 day. The dotted line indicates the variation in STJ with in a period of P-5 to P+15 days.

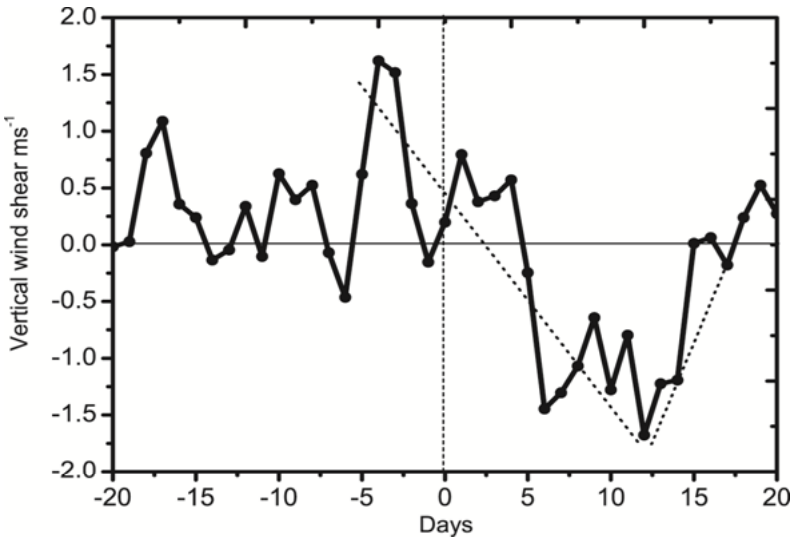

FIG.4.14. Standard deviation of vertical wind shear between 100 hPa and 200 hPa during late-winter stratwarm. The dashed vertical lines denote the peak day.

The transport of high-latitude air to mid-latitude is very pronounced before (Fig.4.13a) and after (Fig.4.13e and f) late winter stratwarm event which intensifies the STJ. Final warming events can influence the large scale

circulation pattern and this circulation had a coherent pattern with the polar vortex breakdown (Black et al., 2006).

4.3.3.4. Meridional flow of transient heat flux: 1983/84

Figure 4.15 displays the latitude-time cross-section of meridional heat flux at 10 hPa. The winter of 1983/84 exhibited minor warming in the mid-stratosphere on 6 February 1984. This minor warming is not accompanied by wind reversal. Corresponding to the minor warming on 6 February 1984, positive and negative heat flux (first dashed elliptic) are observed. While analysing the meridional transport of heat flux (Fig. 4.15), high and low values of heat fluxes are alternatively observed in the mid-stratosphere. These variations are observed at high-latitudes up to first week of March 1984.

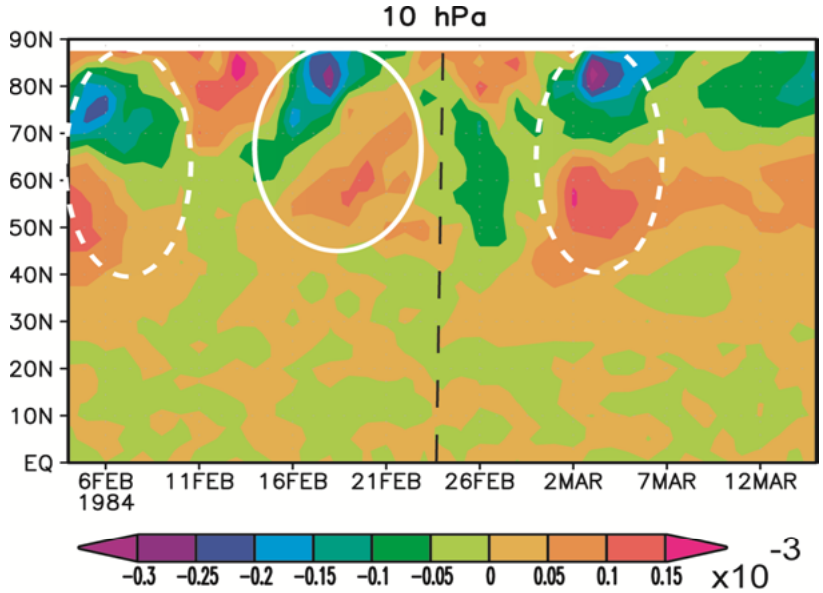

FIG.4.15. Latitude-time cross- section of meridional heat flux ($°Ks^{-1}$) at 10 hPa during 1983/84 late winter stratospheric warming. The dashed vertical lines denote 24 February 1984.

During late winter major warming on 24 February 1984 the heat flux varies of the order of about -0.3×10^{-3} to 0.1×10^{-3} $^{\circ}Ks^{-1}$ (solid circle). After the major event the polar vortex regains its strength within a short time. The winter ended with another pulse of warming in the first week of March 1984 and the corresponding heat flux variation is indicated by second dashed elliptic.

4.3.3.5. Meridional flow of transient heat flux: 2007/08

Meridionally advected transient heat flux for the late-winter stratwarm event in 2007/08 is represented in Fig.4.16 in 2007/08.

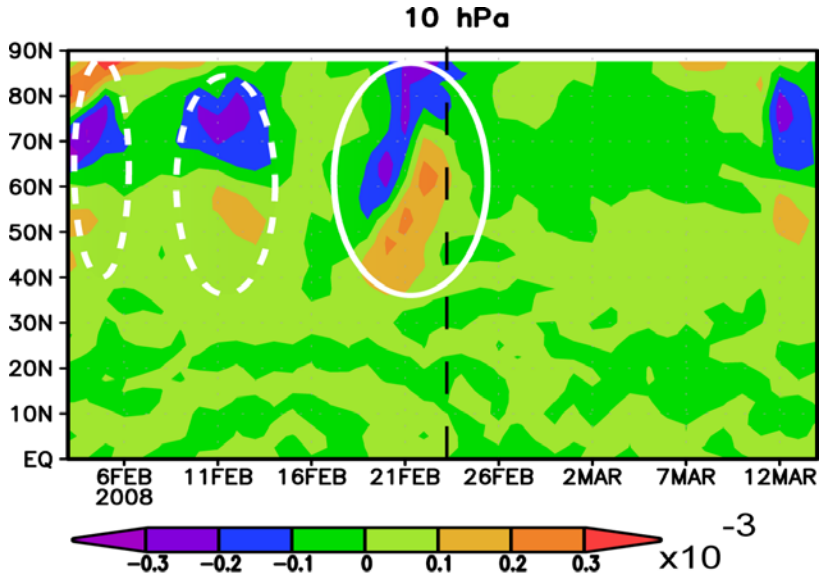

FIG.4.16. Poleward transient heat transport at 10 hPa during 2007/08 stratospheric warming. The time period is from 3February to 14 March 2008. The dashed vertical lines stands on 23 February 2008.

The mid-stratosphere is disturbed and temperature started to increase by early February. Minor warming pulses are noticed on 6 and 16 February 2008, followed by major warming on 23 February 2008. Related to the minor warmings events, positive heat flux 0.2×10^{-3} to 0.3×10^{-3} $^{\circ}Ks^{-1}$ (marked as

dashed elliptic) is noticed about 50°N and negative flux ranges -0.1×10^{-3} to -0.3×10^{-3} $^{\circ}Ks^{-1}$. These enormous heat fluxes can alter the meridional temperature gradient from pole to equator and thus changes the mean westerly wind to easterly in accordance with the onset of warming in the stratospheric levels. The heat flux anomalies are due to the wave activity within a short period of time and downward propagation is stagnant.

4.3.3.6. Total eddy heat flux

Figure. 4.17a and 4.17b show the composite field of northward advected heat flux during two late-winter stratwarm events at high and low-latitude. The cross correlation between 10 hPa and 100 hPa heat fluxes at high latitude and for low-latitudes is given in Fig. 4.17c. From Fig.4.17a (red line) it is clear that high-latitude total heat flux shows strong amplitude on P_{-10} day ranging 0-250 $^{\circ}K\ ms^{-1}$ and it is decreased on P_{+10} day (dotted arrow). This largest amplitude variation of heat flux arises due to the presence of minor warming in both the cases. As explained in Fig. 4.15 and Fig.4.16 minor warming does have the prominent heat flux.

The tropospheric heat flux varies from 0-100 $^{\circ}K\ ms^{-1}$ (Fig 4.17a. black solid line) at high latitudes. While comparing the 100 hPa heat flux over high latitude with early and mid winter stratwarm cases in section 4.3.1.5 and 4.3.2.6, this late winter heat flux shows the maximum amplitude. The moderate correlation coefficient of 0.15 shows the lead correlation of 6 days with 10 hPa level. The 100 hPa signal of positive heat flux is noted 6 days prior to the signal at 10 hPa. Haklander et al (2007) computed the correlation coefficient between 100 hPa heat flux and meridional heat flux from 1000 hPa to 1 hPa in

the latitudinal belt 20°N-90°N. He found significant positive correlation coefficient 100 hPa with poleward eddy heat flux.

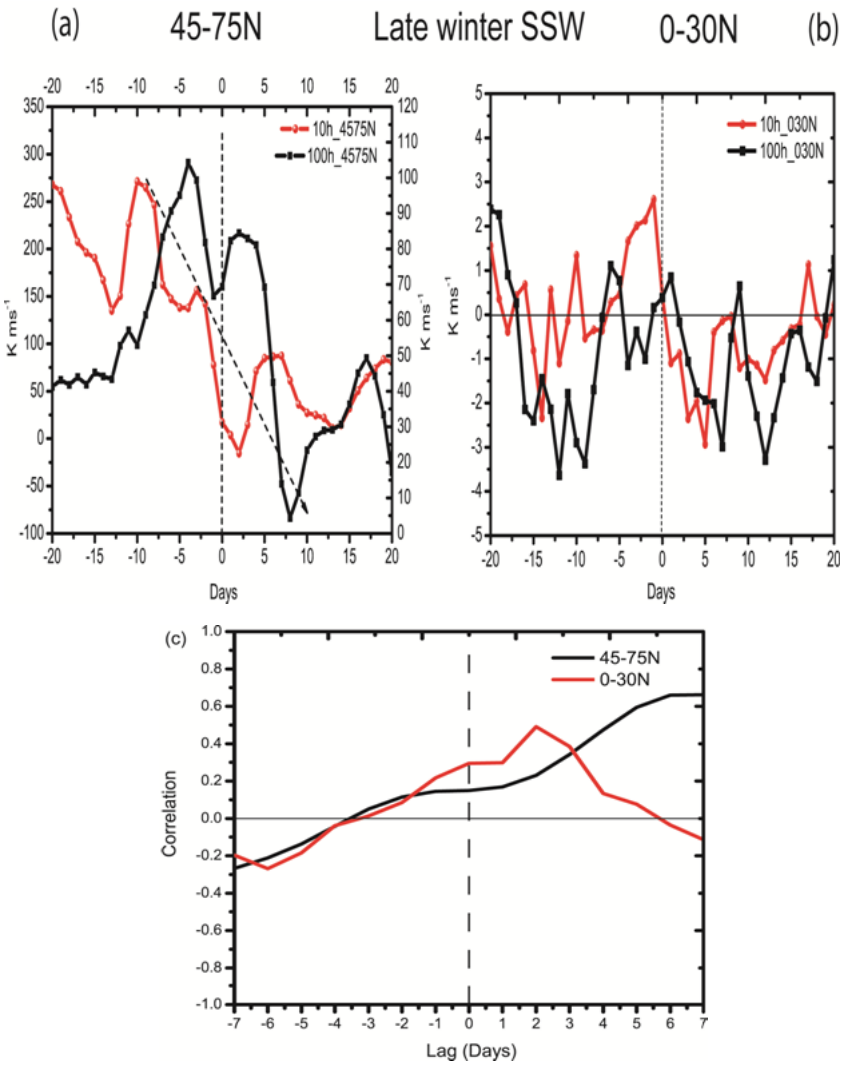

FIG.4.17. Time series of northward advection of heat flux at 10 hPa and 100 hPa for high (left) and low latitudes (right) respectively. The dashed vertical line denote the peak day.(c) cross correlation with 10 hPa and 100 hPa heat flux over high latitude and the same for low latitudes. Days with positive sign indicate lead correlation of 100 hPa with 10 hPa and negative for lag correlation.

Low-latitudes heat flux shows an out of phase association just before the peak day (Fig.4.17b). The amplitude of heat flux ranges -3.5 to 3 °K ms^{-1} and it shows a positive correlation of 0.29. The mid-tropospheric heat flux has a lead correlation of 2 days with 10 hPa which explains that the wave activity starts at 100 hPa two days before then it reaches at 10 hPa level. Table 4.1 summarizes the lead lag correlations during each stratwarm event.

ABLE. 4.1. Cross correlation results of heat fluxes between 10 hPa and 100 hPa levels over high (45°-75°N) and low (0°-30°N) latitude.

Type of SSWs	High latitude (45°-75°N)	Low latitude (0°-30°N)
Early	3 day lag	Zero lag
Mid	5 day lag	One day lag
Late	6 day lead	Two day lead

4.4. Summary and conclusion

The study reported in this chapter addressed the circulation pattern in the Eastern Arctic domain using composite analysis of two cases each for early, mid-winter and late-winter stratospheric warming events. For each stratwarm case, ±20 days (around the central date) are considered for the calculation. Consistent patterns are found between 10 hPa geopotentail height contours and 200 hPa circulation pattern during the above selected cases. This qualitative analysis explains that intense north-westerly wind flows from high to mid-latitudes around the peak days of SSWs through the low geopotential area (displaced cold polar vortex from North Pole). The north-westerly wind

merges with subtropical westerly jet stream (STJ) at mid-latitudes. As a result, significant amount variation is observed in the subtropical jet stream during stratwarm days. That shows an intensification of STJ is associated with the air from the cold polar vortex. Normalized vertical wind shear explains the intensity of STJ is prominent on P_{-5} to P_{+5} day for early and mid winter cases, and maximum perturbation is noticed during late winter case from P_{-5} to P_{+15} days with an increase of 1.5 standard deviation prior to the warming.

Meridionally advected heat flux is computed for each stratwarm cases for the longitudinal sector 0-180°E at 10 hPa level. Positive and negative heat flux show the perturbed wave activity associated with each cases. Negligible amount of variation is observed from equator to mid-latitudes during stratwarm days and maximum amount of variation is concentrated over high-latitudes (45°-75°N). The strongest meridionally advected transient heat flux is seen in 2008/09 stratwarm event. That explains the most perturbed wave activity is over high-latitudes and it getting reduced at mid-stratospheric level after the onset of stratospheric warming.

Total heat flux analysis over high-latitude is also shows prominent wave activity prior to the peak day of each warming at 10 hPa and 100 hPa levels. This feature is in accordance with the observation by Charlton and Polvani (2007). Maximum heat flux is noted at 10 hPa level over 45°-75°N during the composite of mid and late winter stratwarm events compared to early winter cases. The mid tropospheric (100 hPa) heat flux over the same area are correlated, with coefficients is of 0.82, 0.038, 0.15 respectively for early mid and late winter cases.

Low-latitude heat flux analysis shows enhancement of heat flux after the peak .i.e., after the onset of SSW over high latitudes. Mid-tropospheric and stratospheric heat flux shows an out of phase relation during the peak days. The cross correlation analysis between 10 hPa and 100 hPa heat flux over high latitude shows a lag correlation of 3 day, lead correlation of 5 day and also lead correlation of 6 day respectively for early, mid and late winter stratwarm events. Over low-latitudes cross correlation shows zero lag, lag of one day and lead of two days for above three events respectively.

Chapter 5

The Coupling between Polar and Tropical Stratosphere during Intense Major Warming events with Special Emphasis on Indian regions

5.1. Introduction

Sudden stratospheric warming (SSW/stratwarms) is one of the most dynamic aspects of the high-latitude regions during winter. The Thermal structure of both the tropical and subtropical stratosphere is also influenced by the dynamics of SSW. Tropical stratosphere is found to undergo a slight cooling in association with high-latitude warming. The observation on a tendency of the low latitude stratosphere to cool during SSWs is first reported by Reed et al. (1963) and then supported by Julian and Labitzke (1965). They analyzed the polar temperature increase and tropical cooling of the tropical stratosphere up to a latitudinal belt of 35°N to 10°N. The data derived from Nimbus satellite clearly illustrated the global extent of this cooling effect (Fritz and Soules 1970) as shown in Figure 5.1. The deviation of average latitudinal radiance [m $W.m^{-2}$ $(ster)^{-1}$ $(cm^{-1})^{-1}$] from a finite Fourier-series fit for 80°N-80°S from 14 Apr, 1969 to 13 Apr, 1970. The figure is adapted from Fritz and Soules, (1972) and they have used the data from one channel centered at 669.3 cm^{-1} in the 15-μm band of CO_2. The energy in this channel comes mainly from the stratosphere and indicates changes in weighted temperature of the upper 100 hPa of atmosphere. The seasonal variations of outgoing radiance for the period from mid-April, 1969 to mid-March, 1970 are presented for latitudes from

80°N to 80°S. The latitudinal and seasonal variations are removed and the residual variations are discussed as a function of time and latitude.

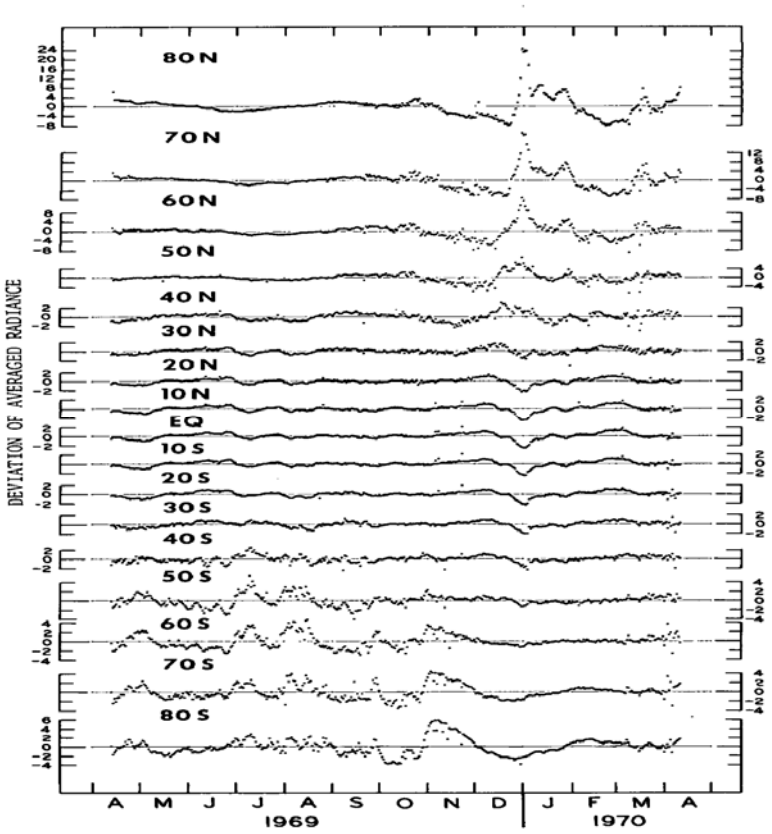

FIG. 5.1: Deviation of average latitudinal radiance [m W.m^{-2} (ster)$^{-1}$ (cm^{-1})$^{-1}$] from a finite Fourier-series fit for 80°N-80°S from Apr. 14, 1969, to Apr. 13, 1970. (Adapted from Fritz and Soules, 1972) Courtesy: American meteorological society Reprinted with permission.

The main result is that, when a temperature rise occurred in the winter polar stratosphere as a part of SSW (or Southern Hemisphere), a temperature decrease occurred in the stratosphere of the tropics of both the winter and summer hemispheres, at least up to latitude 40°N. They found that stratwarms are accompanied by slight cooling in the stratosphere over the tropics and subtropics. This coupling feature is later explained by Dunkerton et al. (1981).

More studies on this aspect of the tropical response of SSW were reported using the weekly meteorological data obtained from an equatorial station Thumba (8 32, 76.52) by Appu (1984); Mukherjee et al. (1985); Mukherjee et al. (1987) and Mukherjee, (1990). Analysis on this rocket data also revealed the presence of high-level warmings in the strato-mesospheric region over Thumba (Mukherjee et al. 1972).

The mechanism responsible for SSW is due to the increase in planetary wave activity and its interaction with the wave mean flow (Matsuno 1971). Using various satellite and ground based radar data more studies were reported on the dynamics of SSW. Calculations on Eliassen-Palm (E-P) flux using ECMWF reanalysis data, showed clear evidence of an equatorward propagation of planetary waves consecutive to a major warming episode over polar region (Sivakumar et al. 2004). This study showed that the SSW is not only focused towards high/mid-latitudes depending on the strength of the warming it can also extend to low-latitudes. Kodera (2006) analysed meridional circulation change associated with high-latitude warming of polar region using a composite analysis of twelve stratwarm events. They concluded that the warming produces lowering of temperature in equatorial lower stratosphere and upper troposphere. This leads to a see-saw convective activity in the troposphere near to the SH (10°S-equator) and over NH tropical (5°–15°N) stratosphere. Sub-tropical (5°-15°N) mesospheric temperature field shows a cold anomaly with a downward progression of 1 km d^{-1} (Shepherd et al. 2007) during the period of warming events. Yoshida and Yamazaki (2011) showed that tropical tropopause layer experience a cold anomaly during January, 2009 SSW event.

5.2. Data and methodology

The ECMWF ERA-40 and interim reanalysis data set at 00 GMT with a resolution of 2.5º×2.5º and 1.5º×1.5º, respectively were used for the study. Four typical cases were selected for the present analysis. The chosen cases are (i) Case 1 - mid-winter event (984/85), (ii) Case 2 - early winter (1987/88), (iii) Case 3 – double pulse event (1998/99) and (iv) Case 4 - Major (2008/09). Stratospheric temperatures at 2 hPa, 5 hPa, 7 hPa and 10 hPa levels at 80°N during December to March period for the aforementioned SSW years are considered. Daily temperature anomalies for the winter period are calculated from the long term mean period comprising of 21 year period (1969-1989) for the two events of 1984/85 and 1987/88.

ECMWF interim reanalysis data set for the period of 1990-2010 are used for the other two events to compute the daily anomalies. The daily anomalies are calculated for winter period (November through March) for the latitudinal belt of 30ºN-30ºS. Seasonal means are computed separately for each station from the daily data for the above time period. The anomalies are calculated as the deviations (ΔT) from the seasonal means (T). Normalized temperature anomalies are calculated for one year the period from November-October for each stratwarm case at 2 hPa, 5 hPa, 7 hPa and 10 hPa levels.

Six locations over Indian regions are selected to find out the intensity of upper stratospheric cooling during the period of the chosen stratwarm events. The selected locations are shown in Fig. 5.2. There are (1) Delhi (28º38′N, 77º12′E), (2) Jodhpur (26º18′N, 73º04′E), (3) Ahmedabad (23º00′N, 72º 40′E), (4) Hyderabad (17º22′N, 78º02′E), (5) Bangalore (12º58′N, 77º35′E), and (6) Trivandrum (8º4′N, 77º.02′E).

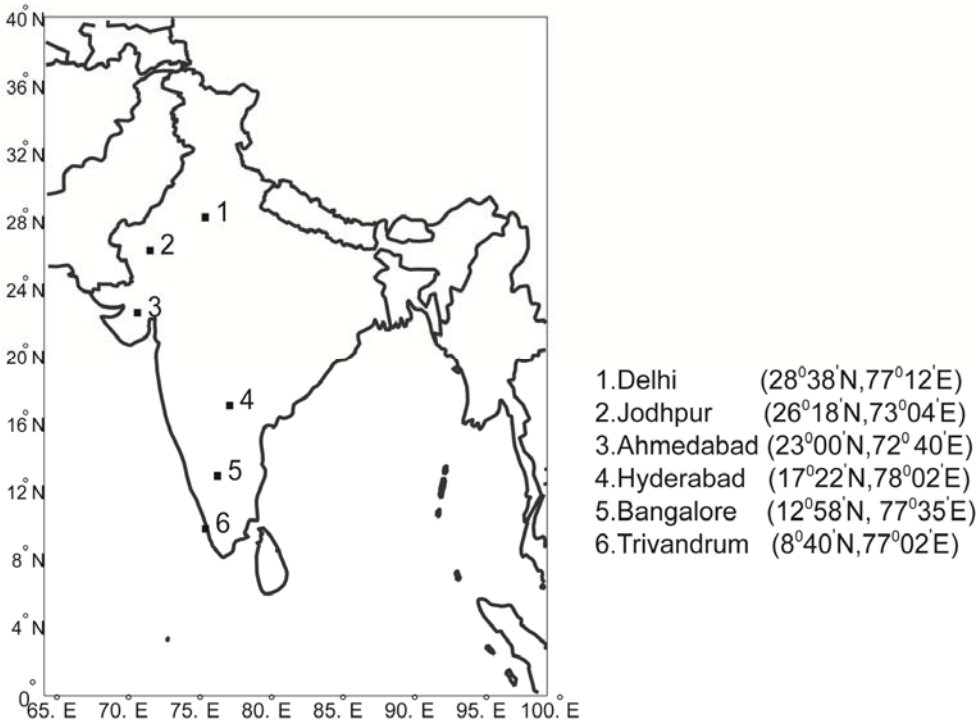

FIG. 5.2. Map of India to show the six selected locations.

The following notations are used:

M_W	: Major warming
m_{w1}	: Minor warming 1
m_{w2}	: Minor warming 2
M_c	: Major cooling: cooling associated with major warming
m_{c1}	: Minor cooling 1: cooling associated with minor warming
m_{c2}	: Minor cooling 2
P_0	: Peak day of the warming event
P_-	: Pre- phase of the warming event
P_+	: Post- phase of the warming event
P_x	where x denotes the number of days after/before the warming

5.3. Results and Discussion

5.3.1. Characteristics of the 'intense major' stratwarm events

Figure 5.3 depicts the time series of the zonal polar upper stratospheric temperatures at 2 hPa, 5 hPa, 7 hPa and 10 hPa levels over 80°N latitude during the major stratospheric warming events on 1984/85 (mid-winter), 1987/88 (early), 1998/99 (double pulse) and 2008/09 (major) from the time period November to March. The behavior of the winter warmings are studied from the these figures

5.3.1.1. Warming event of the winter: 1984/85

Figure 5.3a reveals the time series of the winter 1984/85. Earlier studies (Randel and Boville, 1987 and Fairlie et al. 1988) described the evolution and dynamics of this major warming using geopotential height and temperature, fields of Q vectors, isentropic maps of Ertel's potential vorticity and zonal wave numbers. The winter 1984/85 is characterized by three warming pulses. An intense major warming is developed in the last week of December and peaked in the first week of January 1985. This event is followed and preceded by one minor warmings each. The major warming is clearly delineated at 80°N at different stratospheric levels. The major stratwarm which peaked in the first week of January 1985 propagated to mid-stratospheric level (Fig. 5.3a, M_w). The peak day of this event at 10 hPa was on 2 January 1985. In addition, the winter polar upper stratosphere is experienced one minor warming on 10 December 1984 (m_{w1}) and another on 15 March 1985 (m_{w2}) at the same level. The second minor warming accompanied the transition of easterly flow towards the spring season (Randel and Boville, 1987). These three warming pulses registered at the upper stratospheric level with maximum amplitude at 2 hPa level. Table 5.1

shows the peak days of the three events, the location of the warm centers and the temperature anomaly at the peak phase.

TABLE. 5.1. Temperature deviations (ΔT) at the warm centers at different levels for the major and the two minor warming events in the winter 1984/85.

ht (hPa)	Major warming (M_w)			Minor warming 1 m_{w1}			Minor warming 2 m_{w2}		
	P_0 day	Max ΔT(° C)	Core Lat/Lon degree	P_0 day	Max ΔT(° C)	Core Lat/Lon degree	P_0 day	Max ΔT(°C)	Core Lat/Lon degree
2	31/12/84	86	65/120	09/12/84	34	75/ 60	15/03/85	25.5	50/ 5
5	31/12/84	60	55/60	10/12/84	35	70/ 130	15/03/85	34.5	70/ 110
7	01/01/85	58.5	60/58	09/12/84	33	70/80	15/03/85	34	70/ 110
10	02/01/85	54.5	70/ 38	10/12/84	25	70/ 110	15/03/85	27.8	68/ 118

5.3.1.2. Warming event of the winter: 1987/88

The stratospheric warming in this winter is characterized by the earliest intense major warming event ever recorded in the northern hemisphere. The warming began on the first week of December and peaked on 09 December 1987 (Fig. 5.3b, M_w). The event developed by the intensification of planetary wave number 1 (Baldwin and Dunkerton, 1989). Prior to the major stratwarm event, the upper stratospheric levels experienced a minor warming on 21 November 1987 (Fig. 5.3b, m_{w1}) and consequently stratospheric vortex regained its strength with temperatures -80°C. It is then followed by a major and a minor warming occurred at 2 hPa level on 01 March 1988 (Fig. 5.3b, m_{w2}). The minor warming marked the transitional phase of the season. Details of the peak intensity of this event are given in Table 5.2.

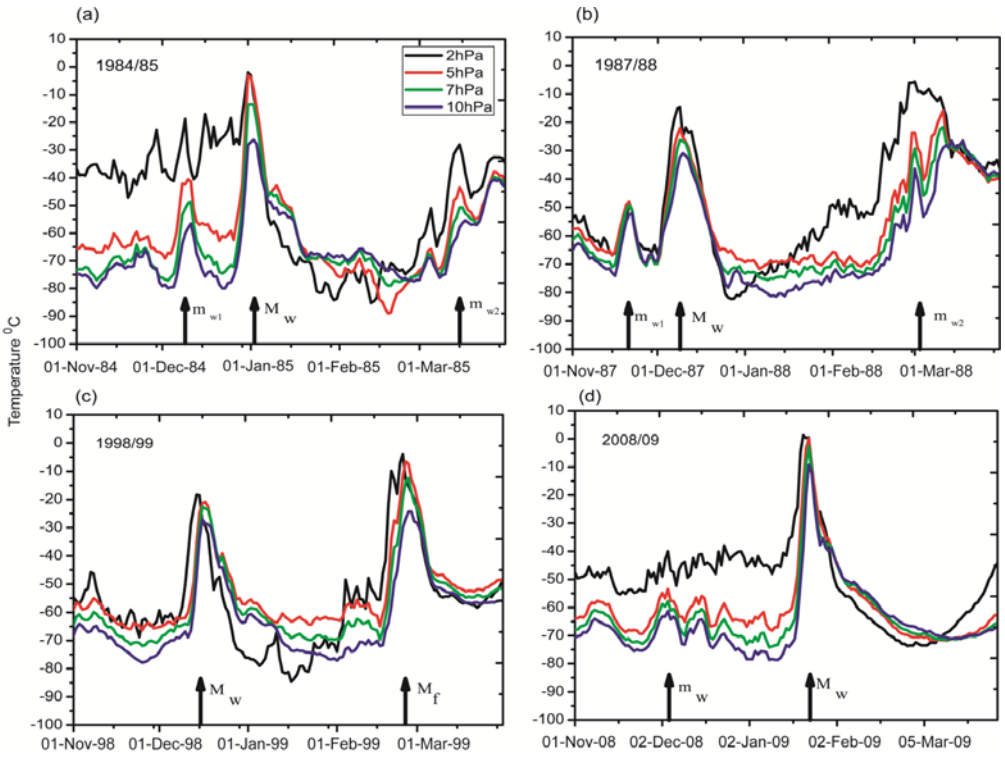

FIG.5.3. Daily variation of polar stratospheric temperatures (°C) at different stratospheric levels during four different SSW winters (a) 1984/85, (b) 1987/88, (c) 1998/99 and (d) 2008/09. The arrow with M_w represents the peak days of the major warming events. The first and second minor warming events are denoted by m_{w1} and m_{w2}. M_f represents the Final warming event.

TABLE. 5.2. Temperature deviations (ΔT) at the warm centers at different levels for the major and the two minor warming events in the winter 1987/88.

ht (hPa)	Major warming (M_w)			Minor warming 1 m_{w1}			Minor warming 2 m_{w2}		
	P_0 day	Max ΔT (°C)	Core Lat/Lon (degree)	P_0 day	Max ΔT (°C)	Core Lat/Lon (degree)	P_0 day	Max ΔT (°C)	Core Lat/Lon (degree)
2	09/12/87	58	55/62	21/11/87	6.5	80/ 80	01/03/88	55	75/ 60
5	09/12/87	59.2	65/40	21/11/87	19	80/ 130	01/03/88	44.5	80/ 90
7	09/12/87	57.8	60/40	21/11/87	23	80/ 140	01/03/88	45	80/ 100
10	10/12/87	52	65/51	21/11/87	25	80/ 130	01/03/88	45	80/120

Stratospheric temperature rose to -10°C at 2 hPa levels on first week of March, and then it entered into a transition period of winter to spring. This minor warming shows fluctuation at 5 hPa, **7** hPa and 10 hPa levels i.e., increase in temperature, then a sudden fall and again a slight increase (denoted as arrow) before entering into the transition phase.

5.3.1.3. Warming event of the winter: 1998/99

The winter of 1998/99 experienced two significant warming pulses. The first pulse occurred in the early December (Fig. 5.3c, M_w) and the second one in late February (M_f). The first event stands as the second earliest major warming. The overall vortex evolution of this event is reported by Manney et al. (1999) using 3D mechanistic model simulation. They reproduced the warming and zonal wind reversals at 10 hPa level in their model studies. At upper stratospheric levels, both the early and late winter warmings, registered their intensity with higher gradient. Details of the peak intensity of the two warmings are given in table 5.3. The maximum temperature rise is not uniform in the whole of the stratospheric region because of the downward propagation of the warm centers from upper to lower stratospheric levels. Peak date of the final warming at different upper stratospheric levels vary from 24 to 27 February 1999 respectively.

5.3.1.4. Warming event of the winter: 2008/09

The winter period is relatively undisturbed till the first half of January. A warming developed in the beginning of the second half of January and attained its peak intensity on 23 January 2009 (Fig 5.3d, M_w).

TABLE. 5.3. Temperature deviations (ΔT) at the warm centers at different height levels for the major and the final warming events in the winter 1998/99.

ht (hPa)	Major warming (M_w)			Final warming 1 (M_F)		
	P_0 day	Max ΔT(°C)	Core Lat/Lon degree	P0 day	Max ΔT(°C)	Core Lat/Lon degree
2	14/12/98	63.8	70/ 40	24/02/99	74.6	75/09
5	17/12/98	36.6	75/ 80	25/02/99	70	75/30
7	16/12/98	42	65/ 75	26/02/99	62.5	75/30
10	16/12/98	43.2	70/ 90	27/02/99	56.5	75/25

Out of the four selected stratwarm events, this event is the strongest and it is distinguished by the zonal wave number-2 pattern. Its evolution is detailed by Labitzke and Kunze, (2009); Manney et al. (2009) and Harada et al. (2010). Similar to the major stratospheric warming events in 1984/85 and 1987/88, the final warming in February 1999 also undergone split in the polar vortex during the warming phase. There is a minor temperature increase in the upper stratospheric levels on the first week of December 2008, which is denoted by m_{w1} (Fig 5.3d). In this chapter, the day in which polar stratospheric temperature increase at 80°N for each level is considered as the peak days for the selected stratwarm event.

TABLE. 5.4. Temperature deviations (ΔT) at the warm centers at different levels for the major warming events in the winter 2008/09.

ht (hPa)	Major warming (M_w)		
	P_0 day	Max ΔT(°C)	Core Lat/Lon (degree)
2	23/01/09	62.5	75/80
5	23/01/09	73.2	85/10
7	23/01/09	71.8	85/10
10	23/01/09	75.2	80/10

5.3.2. Zonal average temperature anomalies over the tropics during SSWs period

To study this aspect, the anomaly in the daily data are calculated from the mean of 21 year period (1969-1989) using ERA-40 for the first two events (1984/85 and 1987/88) and for the other two (1998/99 and 2008/09), the period is 1990-2010. Fig. 5.4 illustrates the thermal pattern of the tropics (30°N-30°S) during the two events at the four different stratospheric levels (2 hPa, 5 hPa, 7 hPa and 10 hPa). Associated with the SSW, cooling in the tropical region is evident during the days of warming. The peak days of tropical cooling connected with the major warmings are denoted by arrows with M_c and linked with the minor warmings by m_{c1} and m_{c2}.

5.3.2.1. Thermal structure of the tropical stratosphere: 1984/85

Time series of temperature anomaly for 1 December through 31 March 1985 is prepared and shown in Fig.5.4a-d. During this winter, apart from the major warmings minor warmings are also noticed, one before and one after the major warming pulses (see Fig. 5.3a). These 3 warming pulses exhibited a decrease in the prevailing temperatures over tropics. The low temperatures during the major warming on 1 January 1985 are denoted by M_c in each in Fig. 5.4 (a-d). Cooling associated with the m_{w1} and m_{w2} warming are also very evident in the figure.

A minor cooling (m_{c1}) of -2° to -4°C is noticed at 2 hPa level on 14 December 1984, which is then followed by a major cooling (M_c) of -4° to -6°C. The major warming peaked on 1 January 1985. After these two events, the tropical upper stratospheric temperature regained to the positive temperature gradient. This gradient ranges from 0 to 4°C to the first week of February 1985. A minor cooling weakened on 14 March 1985. These

three cooling pulses and positive temperature gradient over tropics are associated with the high- latitude temperature gradient as described in Fig. 5.3a. The high-latitude maximum and equatorial minimum temperatures are observed on the same peak days. This implies the presence of strong coupling between high-latitude and equatorial upper stratospheres in association with SSWs.

Fig. 5.4b-d explains how these tropical cooling pulses are propagate downward from upper to mid-stratosphere during the major and minor warmings. Associated with the minor warming at 5 hPa (Fig. 5.4b, m_{c1}), a cooling of -2° to -4°C is noticed in the latitudinal belt 15°N - 15°S. This minor cooling is merged with lower temperatures of -6° to -8°C around 1 January 1985 (M_c). Another cold anomaly is again noted at the same level associated with the minor warming during the transition period from winter to spring season. This equatorial cooling continued till the end of the season with -4° to -8°C. In between the major and the second minor cooling, tropical upper stratosphere experienced a cold anomaly of -4° to -10°C.

The intensity of the cooling is reduced as it propagated from 5 hPa to 7 and 10 hPa levels. The magnitude of the cooling ranges from -4° to -8°C during minor 1 and major (Fig. 5.4c, m_{c1} and M_c) warming episodes. The cooling takes place around the peak days. At the mid-stratospheric level, the lowest temperature of -4° to -6°C (Fig. 5.4d, m_{c1} and M_c) are found during the peak phase of minor 1 and major warming events. Positive temperature gradient of 0-4°C is also noticed after the two cooling phases. The temperature drop associated with the minor warming (Fig. 4.4d, m_{c2}), is -2° to -4°C. The time of maximum cooling is on the peak days of the major warming.

5.3.2.2. Thermal structure of the tropical stratosphere: 1987/88

Similar to the 1984/85 event, an out of phase relation of temperature anomalies over the tropics is noted during the SSW of 1987/88 at Polar regions. Fig. 5.4e-h depicts the time period from 10 November 1987 - 30 March 1988. This winter is characterized by three warming pulses on (1) 21 November 1987 (minor 1, m_{w1}), (2) 10 December 1987 (major, M_w) and (3) 01 March 1988 (minor 2, m_{w2}).

Corresponding to the minor warming on 21 November 1987, equatorial regions (Fig. 5.4e, m_{c1}) is experienced a negative temperature gradient ranging from 0 to -4°C. This cooling merged with an intensified severe cooling of -8 to -12°C on 11 December 1987. At 2 hPa and 5 hPa levels a well pronounced low temperature is occurred during the peak phase of the major warming event on 11 December 1987.

Temperatures over the tropics are returned to the normal seasonal state after the decay of the warming. A cooling is also noticed in the upper stratosphere associated with the third minor warming; which occurred in the first week of March 1988. The intensity of cold anomalies decreased while propagating from upper to mid-stratosphere during the major as well as minor warmings. A positive temperature gradient of 0-2°C is noticed over tropics soon after the major cooling (M_c). These tropical temperature perturbations are directly related with the polar stratospheric temperature variations. This out of phase relation is visible throughout the winter season of 1987/88 at the time of SSWs. Maximum cooling of -8° to -10°C is observed in the latitudinal belt of 5°N- 5°S simultaneously with the highest temperature occurred in the high- latitude in early December 1987 (M_w). A negative gradient of -4° to -6°C is visible corresponding to the minor 2 in March 1988. At mid-stratosphere (Fig. 5.4h, M_c), low departures of -4° to -

6°C is linked with the major warming. The maximum cooling is found in the latitudinal belt of 10°N-10°S; i,e., in the equatorial region

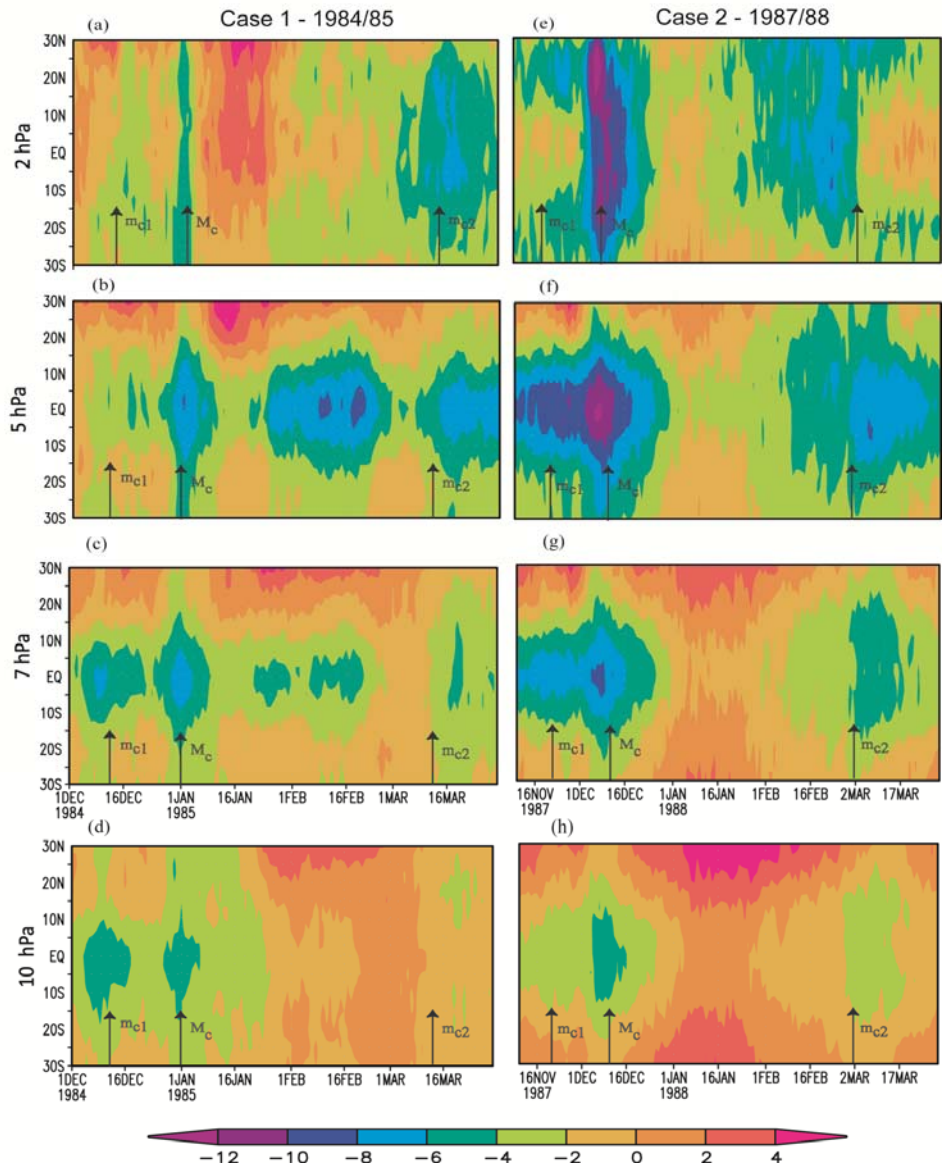

FIG. 5.4. Time-latitude cross-section of the daily temperature anomalies during stratwarm events 1984-85 (left) and 1987-88 (right) using ERA-40 data. Time period ranges 1 December 1984 - 31 March 1985 and 10 November 1987 – 31 March 1988 at 2 hPa (top row), 5 hPa (second row), 7 hPa (third row) and 10 hPa (fourth row). Arrow with M_c denotes the major cooling, m_{c1} and m_{c2} stand for the minor cooling1 and minor cooling 2, during the peak days of the major and minor warmings.

.

5.3.2.3. Thermal structure of the tropical stratosphere: 1998/99

Spatial and temporal variability of the stratospheric cooling during this event is very evident from fig. 5.5a-d as in the case of the above two cases. The winter of 1998/99 is experienced a major warming in the first half of December.

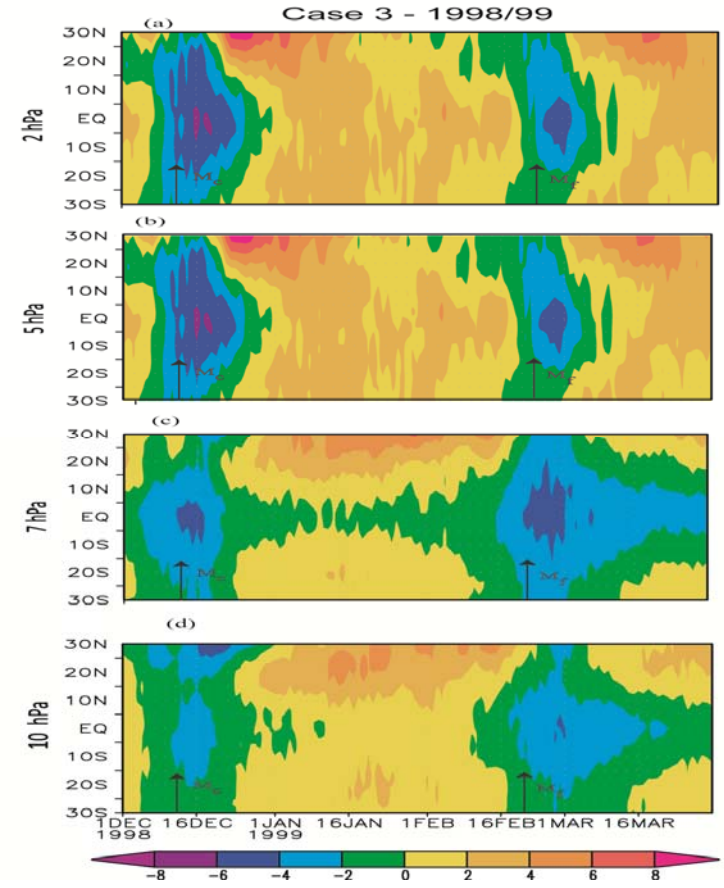

FIG. 5.5. Time-latitude cross-section of the daily temperature anomalies during the 1998/99 SSW event at different stratospheric levels: 2 hPa (top row), 5 hPa (second row), 7 hPa (third row) and 10 hPa (fourth row) level. Time period ranges 1st December to 31 March 1999.

Around the peak days, a cooling of -4° to -6°C is noted at 2 hPa level (Fig. 5.5a, M_c) covering the latitudinal belt of 20°N-20°S. This cooling pattern exists at 5 hPa during 10 - 20 December 1998 with an intensity of -

6°C (Fig. 5.5b) in the same latitudinal belt. At lower level (7 hPa), the temperatures of -4°C are found in between 10°N-15°S (Fig. 5.5c, M_c), while at mid-stratospheric level (10 hPa) an intensified cooling of -5°C is seen in the 30°N-20°N region. The anomalies seem to propagate downward and towards the equatorial regions.

The winter of 1998/99 had the final warming during the end of February: peak phase begins on 24-27. A cooling of -5°C is seen at 2 hPa level (Fig. 5.5b, M_f) between 15°N-15°S. These cold anomalies propagated downward with the same intensity at the lower levels at 5 hPa and 7 hPa. During these processes the cold region covers more tropical areas. After the early warming in December 1998, upper stratospheric temperatures attained its seasonal state of the non-event period with strong polar vortex which continued till the final warming in the late February. The stratospheric temperature over the tropics shows two reversals in temperature gradient which resulted in cooling at par with the two warmings. The value of the temperature gradient is 0-4°C over tropics. The coupling between low and the high- latitudes regions is also evident in this winter.

5.3.2.4. Thermal structure of the tropical stratosphere: 2008/09

Figure 5.6a-d depict the spatial and temporal variability of equatorial cooling during the case 4 SSW (left) event at different pressure levels. Figures in the right panel show the corresponding peak days of temperature anomalies. Along with the sharp temperature increase in the Polar regions, a drop in tropical stratospheric temperature is very evident. At 2 hPa level, the tropical cooling of -4° to -6°C is noticed over the region 10°N-30°S. Prior to the peak day maximum cooling is observed at 25°N (Fig. 5.6e) and also at 5 hPa level cooling is at 20°N on 20 January 2009 (P_{-3} day). The cooling extends both to the northern and the southern hemispheres.

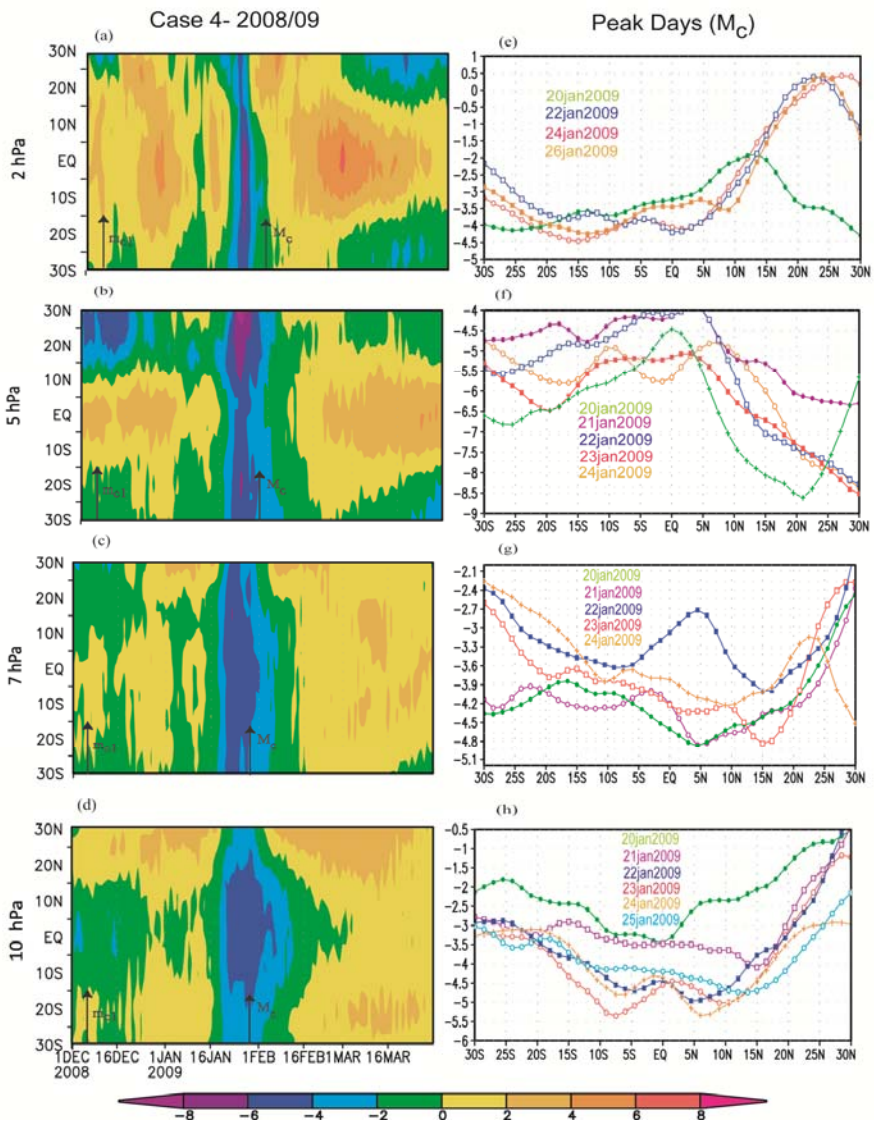

FIG.5.6. Time-latitude cross-section of the daily temperature anomaly (left) for the stratwarm events at 2 hPa (top row), 5 hPa (second row), 7 hPa (third row) and 10 hPa (fourth row). Time period is from 1st December to 31 March 2009. The temperature anomaly variation during peak days are plotted (right).

At 7 hPa and 10 hPa levels that maximum cooling is noticed during 20-24 January 2009, then after it intensity decreased. The lower temperatures of -4.8°C (Fig. 5.6g) are noticed at 5°N on 20 January 2009.

At the same time, at 10 hPa level (Fig. 4.6d, M_c) the lower temperature is -5.4°C on 23 January 2009 and 24 January 2009 at 10°S and 5°N (right).The cooling associated with the major warmings stands as the seasonal minimum value in the tropical stratosphere.

When the center of warming propagate downwards, the area of the cold regions are effective to larger areas. Downward propagation of the warming and the area of the cold center are interlinked. This study also indicate that there is a relation between the altitude of cold centers and the area of the cold regions, when the cold center is in the upper most stratospheres the cold region is comparatively confined to lower areas.

The minor perturbations in the winter also causes 0 to -2°C (Fig. 5.6d, m_{c1}) of cooling in the latitude of 10°N - 10°S. Temperature regains to the pre- SSW state at both the high and low latitude regions soon after the decay of SSW.

5. 3. 3. Tropical cooling over Indian regions

From the above analysis it is very clear that SSWs are always accompanied by a cooling in the stratosphere over the tropics from 30°N-30°S. In this section, the effects of SSW on cooling over Indian regions are discussed. For this purpose six Indian stations, such as Delhi (DLH), Jodhpur (JDP), Ahmedabad (AHD), Hyderabad (HYD), Bangalore (BNG), and Trivandrum (TRV) are selected. The first three stations represent the north Indian sectors and the rest are in the south Indian sectors (Fig.5.2). The analysis is carried using the four SSW events occurred during the winter 1984/85, 1987/88, 1998/99 and 2008/09. The vertical cross-sections of temperature anomalies for the stratospheric regions are prepared for all the four winters and delineated the various features on the tropical response of stratwarm pertaining to the Indian regions.

5.3.3.1. Intensity and time of cooling over Indian regions: 1984/85

Figure 5.7a-f depicts the thermal behavior of the stratospheric layers over the stations during the case 1 (1984/85) stratwarm event.

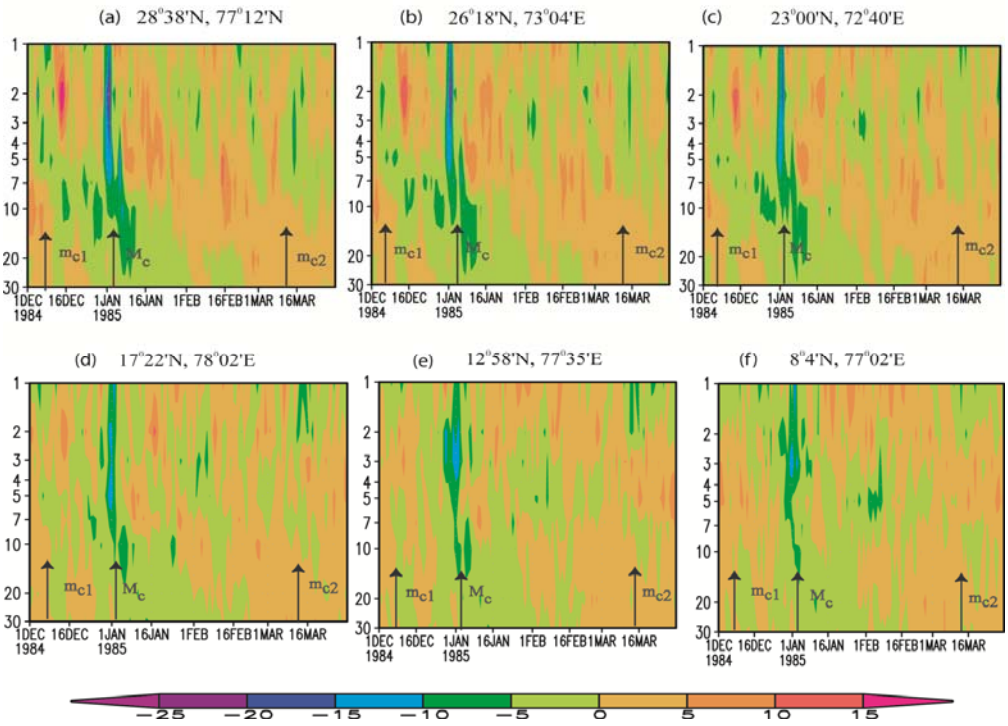

FIG.5.7. Height-time cross section of stratospheric temperatures over the six Indian stations viz (a) DLH (28°38'N, 77°12'E), (b) JDP (26°18'N, 73°04'E), (c) AHD (23°00'N, 72° 40'E), (d) HYD (17°22'N, 78°02'E), (e) BNG (12°58'N, 77°35'E), and (f) TRV (8°4'N, 77°.02E). The arrow with Mc represents the peak day of major SSW with m_{c1} and m_{c2} for that of the minor SSW events.

During this winter there are three warmings, two minor and one major (Fig. 5.3). Major warming peaked on 2 January and the minor warmings peaked on 10 December and 15 March 1985 respectively. From the figure it is very evident that temperature the Indian stations undergone an out of phase variations with respect to the warming periods over the Polar region. The stratosphere over the Indian region shows a very strong cooling during the peak phase of the warmings. The intensity of the cooling is very strong in the upper stratosphere (2 hPa and 5 hPa levels).

TABLE.5.5. Maximum cooling and its corresponding time in days with respect to the Peak day (P_0) of the major 1984/85 SSW at the six stations.

ht (hPa)	Peak day (P_0)	$\frac{Maximum\,deviation\ \Delta T\ ^oC}{Corresponding\,day\,wrt\ P_0}$					
		DLH 28º38′N, 77º12′E	JDH 26º18′N, 73º04′E	AHD 23º00′N, 72º40′E	HYD 17º22′N, 78º02′E	BNG 12º58′N, 77º35′E	TRV 8º4′N, 77º02′E
2	31/12/84	-24.2	-24.51	-18.84	-11.74	-12.37	-9.24
		P_{+2}	P_{+2}	P_{+2}	P_0	P_{+2}	P_{+1}
5	31/12/84	-14.67	-13.57	-14.48	-12.95	-6.88	-8.12
		P_{+5}	P_{+1}	P_{+1}	P_0	P_{+1}	P_{-1}
7	01/01/85	-12.38	-11.51	-10.02	-8.99	-5.64	-6.42
		P_{+1}	P_{+1}	P_{+2}	P_0	P_0	P_0
10	02/01/85	-11.24	-10.17	-6.1	-9.04	-6.31	-6.16
		P_{+5}	P_{+5}	P_0	P_{+4}	P_{-1}	P_{+1}

The cold centers are propagated to the lower altitudes irrespective of the intensity of the stratwarm events. The maximum warming over the Polar regions and the lowest temperature over the Indian region are almost simultaneous. The stratospheric temperature over Indian stations during the peak phase of major SSWs stands out as the lowest of the season. The maximum negative departure of -24.2°C is noticed at 2 hPa on P_{+2} day. i.e., two days after the peak day. The magnitude of the stratospheric cooling (M_c) associated with major SSW and the day in which maximum deviation is noticed are summarized in Table 5.5.

The intensity of cooling and the day in which the low temperatures are noticed are tabulated in Table 5.6 and 5.7, during minor 1 and minor 2 stratwarms. Maximum lower temperature is noticed at 2 hPa level (m_{c1}) on P_{-4} day for the first four Indian regions and P_{-5} and P_{-3} day on remaining two stations. It indicates that less intensified cooling also happened during the two minor warmings. Here we can infer that minor warming also cause

a low temperatures. The time of maximum cooling varies from P_{-5} to P_{+4} (Table 5.7) days. The intensity of cooling goes on decreasing at each level as it moves from 28°N to 8°N. In the case of second minor event the tropical minimum is -8.37°C at 2 hPa.

TABLE 5.6. Maximum cooling and its corresponding time in days with respect to the Peak day (P_0) during the 1984/85 minor SSW at the six stations.

ht (hPa)	Peak (P_0)	$\frac{Maximum\,deviation\ \Delta T\ ^oC}{Corresponding\,day\,wrt\ P_0}$					
		DLH 28º38′N, 77º12′E	JDH 26º18′N, 73º04′E	AHD 23º00′N, 72º40′E	HYD 17º22′N, 78º02′E	BNG 12º58′N, 77º35′E	TRV 8º4′N, 77º02′E
2	09/12/84	-12.27	-09.73	-06.52	-04.27	-02.60	-00.53
		P_{-4}	P_{-4}	P_{-4}	P_{-4}	P_{-5}	P_{-3}
5	10/12/84	-06.78	-04.68	-06.46	-05.87	-04.59	-03.67
		P_0	P_{-2}	P_{-3}	P_{-4}	P_{-4}	P_{-4}
7	09/12/84	-00.26	-01.32	-00.06	-01.10	-01.02	01.51
		P_0	P_0	P_{+1}	P_{-1}	P_{-2}	P_{-1}
10	10/12/84	-02.55	-00.77	01.09	-02.48	-02.88	01.80
		P_{+4}	P_{+2}	P_{-5}	P_0	P_0	P_{-5}

TABLE 5.7. Maximum cooling and its corresponding time in days with respect to the Peak day (P_0) during the 1984/85 minor SSW at the six stations.

ht (hPa)	Peak (P_0)	$\frac{Maximum\,deviation\ \Delta T\ ^oC}{Corresponding\,day\,wrt\ P_0}$					
		DLH 28º38′N 77º12′E	JDH 26º18′N, 73º04′E	AHD 23º00′N, 72º40′E	HYD 17º22′N 78º02′E	BNG 12º58′N 77º35′E	TRV 8º4′N, 77º02′E
2	15/3/85	-8.37	-7.28	-4.03	-7.09	-6.42	-0.73
		P_{+3}	P_0	P_{-3}	P_{+3}	P_{+3}	P_{+2}
5	15/3/85	-8.60	-4.94	-4.54	3.73	0.63	2.96
		P_0	P_0	P_{-2}	P_{+2}	P_0	P_{+3}
7	15/3/85	-3.73	-2.89	-3.31	-3.46	-1.07	-1.32
		P_0	P_{+1}	P_{-1}	P_{+3}	P_0	P_{+4}
10	15/3/85	0.59	1.48	1.13	-1.18	-0.31	-2.64
		P_0	P_0	P_0	P_0	P_{+2}	P_{+3}

5.3.3.2. Intensity and time of cooling over Indian regions: 1987/88

Stratospheric temperatures over the six Indian regions associated with the case 2 (1987/88) warming shows almost similar pattern as in the case of 1984/85 event. The seasonal minimum temperatures in the Indian station during the winter 1987/88 falls on the peak day of the major stratwarm.

The latitudinal variation of seasonal minimum temperatures at different altitudes is shown in Figure 5.8. It illustrates the peak of three cases of warmings of the winter 1987/88: (a) major, (b) minor 1 and (c) minor 2 and the corresponding latitude. From the Fig 5.8a it can be seen that, northern part of the Indian regions experienced the lowest temperatures, with magnitude exceeding -18°C between 23°N and 17°N latitudes at 2 hPa level on 8 December 1987 (i.e., P_{-1} day). The behavior of the remaining 3 levels is identical. This indicates the downward propagation of cold centers from high- to lower latitudes. The days in which the maximum cooling noticed are tabulated in Table 5.8.

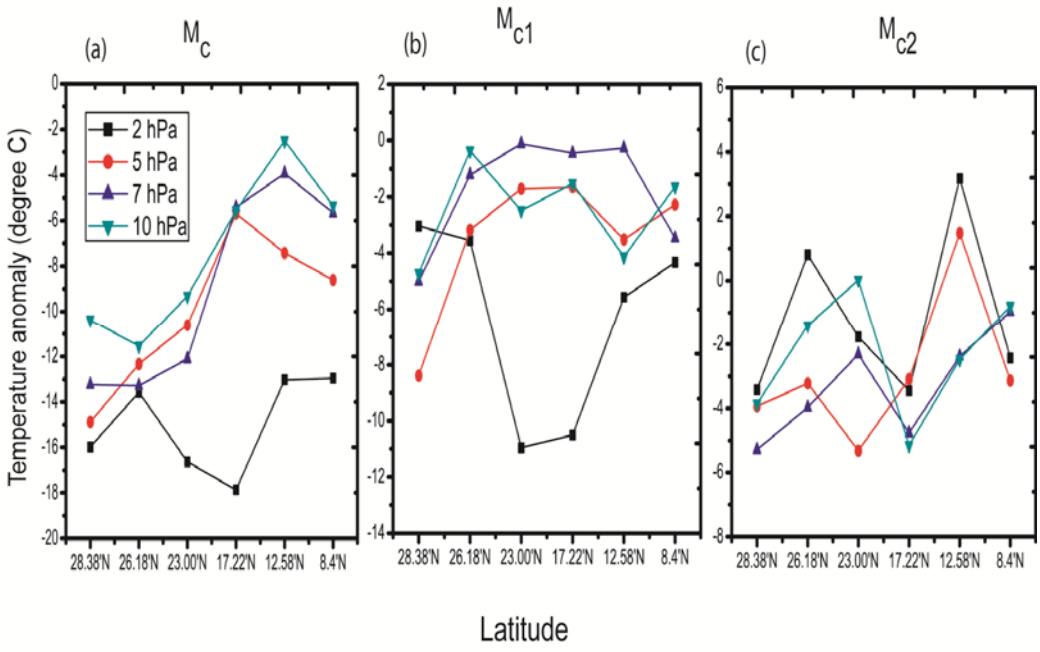

FIG. 5.8. Examples for the three cases of SSW in the winter 1987/88. Stratospheric seasonal temperature anomaly for the Indian stations indicates the out of phase relation during (a) major, (b) minor 1, and (c) minor 2 stratwarm days.

TABLE 5.8. Maximum cooling and its corresponding time in days with respect to the Peak day (P_0) of the 1987/88 major SSW at the six stations.

ht (hPa)	Peak (P_0)	$\frac{Maximum\ deviation\ \Delta T\ ^oC}{Corresponding\ day\ wrt\ P_0}$					
		DLH 28°38′N, 77°12′E	JDH 26°18′N, 73°04′E	AHD 23°00′N, 72°40′E	HYD 17°22′N, 78°02′E	BNG 12°58′N, 77°35′E	TRV 8°4′N, 77°02′E
2	09/12/87	-15.98	-13.58	-16.63	-17.87	-13.03	-12.96
		P_{-1}	P_{-1}	P_{-1}	P_{-1}	P_{-1}	P_{-1}
5	09/12/87	-14.88	-12.34	-10.06	-05.69	-07.42	-08.61
		P_0	P_0	P_0	P_{-1}	P_{+1}	P_{+1}
7	09/12/87	-13.24	-13.29	-12.01	-05.42	-03.93	-05.67
		P_{-1}	P_{+1}	P_{+1}	P_{+1}	P_{-1}	P_{-2}
10	10/12/87	-10.38	-11.54	-9.32	-5.57	-2.5	-5.35
		P_{+2}	P_0	P_0	P_{-3}	P_{-1}	P_{-2}

There is a minor thermal perturbation in the northern stratosphere on 21 November 1987 (M_{w1}). This led to an enhanced negative temperature gradient in the equatorward upper stratosphere (m_{c1}). The minor warming in polar stratosphere accompanies a negative impulse in the equatorial stratosphere without any time lag (Fig. 5.8, m_{c1}). The stations Ahmedabad and Hyderabad underwent the maximum cooling of -10.9°C on 16 November 1987 at 2 hPa on P_{-5} day. The temperature perturbations (Fig. 5.8, m_{c2}) around 20 November 1987 appear very close in time to the SSW event registered on 21 November 1987.

5.3.3.3. Intensity and time of cooling over Indian regions: 1998/99

As in the above two cases, tropical stratospheric temperatures over different stations already shows the presence of cooling. The intensity of the maximum cooling occurred at different pressure levels and the time of occurrence with respect to the peak day of SSW are presented in Figure. 5.9. The peak days at each altitude are already given in Table 5.3. At Delhi station (Fig.5.9a) the maximum cooling are -13°C, -8°C, -7°C and -11°C at 2 hPa, 5 hPa, 7 hPa and 10 hPa levels respectively. The corresponding peak days are P_{+7}, P_{+1}, P_{+3} and P_{+5}. The intensity of the cooling is sustained from upper to mid-stratospheric levels (Fig. 5.9a-c) over the north Indian stations. Bangalore station experienced cold temperature anomalies of -13.6°C, -6.7°C on P_{+3} day and -3.2°C on P_{+5} day, and -3.1°C on P_{+7} day at respective levels. The intensity of cooling is linearly decreased over these stations (Fig. 5.9e) and in most of the cases it is on post-phase of warmings (P_{+}) days. In general cooling is noticed just after the peak days. The seasonal minimum temperatures can be seen at northern as well as southern sectors.

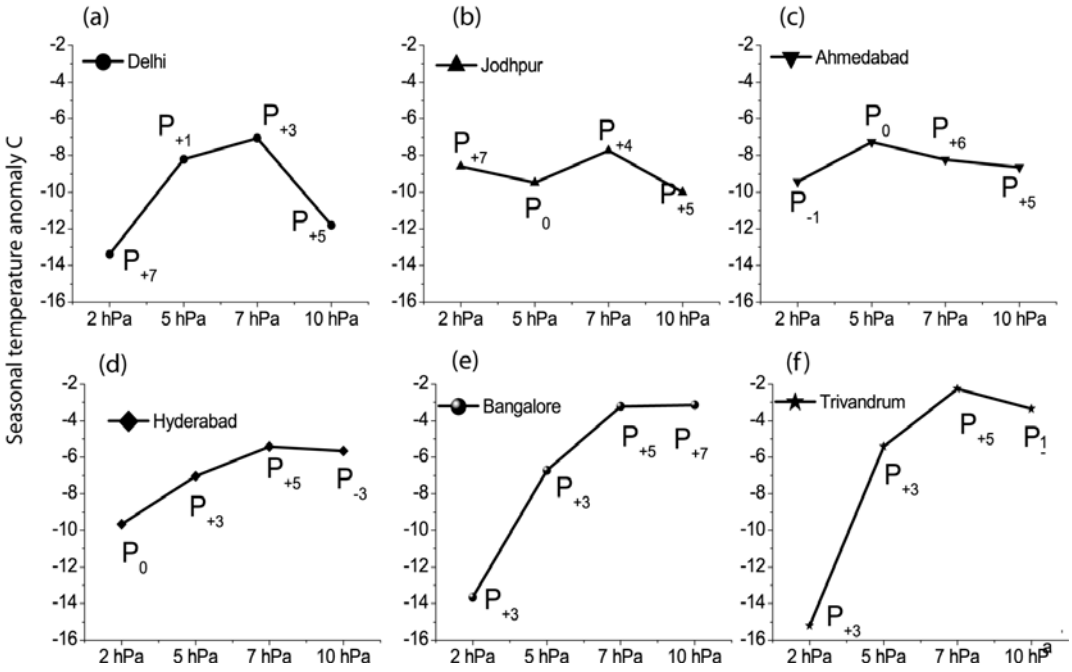

FIG. 5.9. The magnitude of peak cooling and their corresponding time in days with respect to the peak of SSW during the major SSW of the winter 1998-99.

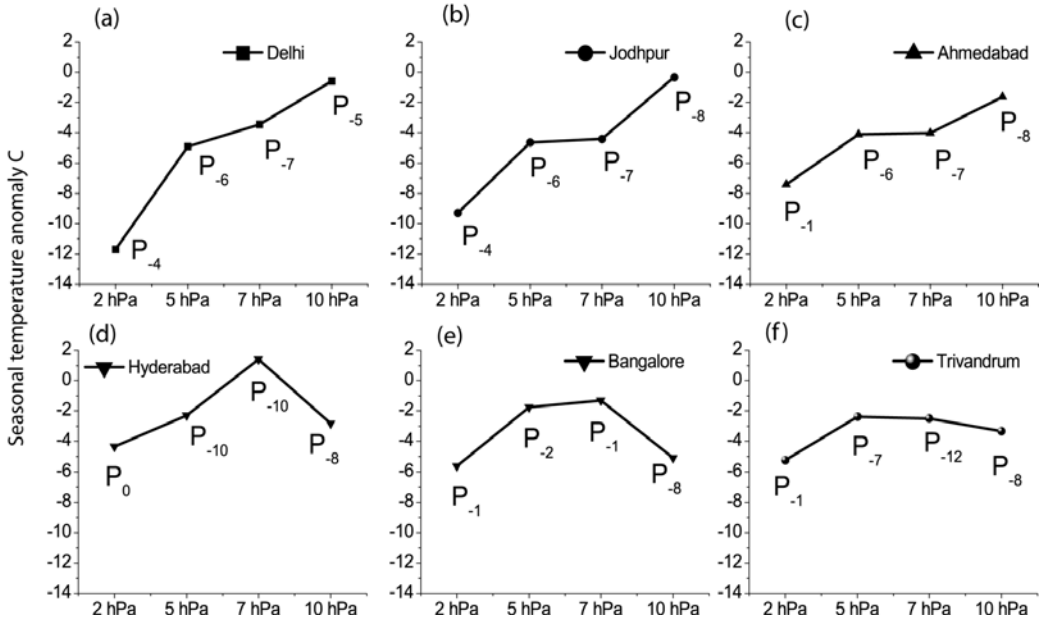

FIG. 5.10. Same as fig 5.9 but for the final warming in February 1999.

The effect of high-latitude final warming (February 1999) over the Indian region from upper to mid- stratospheric level is illustrated in Fig. 5.10a-f. The abscissa with each line denotes the day in which lower temperatures are noticed with reference to peak day. The intensity of the cooling is largest over the three north Indian stations at 2 hPa level. The intensity is reduced as it propagated from upper to mid-stratospheric levels.

Over Delhi station (Fig.5.10a) the temperature decreased by -11.7°C, -4.9°C, -3.4°C, and -0.59°C at four stratospheric pressure levels on P_{-4}, P_{-6}, P_{-7} and P_{-5} days. Similar is the pattern of cooling over Jodhpur and Ahmedabad stations. It indicates that the intensity of cooling reduced as the cold center propagates to lower levels. The intensity of cold temperature anomaly over the south Indian station (Trivandrum) varies -5.2°C, -2.3°C, -2.4°C and -3.32°C at 2 hPa, 5 hPa, 7 hPa and 10 hPa levels respectively. This coldest departure throughout the region is noticed just after the peak day of the event.

5.3.3.4. Intensity and time of cooling over Indian regions: 2008/09

The thermal behavior in the stratospheric layers over the six stations during the SSW phases of the winter 2008-09 is similar to that of the above 3 cases. The intensity of upper stratospheric cooling during the peak day of major stratwarm event on 23 January 2009 over Indian stations presented in Fig. 5.11 in a different way. The lowest temperatures observed at different stratospheric levels are presented against the latitudes of the six stations. The response time of high- latitude warming over these stations with reference to the peak days are depicted in Fig. 5.11b.

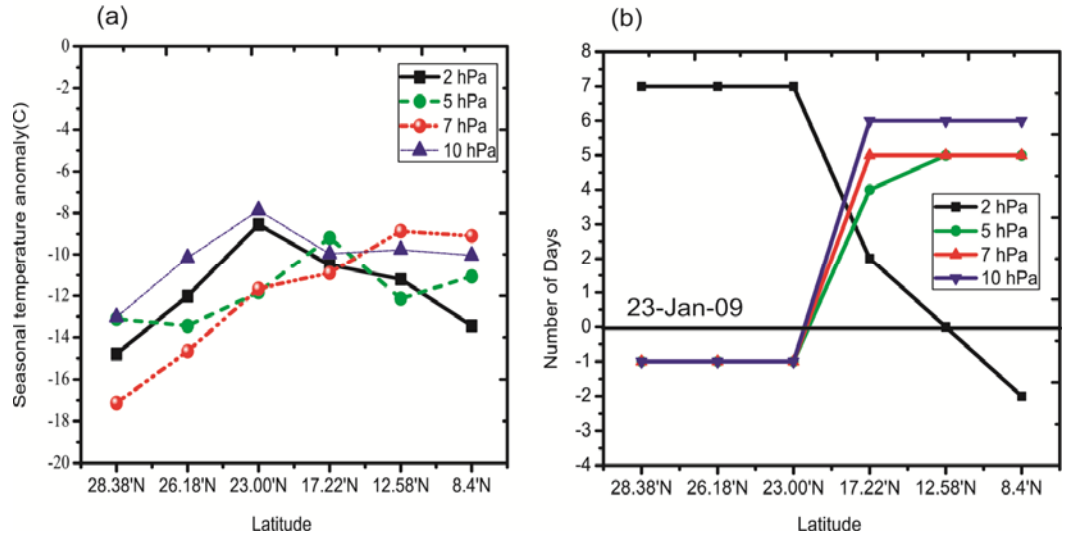

FIG. 5.11. illustrates the maximum low temperatures at the upper stratospheric levels against latitude of the six Indian stations (a). The days on the maximum cooling with reference to the peak day are represented for the four levels (b).

In the upper stratosphere (2 hPa) winter temperature anomaly shows a decrease corresponding to the warming. The coldest temperature anomalies at this level are -14.7°C, -12°C, -8.5°C, -10°C, -11°C and -13°C respectively for the stations from Delhi to Trivandrum. This temperature decrease is noticed (Fig.4.11b, black) on P_{+7} day for Delhi, Jodhpur and Ahmedabad station, P+2 day for Hyderabad, P_0 day for Bangalore and P_{-2} day for Trivandrum stations. The most pronounced cooling of -17°C is seen at 7 hPa and its amplitude decreases towards northern latitude with minimum at around 8°N. The lowest temperature is noticed on 22 January 2009 (P_{-1}) for the first three stations and on P_{-5} day for the other stations (Fig.4.11b).

5.3.4. The intensity of stratospheric cooling in the annual period

In order to compare the intensity of cooling over Indian regions in the annual scale, normalized temperature anomaly in the daily data at different pressure levels (2 hPa, 5 hPa, 7 hPa and 10 hPa) are calculated for

a period of a year from November to October for the four years and shown in Figure 5.12 to 5.15. Temperature anomalies are calculated for the six stations corresponding to four (1984/85, 1987/88, 1998/99 and 2008/09) events and presented Figures 5.12 to 5.15 respectively. The magnitude of cooling during the SSW phase in the one year for period can be evaluated from these figures. The peak days of the major warmings are denoted by dotted vertical lines in all the years. The peak days for the major warmings are 2 January 1985, 10 December 1987, 15 December 1998 and 23 January 2009. The normalized anomaly in the year 1984/85 varies from -6 to 6 at 2 hPa and -4 to 4 for the respective levels.

In earlier sessions it is already presented that the seasonal (winter) minimum temperatures in the stratospheric levels over the Indian regions took place during the peak phase of major SSWs. It is very interesting to report that annual maximum temperature over the polar stratosphere is accompanied by annual minimum temperatures over Indian stratosphere. It is very clear that the annual minimum temperatures over the Indian stations occur during the peak phase of major warmings.

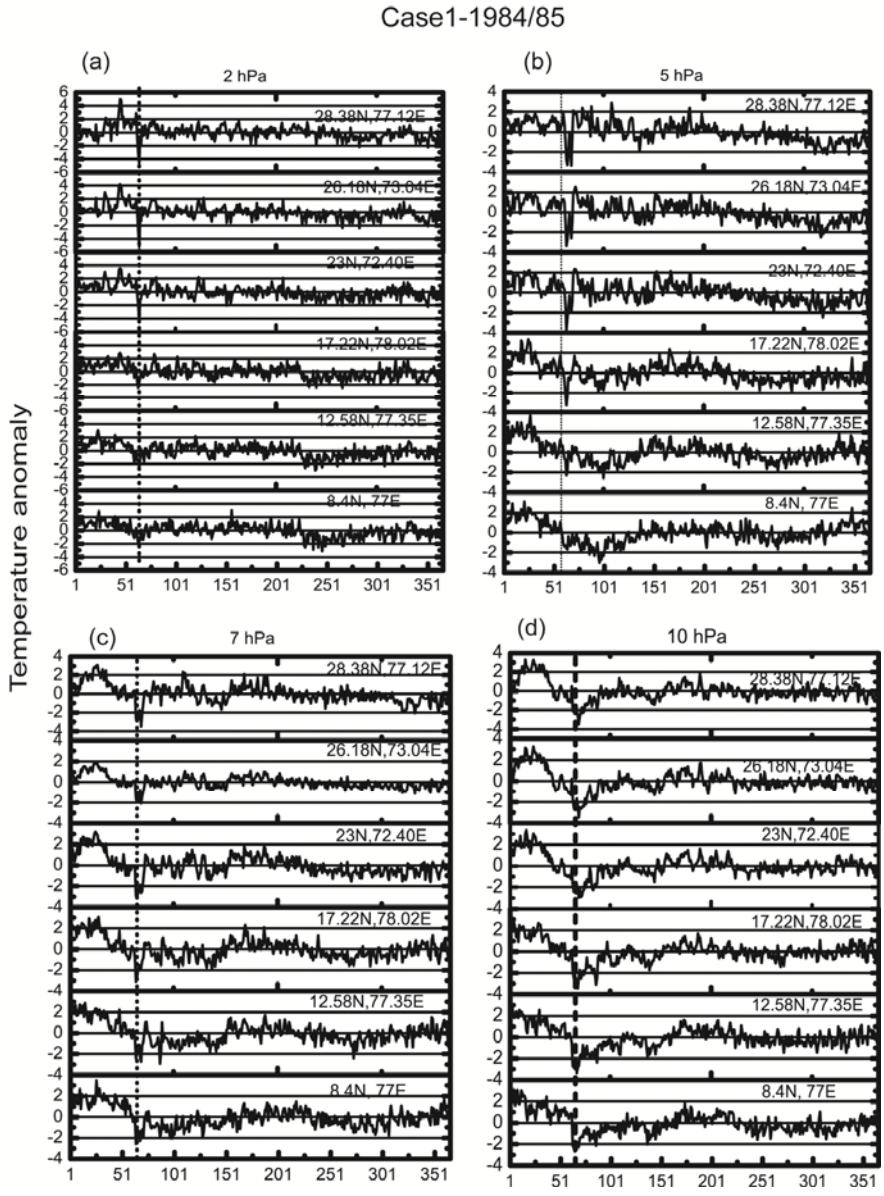

FIG. 5.12. Annual temperature variation at (a) 2 hPa, (b) 5 hPa, (c) 7 hPa, and (d) 10 hPa from 1 November 1984 to 31 October 1985 over six Indian stations. The dotted vertical lines indicate the peak days.

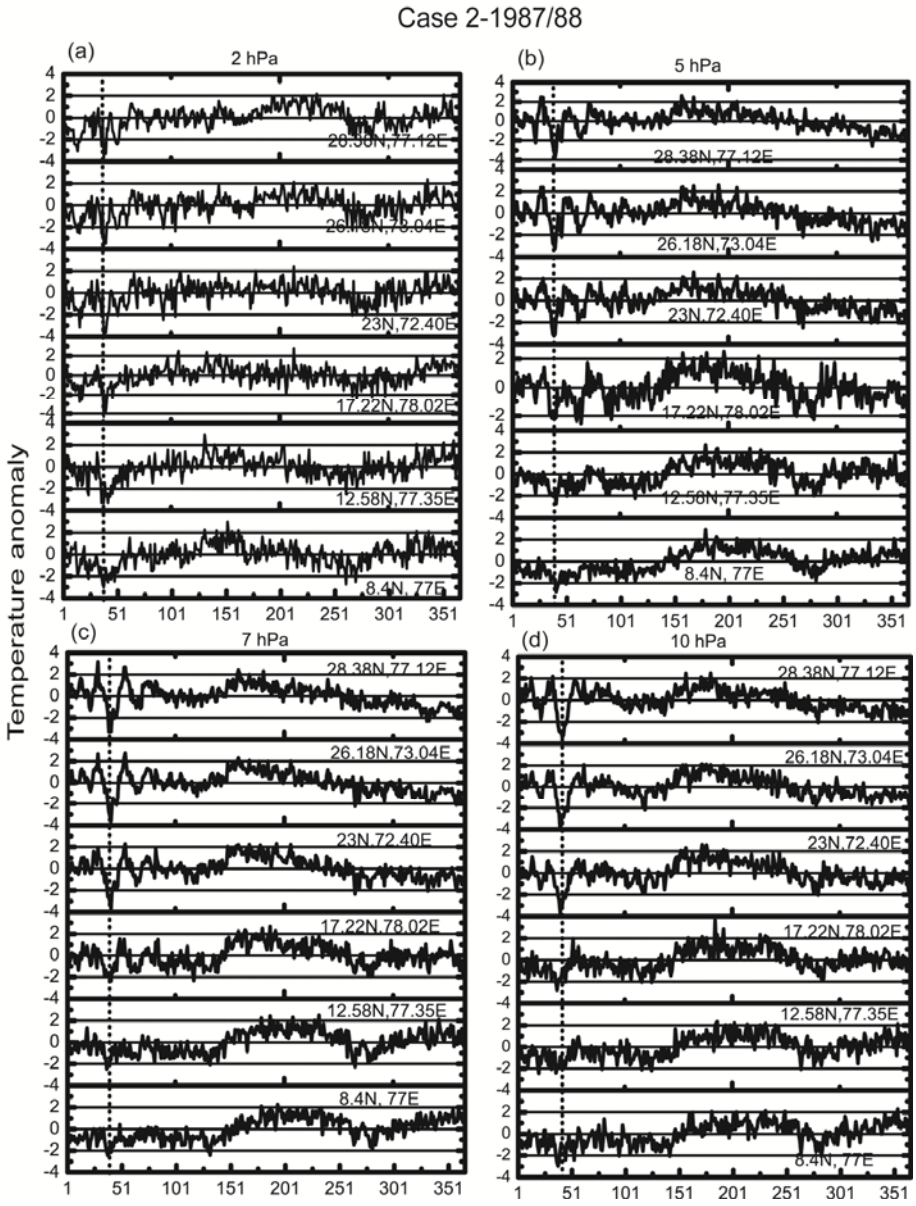

FIG. 5.13. Same as 5.12 but for the period 1 November 1987 to 31 October 1988.

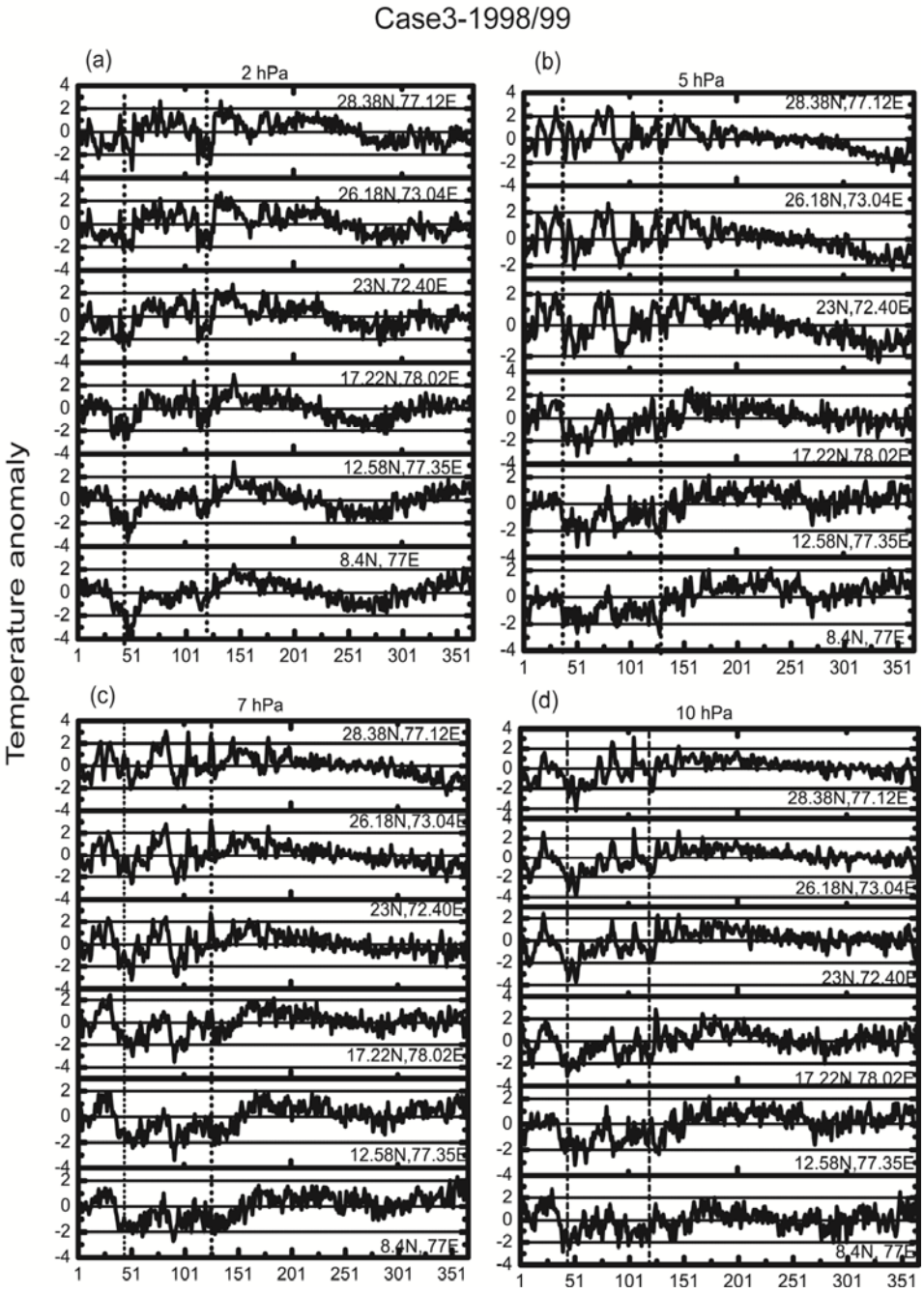

FIG. 5.14. Same as 5.12 but for the period 1 November 1998 to 31 October 1999.

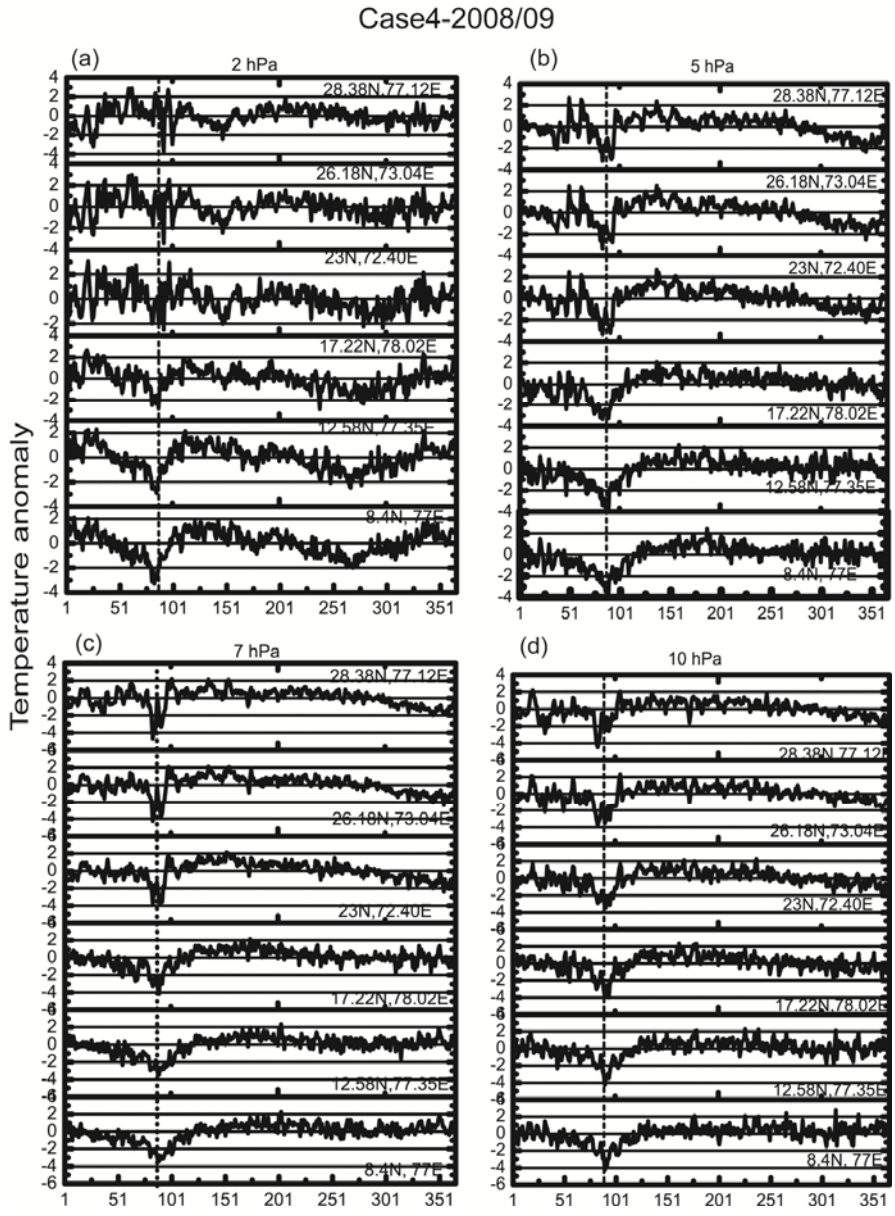

FIG. 5.15. Same as for 5.12 but for the period from 1 November 2008 to 31 October 2009 over six Indian stations.

In all the four cases stratospheric temperatures over Indian regions attained the annual minimum temperatures around the peak intensity of SSW. This indicates the presence of a very strong coupling between Indian regions and high- latitude regions when SSW exists. This result generally

agrees with the results reported from a single equatorial station using weekly rocket data (Appu 1984). The present study shows the spatial structure of the cooling effect over the Indian regions. At 5 hPa, 7 hPa and 10 hPa height levels the intensity is maximum towards north Indian regions. At the upper most level the cooling intensity is almost same.

The mechanism responsible for the out of phase relation is explained due to the increased wave activity which drives the upward motion in the polar stratosphere and as a result temperature decreases in the low latitudes by the induced wave activity (Kodera, 2006). Eguchi and kodera (2007) also examined the relation between stratospheric warming and tropical cooling. The connection between tropics and Polar regions through quasi 16-day wave propagation from equator to pole, and the persistent of zero wind line over tropics ~60 days prior to the major SSW' s is reported by Vineeth et al. (2008). Using thermo dynamical analysis with ERA-interim data Yoshida and Yamazaki (2001) analyzed the temperature in the tropical upper stratosphere during the SSW in 2009. Prior to the peak of major warming on 23 January 2009 at 70 hPa, a cold anomaly propagated downward over tropics between 150 and 200 hPa on 18 January 2009. Kodera et al. (2011) analyzed the tropical strartospheric and tropospheric circulation features associated with the above January 2009 SSW event. The sudden cooling in the stratosphere causes a change in meridional circulation system, resulting in tropical upwelling followed by an enhanced convective activity in the south of the equator.

5.4. Summary and Conclusion

The main focus of this chapter is to study the tropical stratospheric response during the major as well as minor SSWs occurred in the winters of 1984/85, 1987/88, 1998/99 and 2008/09. Zonal mean temperature anomalies give the intensity of tropical (30°N-30°S) perturbations

associated with the high- latitude warmings. The ECMWF ERA-40 and interim reanalysis data are utilized to examine the features of seasonal temperature anomalies for the selected six stations in the Indian regions. This study delineated the nature of the spatial and temporal distribution of the tropical stratospheric cooling during resulting from SSWs. The seasonal minimum temperatures occurred during the major SSW events over the six Indian regions are coincides with annual minimum values. SSWs are accompanied by severe cooling over the stratospheric layers.

The annual maxima over the polar stratospheric temperatures coincide with the annual minimum over the tropical stratosphere. The polar perturbations and its resultant equatorial perturbations are peaked on the same day. Even though the magnitudes of temperature variations are different at both the regions, qualitatively the temperature variations are same. The ratio of the warming in polar stratosphere and cooling equatorial stratosphere is of the order of 5:1.

After the decay of SSWs, the vortex shows the signs of recovery in the upper stratosphere. During this period the equatorial thermal structure shows a positive temperature gradient as result of the coupling between polar and equatorial regions. The above results are evaluated based on only four events. To make a detailed study, more cases are to be analyzed.

From this analysis it is imperative that one can anticipate a severe cold stratosphere over the Indian regions along with major warmings. A strong perturbation in the stratospheric temperature can alter the equilibrium conditions of the tropical stratosphere. Consequently dynamical, chemical and radiative process over the tropical stratosphere may undergo sudden changes.

Presently major warmings can be successfully predicted one or two weeks ahead. When a major warming is predicted, we can expect a very cold stratosphere over the Indian regions with in one-two weeks time. This prior information may have applications in predicting high altitude balloon trajectories, variations in ozone profiles etc. Hence the study indicates certain applicational aspect of the SSWs for the tropical regions.

Chapter 6

Stratospheric and Tropospheric Circulation Features over Tropics and Surface Cooling over Indian Region during SSW events

6.1. Introduction

Sudden stratospheric warmings in the Northern Hemisphere can also affect the tropospheric climate through meridional circulation (Kodera et al. 2006 and Kuroda Y, 2008). Kodera et al. (2011) also analyzed the convective activity in the tropical belt of 20°N-20°S and associated circulation features during January 2009 stratwarm events.

Mesospheric region experienced cooling during sudden stratospheric warming episodes and is reported by Matsuno (1971) and Labitzke (1972). Recently mesospheric cooling is evidenced by measurements from ground based lidars and space born infrared observation (Siskind et al. 2005; Thayer and Livingston 2008 and Waltershceid et al. 2008). Mesospheric warming also reported from an equatorial station, Thumba associated with the SSWs (Appu 1984). These studies (Labitzke 1972 and Appu 1984) showed the mesospheric warming take place above and 52 km altitude while stratosphere undergoes severe cooling.

Liu et al. (2011) reported that strong cooling of 50°K over thermospheric region is noted during January 2009 stratwarm event and it could also influence on the ionospheric regions. In relation with the cooling, zonal wind reverses to easterly at mesospheric and lower thermospheric heights (Gregory and Manson, 1975; Cevolani, 1989, 1991; Singer et al. 1994; Jacobi et al. 1997). Equatorial ionospheric region also exhibits a unique and distinctive daytime pattern during the stratwarm events like December 2000, January 2003 and January 2008 (Chau et al. 2009).

Equatorial winds in the stratosphere act as a wave guide for the midlatitude planetary wave propagation. Thus it can influence the frequency of stratospheric warmings (Gray et al. 2001). Sridharan and Sathishkumar (2008) anlayse the interannual variability of gravity wave variances in the altitude 84-94 km over Thirunelveli. According to them the enhanced gravity wave variances are coincides with the eastward phase of Quasi Biennial Oscillation (QBO) and stratospheric warming events during 2000, 2004 and 2006 years.

The high-latitude stratospheric warming and equatorial cooling is simultaneously observed (Fritzs and Soules 1970, 1972). Associated with the major SSW perturbations, the surface temperature anomalies over Indian regions show a decrease of 6°C (Appu 1984). This result is obtained based on the daily T-maximum temperatures obtained from Indian Meteorological Department (IMD). The out of phase relation between the tropics and the extra tropics temperatures arises as a result of the wave driven Lagrangian mean meridional circulation (Yulaeva et al. 1994). The relation between tropical and high-latitude stratospheric temperatures is explained by a compensating mechanism of adiabatic warming /cooling in the two regions through Brewer Dobson circulations (Young et al. 2005).

The previous chapter 5 examined the temperature perturbation during strawarm events over selected tropical stations. In the present chapter we have analysed the same stratwarm events (1984/85, 1987/88, 1998/99 and 2008/09) and its circulation features over the tropical stratospheric levels. Tropical upwelling and the variations in the meridional circulation is also examined. Consecutive 3-day mean of meriodional wind anomaly is used to calculate the mass stream function. Thus we can analyse the tropospheric circulation features associated with SSWs. To study the effect of SSWs over the surface layers of the Indian regions temperature anomaly from the seasonal mean over the chosen Indian region is also carried out.

6.2. Data and methodology

The ECMWF ERA-40 zonal wind data is used to calculate the anomaly over the tropics (20°N-20°S) for 1984/85 and 1987/88 stratwarm events from the long term mean of 1969-1989 and interim reanalysis data is utilized for the period 1990-2010 for 1998/99 and 2008/09 events. The zonal averaged (0-360) zonal wind anomaly is calculated for the selected pressure levels ranging from mid-to upper stratospheric levels. Vertical velocity is taken from the above two data sets at 850 hPa, 500 hPa, 100 hPa, 50 hPa, and 10 hPa levels. Then zonal mean vertical velocity is averaged over tropics (20°N-20°S) and a seven day running mean is also performed. Meridional (v) and vertical velocity (w) wind from 1000 to 100 hPa levels are plotted for each stratwarm case over tropical region (30°N-30°S). Thus we can examine the tropospheric perturbation associated with SSWs. Mass meridional stream function is used to study the meridional circulation changes during four SSWs. Zonal averaged (0-360) meridional wind anomalies from the long term mean of 1980-2010 period is

utilized to calculate mass stream function. Consecutive 3-day mean of meridional wind anomaly before, during and after the SSW events are used.

Zonally averaged mass continuity equation is computed from the relation

$$\frac{\partial[\bar{v}]\cos\phi}{R\cos\phi}+\frac{\partial[\bar{w}]}{\partial p}=0 \qquad \ldots 6.1$$

Where [v] is the temporal and zonal averaged meridional velocity, ω is the vertical velocity in pressure co-ordinates, *R* is mean radius of earth and p is pressure.

Introducing a Stokes stream function ψ, given by equation

$$[\bar{v}]=g\frac{\partial\psi}{2\pi R\cos\phi\,\partial p} \qquad \ldots 6.2$$

We can calculate the ψ field, assuming $\psi=0$ at the top of the atmosphere and integrating the equation downward to the surface.

$$\psi=\frac{2\pi R\cos\phi}{g}\int_{p}^{p_0}[\bar{v}]dp \qquad \ldots 6.3$$

Using this Stokes stream function, we can analyze meridional circulation changes associated with each stratwarm events.

To investigate the influence of stratospheric warming at surface level (1000 hPa), temperature anomalies from the winter mean are calculated for the selected Indian regions separately.

6.3. Results and Discussion

6.3.1. Features of zonal wind anomalies over tropics associated with the four stratwarm events (1984/85, 1987/88, 1998/99 and 2008/09)

In this section we analyzed the zonal mean zonal wind variations in the stratospheric levels over the tropical region (20°N-20°S) during the four stratwarm events. The high-latitude polar warming events in each case showed maximum tropical cooling on the peak days (chapter 5). At this time, whether the temperature variation in the tropics has the coherent effect on the zonal wind anomalies over the same area is analyzed. Figure 6.1 shows latitude time cross-section of zonal mean (0-360) zonal wind anomalies for 1984/85 (left) and 1987/88 (right) stratwarm events at 2 hPa, 5 hPa, 7 hPa and 10 hPa levels. The peak days of each event is represented by vertical arrows.

The low-latitude circulation responds to the high-latitude warming phenomena only at upper stratospheric or mesospheric levels. During 1984/85 stratwarm event, the intensification of easterly wind anomalies is noticed at 2 hPa levels about one week prior to the peak day. Duration of the easterly wind anomalies at upper stratosphere started from 16 December 1984 to 16 January 1985 (Fig.6.1a). The variations in the zonal wind anomalies are visible only in the upper stratospheric level (2 hPa), the lower levels are dominated by westerly wind anomalies throughout the season. No variation is seen at 5 hPa, 7 hPa and 10 hPa levels (Fig.6b, c, d) with respect to the peak day of stratwarm events.

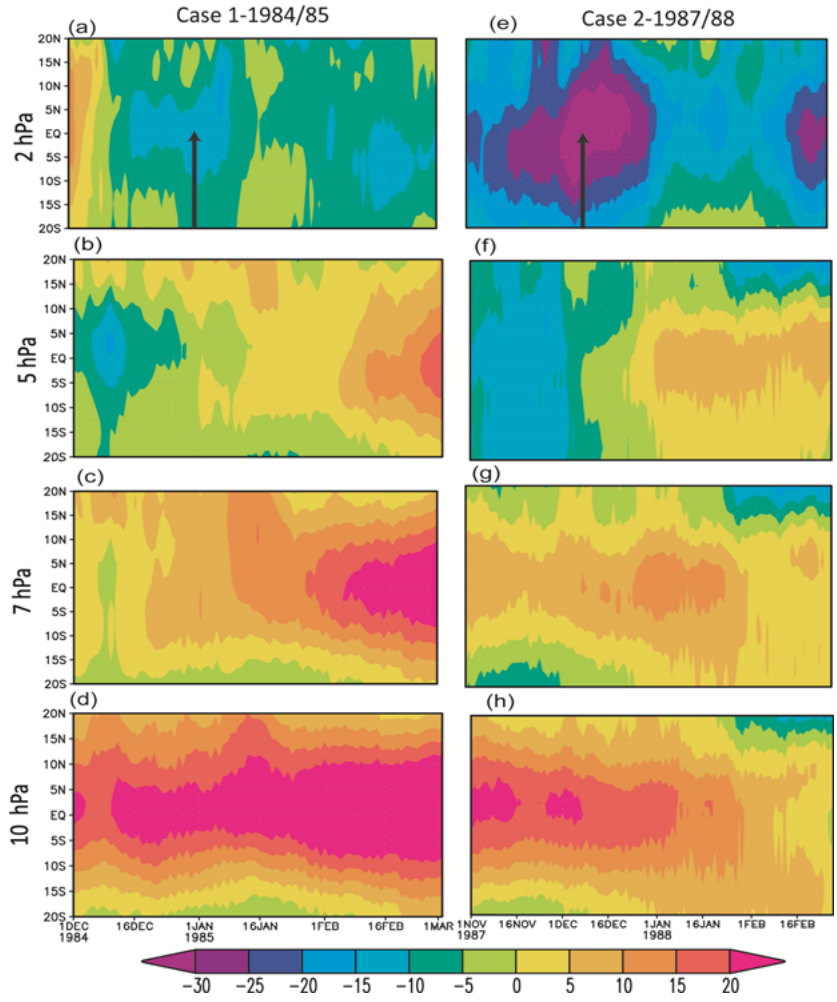

FIG.6.1. Zonal wind anomaly over tropics (20°N-20°S) during 1984/85 and 1987/88 stratwarm events at 2 hPa, 5hPa, 7hPa and 10 hPa levels. The peak days of the event are denoted by arrows.

The same features are evident in fig. 6.1e for the time period 1November 1987 to 28 February 1988. Easterly wind anomalies are observed at 2 hPa level more than one week before and after the peak day with an intensity of -30 ms^{-1}. The intensification of easterly wind is limited to 2 hPa

levels only. It shows that the downward propagation of zonal wind anomalies is confined from mesosphere to upper stratospheric levels.

Hoffman et al. (2007) showed that high-latitude sudden warmings in the stratosphere are connected with mesospheric cooling of about 10-20 °K of the 90 km region over the region Andenes (69°N, 16°E). The cooling process in the mesospheric region leads to the reversal of mean westerly winds to easterly. The mesospheric wind reversal is observed prior to the variation in stratospheric levels associated with SSWs. Mbatha et al. (2010) analyzed the dynamics of mesospheric circulation during the unprecedented southern hemispheric stratwarm event in September 2002. Mesospheric wind reversals are noticed almost one week prior to the reversals in stratosphere.

Figure 6.2a-h depicts the zonal wind anomalies over tropics at different stratospheric levels during 1998/99 and 2008/09 stratwarm events. In this case also the occurrence of the easterly wind at 2 hPa levels coincides with the peak day of the warmings. The intensity of the easterly wind ranges from -10 to -20 ms^{-1} during early winter (December 1998) and late winter (February 1999) warmings. The winter 1998/99 is characterized with mesospheric cooling and wind reversals. As a result, mesospheric variations propagate downward and it is visible in the 2 hPa zonal wind anomalies. The lower levels like 5 hPa, 7 hPa and 10 hPa are distinguished by westerly wind anomalies. In other words, from upper to mid-stratospheric levels the westerly component of wind or the westerly phase of the semiannual oscillation (SAO) is dominated.

In the case of 2008/09 stratwarm event, the circulation reversals from westerly to easterly are absent. The easterly phase of the SAO is noted in the

entire stratospheric levels. Easterly wind anomalies of 30 ms^{-1} are noted at 10 hPa level from the first week of December 2008 to 1 March 2009.

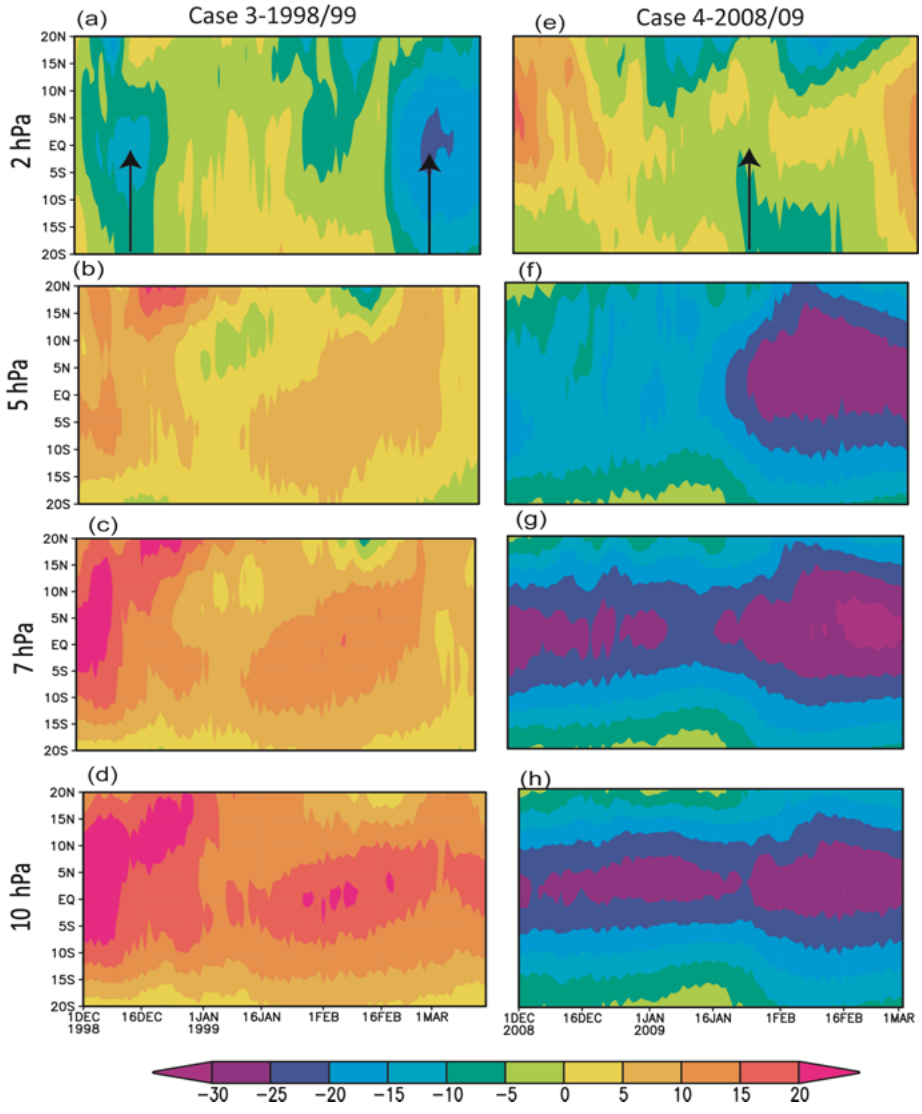

FIG.6.2. Zonal wind anomaly over tropics (20°N-20°S) during 1998/99 and 2008/09 stratwarm events at 2 hPa, 5hPa, 7hPa and 10 hPa levels. The peak days of the event are denoted by arrows.

6.3.2. Tropical upwelling (20°N-20°S) during stratospheric warming event

Figure 6.3a-e illustrates zonal mean (0-360) vertical velocity over tropical region (20°N-20°S) for the time period of 1December 1984 to 31 January 1985 at 850 hPa, 500 hPa, 100 hPa, 50 hPa and 10 hPa levels. The seven day running mean of vertical velocity is performed and it is multiplied by a constant of 1000. Prior to the peak day, a sharp decline (denoted as star sign) in vertical velocity is noticed at 500 hPa and 850 hPa levels (Fig 6.3d and e).

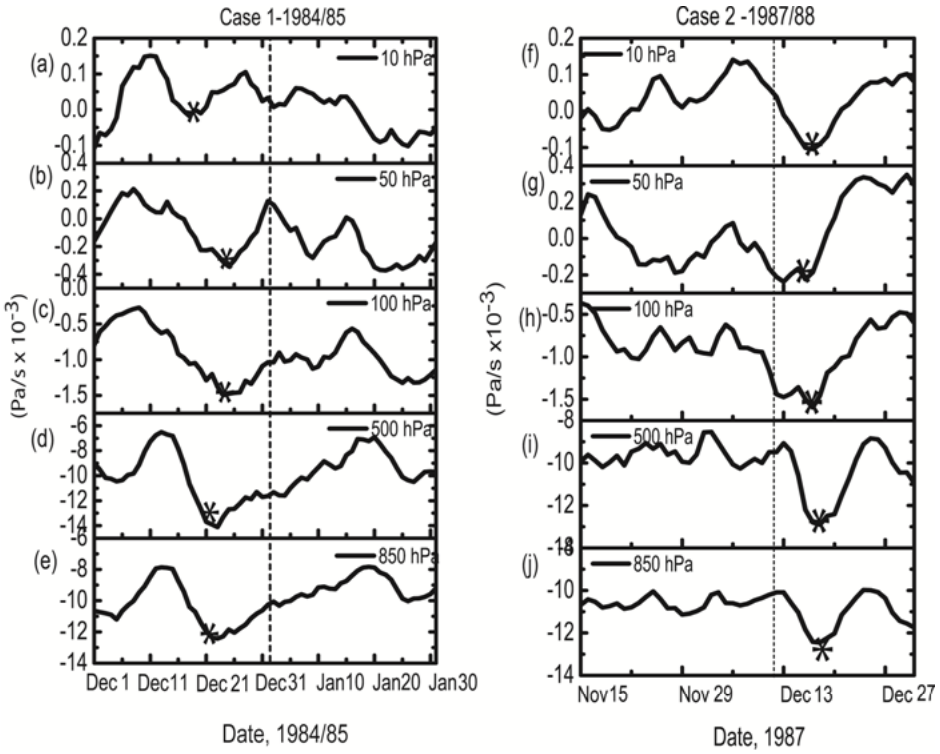

FIG.6.3 Time series of zonally averaged tropical (20°N-20°S) pressure coordinate vertical velocity at 850 hPa, 500 hPa, 100 hPa, 50 hPa and 10 hPa levels for 1984/85 (left) and 1987/88 (right) stratwarm events. The star sign denotes the decline in vertical velocity or upwelling in the tropical atmosphere. The dashed vertical line denote the peak day of warmings.

This sharp decrease started from 13 to 22 December 1984: The decline in velocity actually shows the increased upwelling in the tropical atmosphere during stratospheric warming days. The decrease in tropical temperatures and an increase in upwelling occur simultaneously during the SSW events. At mid-tropospheric and above levels (Fig. 6.3a-c) this decline of vertical velocity takes place especially before after the peak day (dashed line) with varying magnitudes at each levels. Mid-stratospheric (Fig. 6.3a) velocity shows a decline in magnitude on the peak day over tropics.

The case 2 stratospheric (Fig 6.3f-j) warming event for the time period 15 November 1987 to 15 December 1988 also shows the same features over the tropical atmosphere. The decline in velocity is noted after the peak day (13-18 December 1987) from lower tropospheric to mid-stratospheric levels. At lower tropospheric levels (Fig.6.3d and e) it varies from -10 to -12 ms^{-1} over the same time period. The decrease in velocity is taken place after the peak day at 100 hPa and 50 hPa levels (Fig.6.3g and h). At 10 hPa levels we can observe a sharp decline followed by an increase in velocity. The decrease in velocity is started prior to the peak day (dashed line), and then it takes another ten days to reach below normal value (Fig.6.3f, star).

Figures 6.4a-e show the time series of vertical velocity at different pressure levels averaged over tropics (20°N-20°S). The time series ranges from 1 December 1998 to 6 March 1999. Two stratospheric warming pulses in a single winter are noticed in this winter and the peak days are represented by a dashed vertical line. The decline in velocity associated with the early SSW event is denoted by star sign.

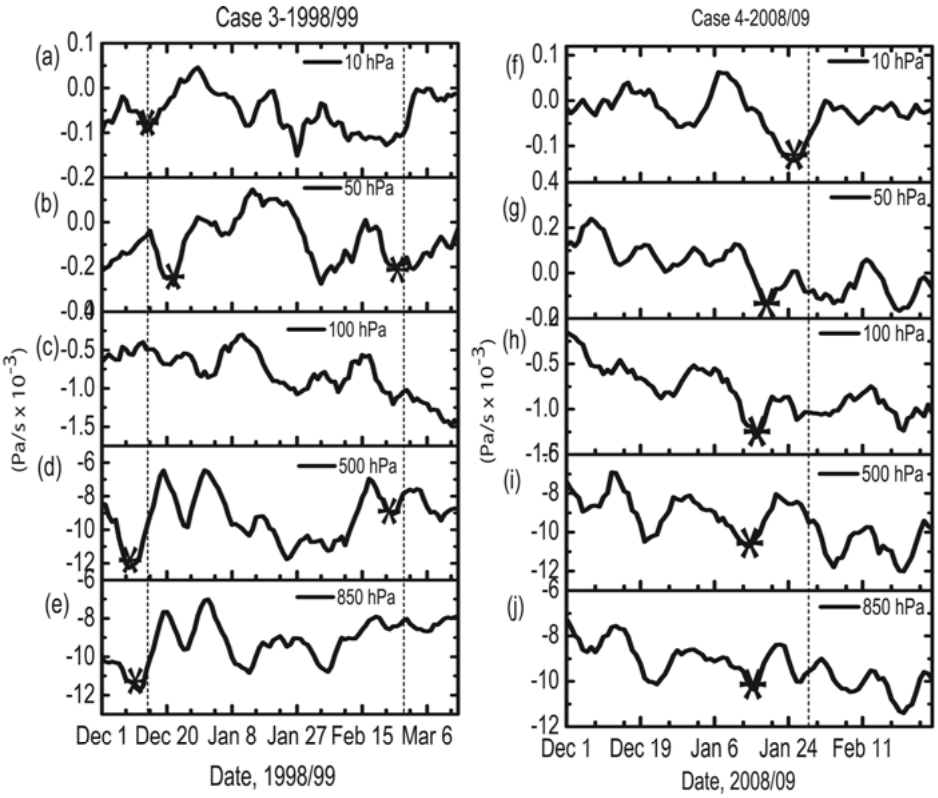

FIG.6.4. Time series of zonally averaged tropical (20°N-20°S) pressure coordinate vertical velocity at 850 hPa, 500 hPa, 100 hPa, 50 hPa and 10 hPa levels for 1998/99 (left) and 2008/09 (right) stratwarm events. The dashed line represents the peak days and the star sign denote the decline in vertical velocity associated with the peak days.

The tropical tropospheric layers like 850 hPa and 500 hPa levels show considerable variations prior to the peak day. The magnitude of variation ranges from -12 ms^{-1} to -6 ms^{-1} with in period of 12-20 December, 1998 followed by an upwelling up to 25 December, 1998. The lower stratospheric upwelling (Fig.6.4b) coincide with the peak day on 15 December, 1998 up to 22 December, 1998. It indicates the duration of the variations in velocity with respect to the peak day; approximately it takes 8 days from minimum to a

maximum peak phase. The mid-stratospheric variations in velocity nearly coincide with the peak day (Fig. 6.4a).

Over the tropical regions the upwelling of vertical velocity is also noticeable from troposphere to stratospheric levels during the 2008/09 stratwarm event (Fig. 6.4f-j). The time series ranges from 1 December 2008 to 28 February 2009 at different pressure levels. The upwelling is observed prior to the peak day from lower troposphere to mid-stratopsheric levels. At mid-tropospheric (100 hPa) level the vertical velocity declined from 6 January, 2009 and peaked on 16 January, 2009 (-1.31 ms^{-1}) then it is followed by an increase up to 22 January, 2009. It indicates the duration of the perturbations and it takes nearly 20 days to reach the normal value. In the upper levels, like 50 hPa and 10 hPa the perturbation shows similar patterns with varying magnitudes. The upwelling at 50 hPa level in association with the convective activity over SH is already explained by Kodera et al. (2009).

The planetary wave activity during SSW events induces hemispheric meridional circulation (Garcia 1987 and Randel 1993). The decline in the vertical velocity or the tropical upwelling is in evidence from the lower troposphere to mid stratospheric levels. The four stratwarm events show a tropical upwelling prior to the peak or after the peak days. As a result, the upwelling or adiabatic cooling nearly takes 10 days to vary from minimum to a maximum and the magnitudes varies from lower troposphere to mid stratospheric levels.

6.3.3. Circulation features in the tropical tropospheric levels

Figure 6.5 shows the tropical (30°N-30°S) tropospheric circulation patterns during (a) 1984/85, (b) 1987/88, (c) 1998/99 and (d) 2008/09 events.

For each winter period, the meridional wind and vertical velocity are used to examine the circulation features. The peak days are represented by vertical lines.

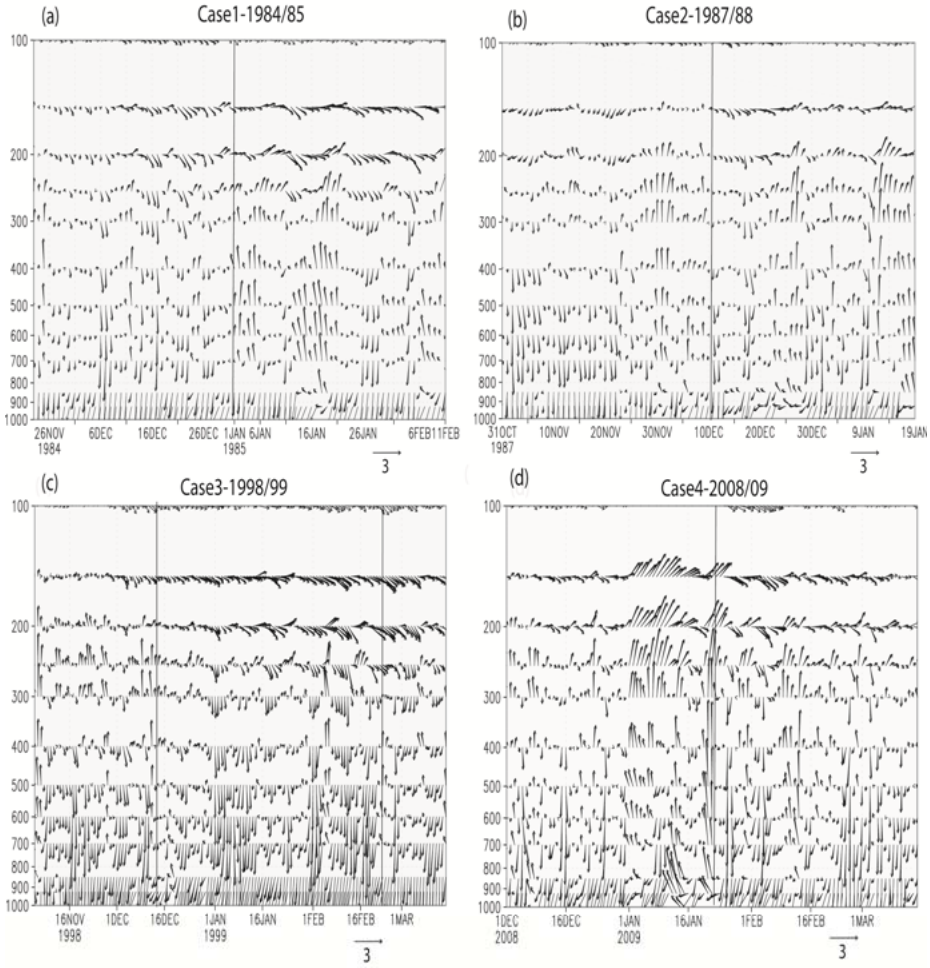

FIG.6.5. Vertical distribution of meridional wind (v) and vertical velocity (w) over the tropics (30°N-30°S) during (a) 1984/85, (b) 1987/88, (c) 1998/99 and (d) 2008/09 events.

In the troposphere, downward motion of circulation is noted prior to the peak day followed by an upward motion (Fig.6.5a). Analysis of case 2 event shows a strong downward motion in the last week of November 1987.

Subsequently the circulation pattern changes prior to the peak day. As a result, highly perturbed state is observed after the warming (Fig.6.5b) in December 1987.

Both the early and late winter warming pulses affect the tropospheric circulation system during the winter 1998/99. Therefore the whole winter period shows an enhanced downward propagation of circulations. The SSW events are found to be followed by the slowly propagating zonal mean zonal wind anomalies (Kodera et al. 2000; Zhou et al. 2002; Black et al. 2006) from stratospheric to tropospheric levels. This feature is evident in our study of the 2008/09 SSW event. Highly disturbed upward and downward motions take place in the tropical tropospheric levels corresponding to the peak phase.

6.3.4. Meridional circulation features

Mass meridional stream function is utilized to examine the evolution of the meridional circulation associated with the stratwarm events. Zonal mean (0-360) meridional wind anomaly from the long term mean of 1980-2010 periods is computed to analyze the wind features. Consecutive 3-day mean of meridional wind anomaly is plotted for the development, peak and decay phases for the four stratwarm events.

6.3.4.1. Mass meridional stream function: 1984/85

The figure 6.6 shows the 3-day consecutive mean of meridional circulation before, during and after the SSW event. Equatorial tropospheric levels are characterized by anomalous clock-wise circulation (SH Hadley cell) during the SSW periods, along with a weakened the polar cells (Fig.6.6a). The southern hemispheric easterly cell is prominent over 500 hPa to 200 hPa levels. Then the cell shows an extension towards the lower levels after the peak day.

The intensity of the tropospheric circulation or the rising motion is reduced after the SSW events (Fig.6.6d).

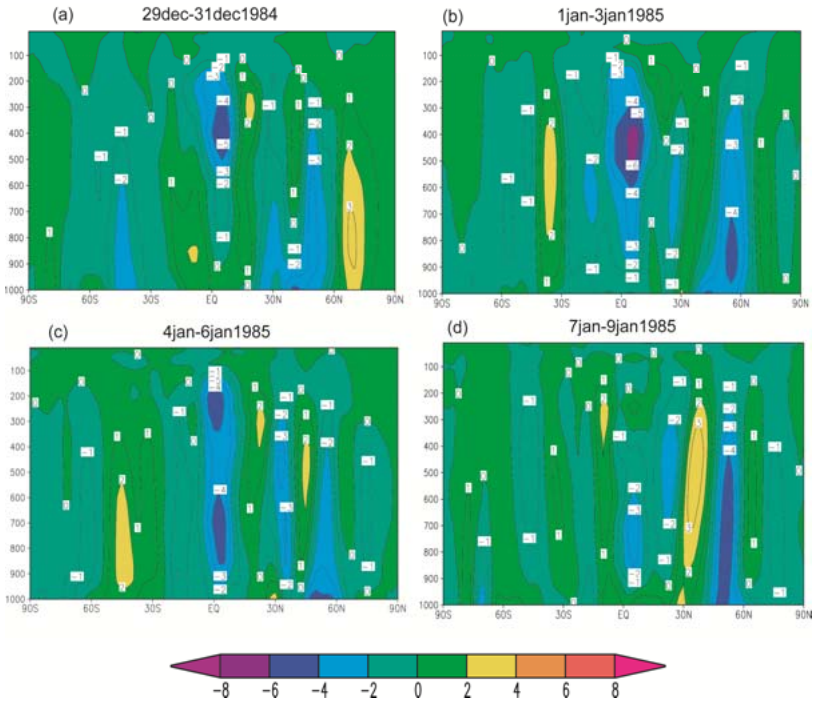

FIG.6.6. Mass meridional stream function for the stratwarm event of 1984/85. Consecutive 3 day mean is carried out (a) before, (b) during and (c and d) after the event. Positive contours indicate anti clockwise circulation, while the negative contours clockwise flow; intervals are $1e^{-10}$ *kg/s.*

6.3.4.2. Mass meridional stream function: 1987/88

Meridional circulation associated with 1987/88 SSW events is depicted in Fig.6.7a-d. During 6-8 December, 1987 the Hadley and Ferrel (Fig.6.7a) cells are noted with clock-wise and anti-clock wise circulations. Whereas during the peak days the Hadley and Ferrel cells are exhibited a weakening of the meridional cell structure (Fig.6.7b) in both the hemispheres. On 15-17 December, 1987 (Fig.6.7d), the anti-clock wise circulation is predominantly

seen over the whole tropospheric layers. The inter-hemispheric circulations during the SSW event are mostly modulating the tropospheric circulations through the meridional circulations.

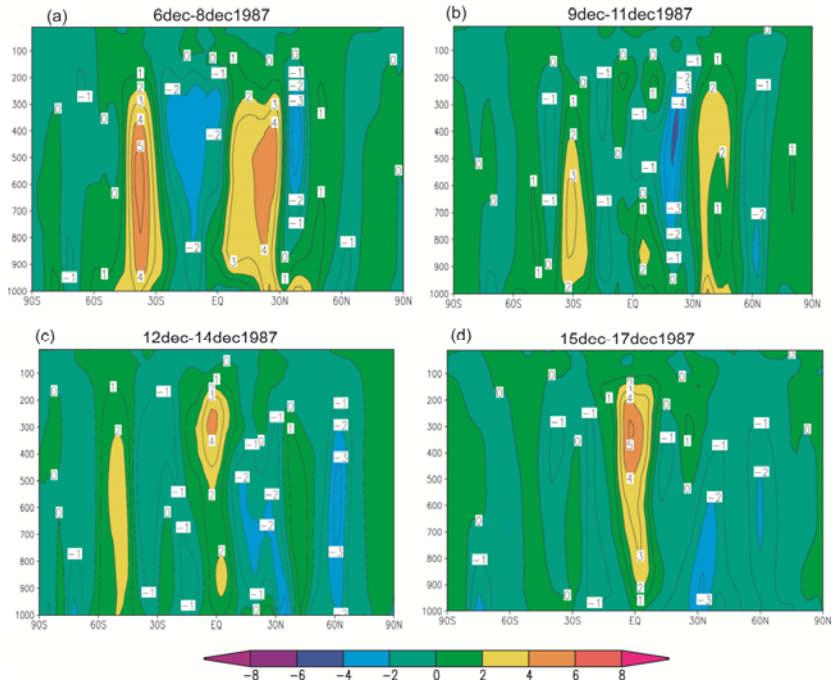

FIG.6.7. Mass meridional stream function for the stratwarm events of 1987/88. Consecutive 3 day mean is carried out (a) before, (b) during and (c and d) after the event. Positive contours indicate anti clockwise circulation, while the negative contours clockwise flow; intervals are $1e^{-10}$ *kg/s.*

6.3.4.3. Mass meridional stream function: 1998/99

The figure 6.8. shows the meridional circulation during the warming event in 1998/99. The Hadley cell in the NH (positive) undergo a weakening in its strength (Fig.6.8a-c) and the mid-latitudes cells are almost undetermined throughout the stratwarm days. The Hadley cell (positive) circulation becomes intensified after the warming episodes. The anomalous negative cell in the

Hadley circulation is not evident in the stratwarm days. It indicates the equatorial cells undergne an abrupt changes during the SSW days.

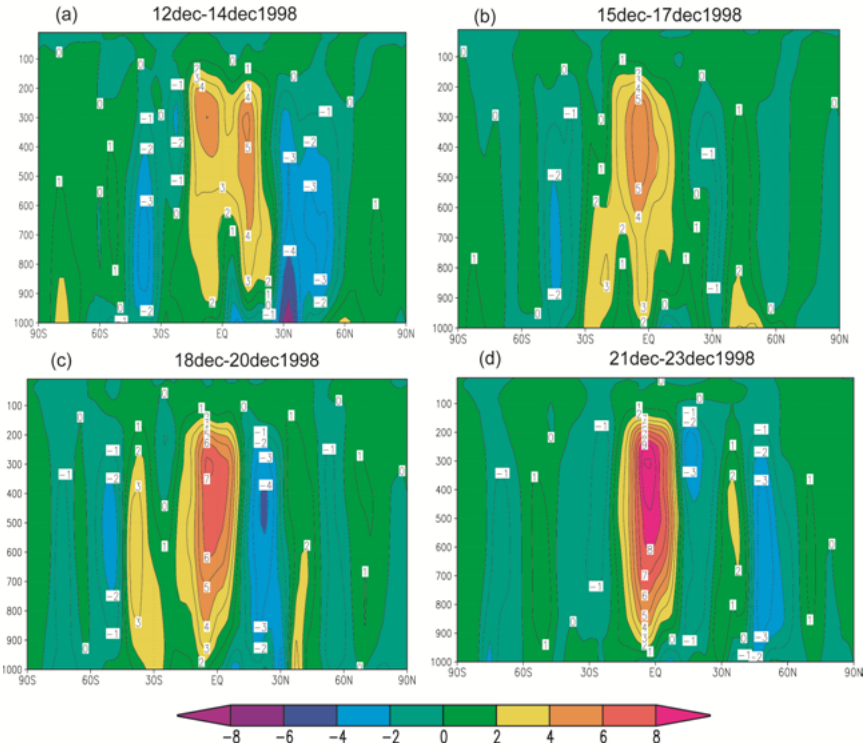

FIG.6.8. Mass meridional stream function for the stratwarm events in 1998/99. Consecutive 3 day mean is carried out (a) before, (b) during and (c& d) after the event. Positive contours indicate anti clockwise circulation, while the negative contours clockwise flow; intervals are $1e^{-10}$ *kg/s.*

6.3.4.4. Mass meridional stream function: 2008/09

The tropsopheric circulation features are explained through stream function in Fig 6.9 during the SSW event. The Hadley cells in both the hemispheres are active prior to the peak day (Fig.6.9a) along with the Ferrel and Polar cells. Along the equator on 22 to 24 January, 2009 the anti-clock wise circulation extend from 900 hPa to 200 hPa levels. After that the cell structure widens up to 30°N (Fig.6.9c). Sudden and abrupt changes in

tropospheric meridional circulation during the 2009 SSW event are noted by Kodera et al. (2011) in association with the inter-hemispheric meridional circulations.

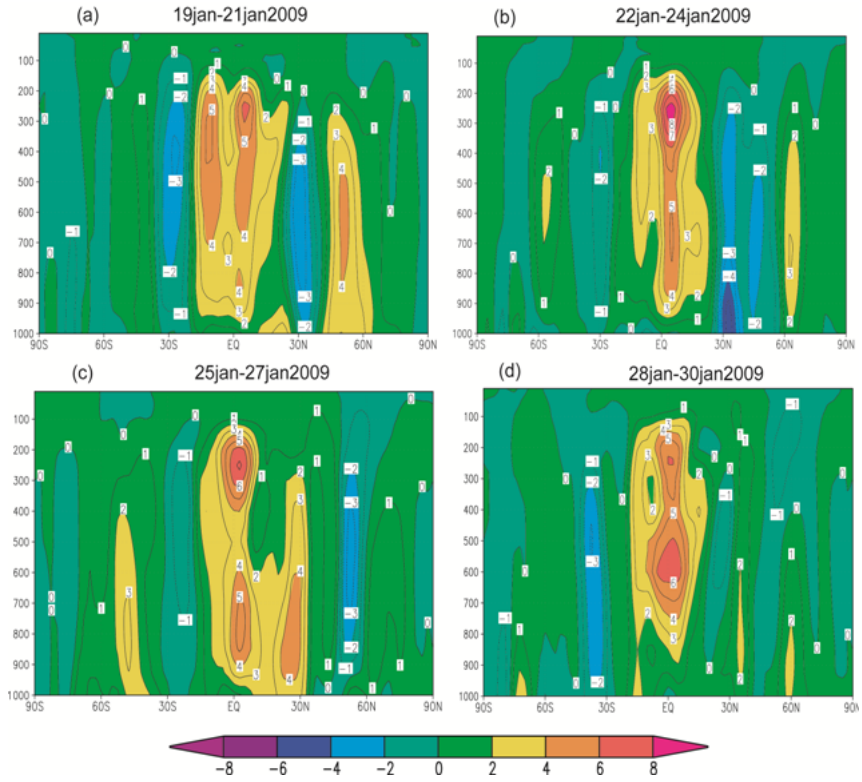

FIG.6.9. Mass meridional stream function for the stratwarm events in 2008/09. Consecutive 3 day mean is carried out (a) before, (b) during and (c& d) after the event. Positive contours indicate anti clockwise circulation, while the negative contours clockwise flow; intervals are $1e^{-10}$ *kg/s.*

6.3.5. Surface (1000 hPa) temperature anomalies during the winter season over the selected Indian regions

The surface temperature anomaly from the winter mean (DJFM) over six tropical Indian stations during 15 December 1984 to 31 January 1985 (left) and 15 November to 30 December 1987 (right) are depicted in Fig. 6.10. The

surface anomaly is found to decrease around 3 January, 1985 for all stations i.e., two days after the major stratwarm event in the year 1984/85.

As described in the chapter 5 equatorial upper stratosphere shows seasonal minimum temperatures during the peak day of high latitude stratospheric warming events. The temperature anomalies at 1000 hPa also show a decrease during the peak phase of stratwarm. Moreover this low temperature is the seasonal minimum values for all the Indian stations. The seasonal minimum values are -8.57°C (Fig. 6.10a), -10.09°C (Fig. 6.10b), on 3 January 1985 and -8.38°C on 2 January 1985 (Fig. 6.10c) and -6.13°C (Fig. 6.10d).

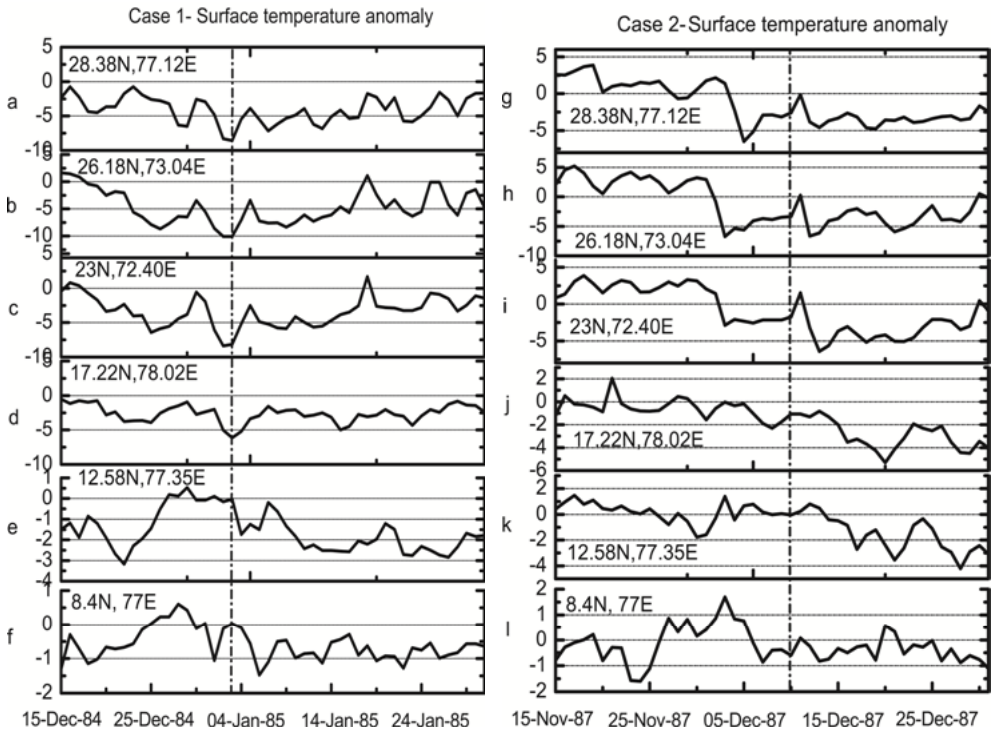

FIG. 6.10. Time series of 00 GMT surface (1000 hPa) temperature anomalies (ΔT °C) at six stations over Indian region for the winter season. The dashed lines denote the peak days of warming on 2 January 1985 and 10 December 1987 respectively.

The seasonal minimum days at surface levels coincide with the peak days of stratospheric warmings for the year 1984/85. The Hyderabad and Trivandrum regions are noticed with -1.74°C and 0.027°C of cooling on 4 January, 1985 and 3 January, 1985(fig.6.10e and f). The effect of minor warming is not evident in this case. The surface temperature anomalies over Jodhpur and Ahmedabad stations shows the seasonal minimum value of -6.63°C (Fig. 6.10h) and -6.42°C (Fig. 6.10i) on 12 and 13 December 1987. It indicates that the seasonal minimum values are noticed two or three days after the peak of case 2 stratwarm. In the North Indian station Delhi, seasonal minimum is observed on P_{-5} day with -6.48°C.

Figure 6.11 (a-f) illustrates temperature anomalies at 1000 hPa for the six chosen Indian stations during the case 3 SSW event for the period of 1 December 1998 to 31 March 1999. The dashed line represents the P_0 day of early major and final warmings. The low temperatures coincide with the P_0 day of the early December stratwarm event. But it does not match seasonal minimum values. In this case lower temperatures are not coincides with seasonal minimum value. During final warming day on 27 February, 1999 (dashed line) the minimum temperatures are not evident as in the case of early December, 1998 for all the selected stations.

The figure 6.11g-l shows the temperature anomalies at 1000 hPa level over six Indian regions for the time period of 20 December, 2008 to 28 February, 2009. The surface cooling is noticed prior to the peak day (P_0) over three north Indian stations during case 4 SSW of 2008/09. Delhi and Jodhpur station shows -8°C and -6°C of cooling on 20 January, 2009 and over Ahmedabad station cooling is -4°C on 26 January, 2009 (P_{+3} day). Such a sudden and severe cooling can affect the seasonal weather anomalies like

winter western disturbances etc over the north Indian regions. The average temperature decrease is noted with -7°C over North Indian stations and -2.5°C for south Indian stations.

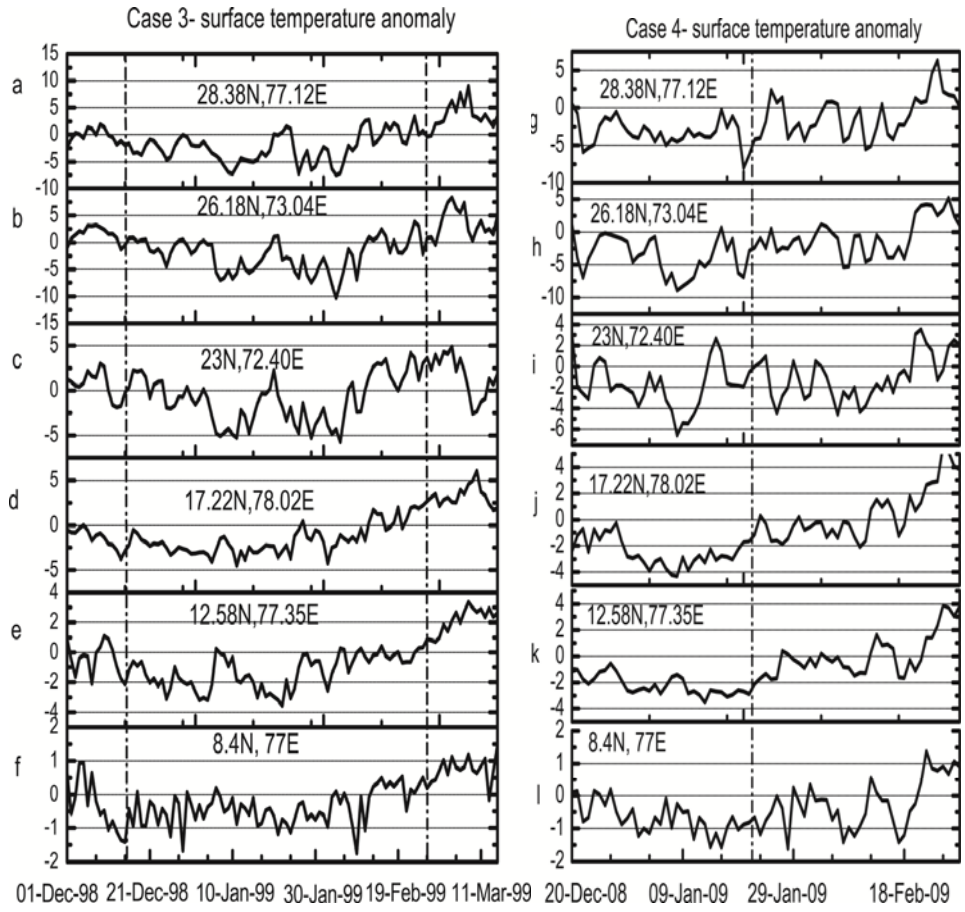

FIG. 6.11: Time series of surface (1000 hPa) temperature anomalies at 00 GMT for the period of 1 December 1998- 31 March 1999 (left), and 15 December 2008 – 15 March 2009 (right), for six Indian regions. The dashed lines denote the peak days of warming.

If the occurrence of major warming is predicted one can anticipate a cooling in the Indian surface regions especially in the North Indian stations within a few days. Further detailed studies are required to facilitate more aspect of the prediction procedures. Ramanathan (1977) in a theoretical study showed that the surface temperatures over the tropics may experience slight cooling as a result of the net reduction in the downward longwave flux from stratosphere to troposphere during SSW period. The net reduction is caused by the cooling in the tropical stratosphere. This study provides some observational evidence for the above prediction. During January 2009 SSW, tropical tropopause shows a cold anomaly especially at 150 hPa and 100 hPa levels. Yoshida and Yamazaki (2011) explained this tropopause cooling using Transformed Eulerian mean equations.

During stratospheric warming days the whole tropical atmosphere is in a perturbed state. Tropical upwelling is takes place from tropospheric to mid stratospheric levels correspondingly meridional circulation shows sudden and abrupt changes associated with the warming. These perturbations can affect the surface temperature anomalies thus we can observe a cooling effect in temperature anomalies within a short span of time.

6.4 Summary and Conclusion

The tropical tropospheric circulation features associated with four stratwarm event (1984/85, 1987/88, 1998/99 and 2008/09) are studied in this chapter. The zonal wind anomalies over tropical (30°N-30°S) stratospheric level (2 hPa) change its sign to easterlies of 30 ms^{-1} about a week prior to the onset of stratwarm. Similar features are found with three warming event except 2008/09 event. The wind anomalies at 5 hPa, 7 hPa and 10 hPa levels do not

undergo changes from westerly to easterlies. The wind anomalies in the lower tropospheric levels are unaffected by the stratospheric warming pulses in the high-latitude. From mid- to upper stratospheric levels westerly wind anomalies are dominating for case 1 to case 3 event, whereas easterly anomalies for case 4 event.

It is seen that a decline in vertical velocity or the tropical (20°N-20°S) upwelling is an inevitable part of the four SSW event. The upwelling takes place from lower troposphere to mid-stratospheric levels. Mostly the upwelling in the lower tropospheric levels is predominantly happened 10 days before and after the peak day. But over mid-stratospheric levels tropical upwelling is coincides with the peak day. The tropospheric circulation features in the tropics are undergone a very strong upward and downward motion after the peak day of high latitude warming. Therefore a high latitude warming is affecting the dynamics of the troposphere. There has been sudden and abrupt changes in meridional circulation are noted during the SSW events.

The tropical upper stratospheric cooling, upwelling in the troposphere regions induces decreases in the surface temperature anomalies. The surface temperature anomalies over six Indian regions show a decrease in temperatures corresponding to the peak day of high- latitude warming. Thus a sudden and severe surface cooling is attributed to the peak of major warmings over the Indian regions. The average surface cooling over North Indian station is -7°C and -2°C for south Indian regions.

Chapter 7

Summary and Future Scope of the Study

7.1. Summary

It is now well evident that stratospheric dynamical process plays an important role in the tropospheric dynamics on an extensive range of time scales through radiative, dynamical and mass transport process emerging from the coupling between stratosphere and troposphere. The doctoral thesis is mainly addressed the different features of Sudden Stratospheric Warming (SSW) events in Arctic hemisphere and its impact on the strato-tropospheric interactions in both the high and low-latitudes. The phenomenon of SSW is involved a two way vertical coupling through wave activity and resulting wave mean flow interaction. The wave activity is also reflected back to the troposphere affecting the dynamical pattern of tropospheric planetary waves. The SSW events are classified and its interaction between high and low-latitude regions, emphasizing Indian regions, is analyzed using ECMWF Era-40, interim and NCEP/NCAR reanalysis data. The major outcome of the study are presented as follows

Depending upon the intensity, zonal wind reversal, and the time of occurrence SSW events are classified as major, minor and final warmings based on 10 hPa level as the reference. In this chapter we classify the events considering two levels of 2 hPa ad 10 hPa. This is done deliberately in the light of observations that warming do occur in upper stratospheric level also. The SSW events are categorized into five groups based on the temperature and zonal wind anomalies over the polar region 60°-90°N. The

events occurred during the period 1980-2010 from 1980 to 2010 are considered. The five groups are (1) 'intense major', (2) 'major 1', (3) 'major 2', (4) 'intense minor' and (5) 'minor' warming depending on the different criteria at two levels: 2 hPa and 10 hPa.

The 'intense major' events at 2 hPa are consistent with the warming events at 10 hPa level in almost all the cases classified based on WMO criteria. The analysis reveals that the major warmings are increased during the decade 2000-2010 at both the levels. The intense major, major 1 and major 2 warmings are commonly termed as major warmings. 'Intense minor' and minor warmings are termed as minor warmings. Fifty percentages of the warmings are of major types and the other 50% are of minor types. The intra-seasonal variability in the intensity as well as frequency of warming events is also studied. Early winter warmings are observed regularly during 1997/98 to 2003/04 period and its average temperature anomaly (ΔT) is 30°C at 2 hPa level. This is high compared to late-winter warmings. Stratwarms are absent during a continuous period of seven years in mid-winter (January) month. The average peak intensity of the late winter warming is 20°C and 15°C at 2 hPa and 10 hPa respectively.

Downward propagation of temperature and zonal wind anomalies are strong around the peak days irrespective of the groups. Thus, each warmings system shows the behavior of downward propagation from upper to mid- stratospheric levels. Composite analysis also explains the position and the intensity of the warm vortex at both the levels. In addition, the position of the displaced polar vortex during major and minor stratospheric warming events is also analyzed. There is a shift in the longitudinal location of the cold centers from 180°W-360°W during the minor and major warmings at both the levels.

Analysis is also carried out on the circulation pattern in the Eastern Arctic domain (0-180°E) of two SSW events pertaining early, mid-winter and late winters. Consistent patterns are found between 10 hPa geopotentail height contours and 200 hPa circulation pattern during the above selected cases. The intense north-westerly wind flows from high to mid-latitudes around the peak days of SSWs through the low geopotential area (displaced cold polar vortex from North Pole). The north-westerly wind merges with subtropical westerly jet stream (STJ) at mid-latitudes. As a result, significant variations in the intensity of the STJ are observed. Normalized vertical wind shear shows the intensity of STJ is prominent duirng P_{-5} to P_{+5} days for early and mid-winter warming cases. The maximum perturbation is noticed during late winter case during P_{-5} to P_{+15} days with an increase in the 1.5 standard deviation prior to the warming.

Meridionally advected heat flux at 10 hPa level shows the perturbed wave activity associated with all the cases. Negligible amount of variation is observed from equator to mid-latitudes during the stratwarm days and maximum amount of variation is concentrated over high-latitudes (45°-75°N). The strongest meridionally advected transient heat flux is seen in the 2008/09 stratwarm event.

Total heat flux analysis at 10 hPa and 100 hPa levels is carried out for high and low-latitude regions. It indicates the presence of prominent wave activity prior to the peak day of warming over high-latitudes. Maximum heat flux is noted at 10 hPa level over the region 45° to 75°N during the composite of mid and late-winter stratwarm events compared to early warming cases. The mid tropospheric (100 hPa) heat fluxes over the same area are correlated. The coefficients are 0.82, 0.038 and 0.15 respectively for early, mid and late winter warming cases.

Mid-tropospheric and stratospheric heat fluxes over the low - latitudes (0-30°N) shows an out of phase relation during the peak days of warming. The cross correlation technique is applied between 10 hPa and 100 hPa heat flux over high-latitudes and it shows a lag correlation of 3 day, lead correlation of 5 day and also a lead correlation of 6 day respectively for the early, mid and late- winter stratwarm events. Over low-latitudes the cross correlation shows zero lag, lag of one day and lead of two days for above three events respectively.

The tropical stratospheric response during the major as well as minor SSWs in the winters of 1984/85, 1987/88, 1998/99 and 2008/09 are generally analyzed. This study delineated the nature of the spatial and temporal distribution of the tropical stratospheric cooling during SSWs. Zonal mean temperature anomalies over the tropical (30°N-30°S) stratosphere shows the intensity of cooling is maxima on the peak day of high-latitude warmings. Seasonal minimum temperatures over the six Indian regions are occurred during the peak phase of major SSW events. These seasonal minimum temperatures stand as the annual minimum values. This showed the presence of the most severe cooling phase in the winter stratosphere over Indian region occurring in association with SSWs. While polar stratospheric regions experience warmest temperatures, the tropical stratosphere experiences the coldest temperatures. The strong cooling over the Indian regions can be predicted when SSWs generate over the Polar regions.

The annual maxima over the polar stratospheric temperatures coincide with the annual minimum over the tropical stratosphere. The polar perturbations and its resultant equatorial perturbations are peaked on the same days. Even though the magnitudes of temperature variations are

opposite direction at both the regions, the temperature variations are the same qualitatively. The ratio between the warming in polar stratosphere and cooling in the equatorial stratosphere varies in 5:1. After the decay of SSWs the vortex shows the signs of recovery in the upper stratosphere, equatorial thermal structure shows a positive temperature gradient. This analysis shows a sudden and severe cold stratosphere over the tropics is predictable along with major warmings.

The zonal wind anomalies in the tropical upper stratosphere (2 hPa) are reversed to easterlies with -30 ms^{-1} with respect to the warming in the high latitude. The tropical upwelling is observed around the peak days from lower troposphere to mid-stratospheric levels during the four stratwarm cases. The meridional circulation also experiences a sudden and abrupt change during the warming episodes. As a result of the coupling process, cooling in the surface layers is also visible over the Indian regions. The SSW associated coupling is well evident from surface to upper stratosphere.

7.2. Future scope

The present study illustrates a classification of SSW and its relation with the dynamics of the tropical atmospheres. The study also brought out more features on the intensity of upper stratospheric cooling over Indian region. In the light of the present results more parameters like stratwarms and QBO, Elnino and Ozone are also to be analyzed for a better understanding on the interaction between polar and tropical regions. The planetary waves play an important role in regulating the warming over polar stratosphere. It could also have a significant contribution in the dynamics over tropics. These aspects are to be analyzed further through observations and modeling in order to have a better understanding of the inter-hemispheric circulation system associated with SSWs.

REFERENCES

Alexander, S. P., and M. G. Shepherd, 2010: Planetary wave activity in the polar lower stratosphere. *Atmos. Chem. Phys.,* **10**, 707-718.

Alexeev, V. A., I. Esau, I. V. Polyakov, S. J. Byam, S. Sorokina, 2012: Vertical structure of recent arctic warming from observed data and reanalysis products. *Climatic change.,* **111**, 215-239.

Ambaum, M. H. P., B. J. Hoskins, and D. B. Stephenson, 2001: Arctic Oscillation or North Atlantic Oscillation? *J. Climate.,* **14**, 3495–3507.

Ambaum, M. H. P., and B. J. Hoskin, 2002: The NAO troposphere-stratosphere connection. *J. Climate.,* **15**, 1969–1978.

Andrews, D. G., J. R. Holton, and C. B. Leovy, 1985: Middle atmosphere dynamics. *Academic Press*, 489 pp.

Appu K. S., 1984: On perturbations in the thermal structure of tropical stratosphere and mesosphere in winter. *Indian J Radio Space Phys.,* **13**, 35-41.

Appu K S., 2001: Cooling over the Indian surface regions associated with the Polar stratospheric winter warming. *J. Mar. Atmos.,*vol 2,no 1, 16-21.

Asnani, G.C., 1993: Tropical Meteorology, 822 Sind Society, Aundh, Pune, India.

Baldwin, M. P., and J. R. Holton, 1988 : Climatology of the stratospheric polar vortex and planetary wave breaking. *J. Atmos. Sci.,* **45**, 1123-1142.

Baldwin, M. P., and T. J. Dunkerton, 1989: The stratospheric major warming of early December 1987. *J. Atmos. Sci.,* **46**, 2863-2884.

Baldwin, M. P., and T. J. Dunkerton, 1999: Propagation of the Arctic oscillation from the stratosphere to the troposphere. *J. Geophys. Res.,* **104**, 30 937–30 946.

Baldwin, M. P., and T. J. Dunkerton, 2001: Stratospheric harbingers of anomalous weather regimes. *Science.,* **294**, 581–584.

Bancalá, S., K. Krüger, and M. Giorgetta, 2012: The preconditioning of major sudden stratospheric warmings, *J. Geophys. Res.*, **117**, D04101, doi: 10.1029/2011JD016769.

Barnett, J. J., 1975: Large sudden warming in the Southern Hemisphere. *Nature* **255**, 387 - 389 (29 May 1975); doi:10.1038/255387a0.

Bencherif, H., D. V. Charyulu, L. E. Amraoui, V.-H Peuch, N. Semane, and A Hauchecorne, 2007: Examination of the 2002 major warming in the Southern Hemisphere using ground-based and Odin/SMR assimilated data: stratospheric ozone distribution and tropic/mid-latitude exchange. *Cana. J. Physics.,* **85**: 1287–1300.

Black, R. X., 2002: Stratospheric forcing of surface climate in the Arctic Oscillation. *J. Climate.,* **15**, 268–277.

Black, R. X., and B. A. McDaniel, 2006: The dynamics of the northern hemispheric stratospheric final warming events. *J. Atmos. Sci*., **64**, 2932-2946

.

Black, R. X., B. A. McDaniel, W. A. Robinson, 2006: Stratosphere–troposphere coupling during spring onset. *J. Climate*., **19** (19), 4891–4901.

Blume, C., K. Matthes and I. Horenko, 2012: Supervised learning approaches to classify sudden stratospheric warming Events. *J. Atmos. Sci.*, **69**(6), 1824-1840. doi:10.1175/JAS-D-11-0194.1.

Boccara, G., A. Hertzog, C. Basdevant, and F. Vial, 2008: Accuracy of NCEP/NCAR reanalyses and ECMWF analyses in the lower

stratosphere over Antarctica in 2005. *J. Geophys. Res.*, **113**, D20115, doi:10.1029/2008JD010116.

Brewer, A. W., 1949: Evidence for a world circulation provided by measurements of helium and water 30 vapor distributions in the stratosphere, *Q. J. Roy. Meteor. Soc.*, **75**, 351–363, 13831.

Brönnimann, S., A. N. Grant, G. P. Compo, T. Ewen, T. Griesser, A. M. Fischer, M. Schraner, A. Stickler., 2012: A multi-data set comparison of the vertical structure of temperature variability and change over the Arctic during the past 100 years. *Climate Dynam.*, 1-22

Butchart, N., S. A. Clough, T. N. Palmer, and P. J. Trevelyan, 1982: Simulations of an observed stratospheric warming with quasi-geostrophic refractive index as a model diagnostic. *Quart. J. Roy. Meteor. Soc.*, **108,** 475–502.

Cevolani, G., 1989: Long period waves in the middle atmosphere: response of mesospheric and thermospheric winds to recent minor stratospheric warmings at mid-latitudes. *Ann. Geophys.*, **7**, 451–458.

Cevolani, G., 1991: Strato-meso-thermospheric coupling at mid-latitudes in the course of mid-winter stratwarmings during DYANA. *Geophys. Res. Lett.*, **18**, 1987–1990.

Chan, S. C., and S. Nigam, 2008: Residual diagnosis of diabatic heating from ERA-40 and NCEP reanalyses: Intercomparisons with TRMM. *J. Climate*., **22**, 414-428.

Chao, W. C., 1985: Sudden stratospheric warmings as catastrophes. *J. Atmos. Sci.*, **42,** 1631-1646.

Charlton, A. J., and L. M. Polvani, 2007: A new look at stratospheric sudden warmings. Part I: Climatology and Modeling Benchmarks. *J. Climate.*, **20**, 449-469.

Charlton, A. J., L.M. Polvani, Ju. Perlwitz, F. Sassi, E. Manzini, K. Shibata, S. Pawson, J. E. Nielsen, and D. Rind, 2007: A new look at stratospheric sudden warmings. Part II: Evaluation of numerical model simulations. *J. Climate*, **10**, 470-488, doi:10.1175/JCLI3994.1.

Charney, J. G., and P. G. Drazin, 1961: Propagation of planetary scale waves from the lower atmosphere to the upper atmosphere. *Geophys. Res.*, **66**, 83-109.

Chau, J. L., B. G. Fejer, and L. P. Goncharenko 2009: Quiet variability of equatorial E × B drifts during a sudden stratospheric warming event. *Geophys. Res. Lett.*, **36**, L05101, doi:10.1029/2008GL036785.

Clark, J. H. E., 1974: Atmospheric response to the quasi-resonant growth of forced planetary waves, *J. Meteorol. Soc. jpn.*, **52**, 143-163.

Cohen, J., J. Jones, 2011: Tropospheric precursors and stratospheric warmings. *J.Climate.*,**24**,6562–6572.doi: http://dx.doi.org/10.1175/2011JCLI4160.1.

Chen, W., and K. Wei, 2009: Interannual variability of the winter stratospheric polar vortex in the Northern Hemisphere and their relations to QBO and ENSO. *Adv. Atmos. Sci.*, **26**. Issues 5, 855-863.

Cordero, E, P. A. Newman, W. Clark, and E. Fleming. "Chapter 6: Stratospheric Dynamics and the Transport of Ozone and Other Trace Gases". *Stratospheric Ozone: An Electronic Textbook*. http://www.ccpo.odu.edu/~lizsmith/SEES/ozone/class/Chap_6/index.htm. Retrieved 25 Jan 12.

Craig, R. A., and W. S. Hering, 1959: The stratospheric warming of January-February 1957. *J. Meteor.*, **16**, 91-107.

Dee, D. P., and 35 co-authors, 2011: The ERA-Interim reanalysis: Configuration and performance of the data assimilation system. *Quart. J. R. Meteorol. Soc.*, **137,** 553-597. DOI: 10.1002/qj.828.

Dee, D. P., and S. Uppala, 2009: Variational bias correction of satellite radiance data in the ERA-Interim reanalysis. *Quart. J. R. Meteorol. Soc.*, **135**, 1830-1841.

Degorska, M., W. B. Rajewska, 1996: The role of stratospheric minor warmings in producing the total ozone deficiencies over Europe in 1992 and 1993. *J. Atmos. Terr. Phys.*, **58**(16), 1855-1862.

Dobson, G. M., 1956: Origin and distribution of the polyatomic molecules in the atmosphere, *Proc. R. Soc. Lon. Ser.-A.*, **236**, 187–193, 13831.
doi: http://dx.doi.org/10.1175/JAS-3316.1

Donfrancesco, G. D., Adriani, A., Gobbi, G. P., and F. Congeduti, 1996: Lidar observations of stratospheric temperature above McMurdo Station, Antartica, *J. Atmos. Terr. Phys.*, 58, 1391–1399.

Dunkerton, T., C-P.F. Hsu and Mcintyre, 1981: Some Eulerian and Lagrangian diagnostics for a model stratospheric warming. *J. Atmos. Sci.*, **38**, 819-843.

Dunkerton, T. J. and Butchart, N. 1984: Propagation and selective transmission of internal gravity waves in a sudden warming. *J. Atmos. Sci.*, **41**, 1443–1460.

Eguchi, N., and K. Kodera, 2007: Impact of the 2002, Southern Hemisphere, stratospheric warming on the tropical cirrus clouds and convective activity. *Geophys. Res. Lett.*, **34**, L05819, doi:10.1029/2006GL028744.

Eichelberger, S. J., and D. L. Hartmann 2005: Changes in the strength of the Brewer- Dobson circulation in a simple AGCM, *Geophys. Res. Lett.*, **32**, L15807, doi:10.1029/2005GL022924.

European Ozone Research Coordinating Unit (EORCU); winter reports 2000/01.

European Ozone Research Coordinating Unit (EORCU); winter reports 2001/02.

Esler, J. G., and R. K. Scott, 2005: Excitation of transient Rossby waves on the stratospheric polar vortex and the barotropic sudden warming. *J. Atmos. Sci.*, **62**, 3661–3682.

Esler, J. G., L. M. Polvani, and R. K. Scott, 2006: The Antarctic sudden stratospheric warming of 2002: A self-tuned resonance?. *Geophys. Res. Lett.*, **33**, L12804, doi:10.1029/2006GL026034.

Finger, F.G., H. M. Wolf and C. E. Anderson, 1965: A method for objective analysis of stratospheric constant pressure charts. *Mon. Wea. Rev.*, **93**, 619-638.

Fairlie, T. D. A. and A. O'Neill, 1988: The stratospheric major warming of winter 1984/85: observations and dynamical inferences. *Quart. J. Roy. Meteor. Soc.*, **114**: 557–577.

Fairlie, T. D. A., A. O'Neill, and V. D. Pope, 1990: The sudden breakdown of an unusually strong cyclone in the stratosphere during winter 1988/89. *Quart. J. Roy. Meteor. Soc.*, **116**, 493, 767–774.

Fritz, S., and S. D. Soules, 1970: Large-scale temperature changes in the stratosphere observed from Nimbus-III. *J. Atmos. Sci.*, **27**, 1091–1097.

Fritz, S., and S. D. Soules, 1972: Planetary Variations of Stratospheric Temperatures. *Mon. Wea. Rev.*, **100**, 582–589.

Fusco, A. C., and M. L. Salby, 1999: Interannual variations of total ozone and their relationship to variations of planetary wave activity. *J. Climate*, **12,** 1619–1629.

Garcia, R. R. 1987: On the mean meridional circulation of the middle atmosphere. *J. Atmos. Sci.*, **44**, 3599–609.

Garcia, R. R., and B. A. Boville, 1994: ‘‘Downward control’’ of the mean meridional circulation and temperature distribution of the polar winter stratosphere. J. Atmos. Sci., 51, 2238–2245.

Geisler, J. E., 1974: A numerical model of the sudden stratospheric warming mechanism. *J. Geophys. Res.*, **79**, 4989-4999.

Gerber, E. P., and L. M. Polvani 2009: Stratosphere- troposphere coupling in a relatively simple AGCM: The importance of stratospheric variability. *J. Climate.*, **22**, 1920–1933.

Gerber, E. P., C.orbe and L.M. Polvani, 2009: Stratospheric influence on the tropospheric circulation revealed by idealized ensemble forecasts. *Geophys. Res. Lett.* **36**, L24801.

Gimeno, L., L. de la Torre, R. Nieto, D. Gallego, P. Ribera, and R. García-Herrera, 2007: A new diagnostic of stratospheric polar vortices. *J. Atmos. Terr. Phys.*, **69**(15), 1797-1812. doi:10.1016/j.jastp.2007.07.013.

Gray et al., 2001: A data study on the influence of the equatorial upper stratosphere on the Northern hemisphere stratospheric sudden warmings. *Quar. J. Royal. Meteorol. Soc.*, **127**(576), 1985-2003.

Gray, L. J., S. Sparrow, M. Juckes, A. O'neill, and D. G. Andrews, 2003: Flow regimes in the winter stratosphere of the northern hemisphere. *Q. J. R. Meteorol. Soc.*, **129** (589), 925-945. doi:10.1256/qj.02.82.

Gregory, J. B., A. H. Manson, 1975: Wind and waves to 110 km at mid-latitudes. III. Response of mesospheric and lower thermospheric winds to major stratospheric warmings. *J. Atmos. Sci.*, **32**, 1676–1681.

Haklander, A. J., P. C. Siegmund, and H. M. Kelder, 2007: Interannual variability of the stratospheric wave driving during northern winter. *Atmos. Chem. Phys.*, **7**, 2575–2584.

Hamilton, K., 1995: Interannual variability in the northern hemisphere winter middle atmosphere in control and perturbed experiments with the GFDL SKYHI general circulation model. *J. Atmos. Sci.*, **52,** 44-66.

Harada, Y., A. Goto, H. Hasegawa, N. Fujikawa, H Naoe, and T. Hirooka, 2010: A Major Stratospheric Sudden Warming Event in January 2009. *J. Atmos. Sci.*, **67**, 2052–2069. doi: http://dx.doi.org/10.1175/2009JAS3320.1.

Harvey, V. L., R. B. Pierce, T. D. Fairlie, and M. H. Hitchman, 2002: A climatology of stratospheric polar vortices and anticyclones. *J. Geophys. Res.*, **107**(D20), 4442, doi:10.1029/2001 JD001471.

Haynes, P. H., C. J. Marks, M. E. McIntyre, T. G. Shepherd, and K. P. Shine, 1991: On the "downward control" of extratropical diabatic circulations by eddy-induced mean zonal forces. *J. Atmos. Sci*., **48**, 651–678.

Healy, S. B., and D. P. Dee, 2010: Assimilation of Global Positioning System Radio Occultation data in the ECMWF ERA-Interim reanalysis. *Quart. J. R. Meteorol. Soc*., **136**, 1972-1990.

Hinssen Y, A.V. Delden, T. Opsteegh, W. de Geus, 2010: Stratospheric impact on tropospheric winds deduced from potential vorticity inversion in relation to the Arctic Oscillation. *Q. J. R. Meteorol. Soc.*, **136**: 20–29. DOI:10.1002/qj.542.

Hirooka, T., T. Ichimaru, and H. Mukougawa, 2007: Predictability of stratospheric sudden warmings as inferred from ensemble forecast data: Intercomparison of 2001/02 and 2003/04 winters. *J. Meteor. Soc. Japan.*, **85**, 919–925.

Hoffmann, P., W. Singer, D. Keuer 2002: Variability of the mesospheric wind field at middle and arctic latitudes in winter and its relation to stratospheric circulation disturbances. *J. Atmos. Terr. Phys.*, **64**, 1229-1240.

Hoffmann, P., W. Singer, D. Keuer, W. K. Hocking, M. Kunze, and Y. Murayama 2007: Latitudinal and longitudinal variability of mesospheric winds and temperatures during stratospheric warming events. *J. Atmos. Sol. Terr. Phys.*, 69, 2355–2366.

Holton, J. R., and C. Mass, 1976: Stratospheric vacillation cycles. *J. Atmos. Sci.*, **33**, 2218-222.

Holton, J. R., and H. Tan, 1980: The influence of the equatorial quasi-biennial oscillation on the global circulation at 50 mb. *J. Atmos. Sci.*, **37**, 2200-2208.

Holton, J. R. 1983: The influence of gravity wave breaking on the general circulation of the middle atmosphere. *J. Atmos. Sci.,* **40**, 2497–2507.

Hood, L. L., and B. E. Soukharev, 2003: Quasi-decadal variability of the tropical lower stratosphere: The role of extratropical wave forcing. *J. Atmos. Sci.,* **60**, 2389-2403.

Hu Y., and K. K. Tung, 2002: Interannual and decadal variations of planetary wave activity, stratospheric cooling, and northern hemisphere annular mode. *J. Climate,* 15, 1659-1673.

Hu, Y., and L. Pan, 2009: Arctic stratospheric winter warming forced by observed SSTs. *Geophys. Res. Lett.*, **36**, L11707, doi:10.1029/2009GL037832.

Jacobi, Ch., R. Schminder, D. KPurschner, 1997: The winter mesopause wind field over Central Europe and its response to stratospheric warmings as measured by D1 LF wind measurements at Collm, Germany. **20** 1223–1226.

Juckes, M. N., and A. O'Neill, 1988: Early winter in the northern stratosphere. *Met O 20 (Dynamical Climatology Branch), Meteorological Office*.

Julian, P. R., and K. Labitzke, 1965: A study of atmospheric energetics during January and February 1963 stratospheric warming. *J. Atmos. Sci.,* **22**, 597-610.

Kalnay et al., 1996: The NCEP/NCAR 40-year reanalysis project. *Bull. Amer. Meteor. Soc.,* **77**, 437-470.

Karpetchko, A., and G. Nikulin, 2004: Influence of early winter upward wave activity flux on midwinter circulation in the stratosphere and troposphere. . *J. Climate,* **17**, 4443-4452.

Kim, Y-J., and M. Flatau, 2010: Hindcasting the January 2009 Arctic Sudden Stratospheric Warming and Its Influence on the Arctic Oscillation with Unified Parameterization of Orographic Drag in NOGAPS. Part I: Extended-Range Stand-Alone Forecast. *Wea. Forecasting.*, **25**, 1628–1644.

Kim. D., and W. Choi, 2006: Decadal and year-to-year variations of the arctic lower-stratospheric temperature for the month of March and their relationship with eddy heat flux. *Int. J. Climatol.* **26**: 1125–1132.

Kirstin, K., B. Naujokat and K. Labitzke, 2005: The Unusual Midwinter Warming in the Southern Hemisphere Stratosphere 2002: A Comparison to Northern Hemisphere Phenomena. *J. Atmos. Sci.*, **62**, 603–613.

Kobayashi, S., M. Matricardi, D. P. Dee, and S. Uppala, 2009: Toward a consistent reanalysis of the upper stratosphere based on radiance measurements from SSU and AMSU-A. *Quart. J. R. Meteorol. Soc.*, **135**, 2086-2099.

Kodera, K., and M. Chiba., 1995. Tropospheric circulation changes associated with stratospheric sudden warmings: A case study. *J. Geophys. Res.*, **100** (D6), 11, 055–11, 068, doi:10.1029/95JD00771.

Kodera, K., Y. Kuroda, and S. Pawson 2000: Stratospheric sudden warmings and slowly propagating zonal-mean zonal wind anomalies. *J. Geophys. Res.*, **105**(D10), 12,351–12,359, doi:10.1029/2000JD900095.

Kodera, K., 2006: Influence of stratospheric sudden warming on equatorial troposphere. *J. Geophys. Res.*, **33**, L06804.

Kodera, K., N. Eguchi, J. N. Lee, Y. Kuroda and S. Yukimoto, 2011: Suddden changes in the tropical stratospheric and tropospheric circulation during January 2009. *J. Meteo. Soc. Jpn* **89**(3), 283-290. doi:10.2151/jmsj.2011-308

Kolstad, E., T. Breiteig, and A. Scaife, 2010; The association between stratospheric weak polar vortex events and cold air outbreaks in the Northern Hemisphere. *Quart. J. Roy. Meteor. Soc.,* Vol **136**, Issue 649, 886-893.

Kuroda, Y. 2008: Effect of stratospheric sudden warming and vortex intensification on the tropospheric climate. *J. Geophys. Res.*, **113**, D15110, doi: 10.1029/2007JD009550.

Kuttipurath, J., and Nikulin, G., 2012: The sudden stratospheric warming of the Arctic winter 2009/2010: Comparison to other recent warm winters. *Atmos. Chem. Phys. Discuss.*, **12,** 7243-7271.

Labitzke, K., and Collaborators, 1972: Climatology of the Stratosphere in the Northern Hemisphere. Part 1: Heights, Temperatures and Geostrophic Resultant Wind Speeds at 100, 50, 30 and 10 mb. Meteor. Abhandl. F.U. Berlin, Band 100, Heft 4.

Labitzke, K., 1977: Interannual variability of the winter stratosphere in the northern hemisphere. *Mon. Wea. Rev.*, **105**, 762–770.

Labitzke, K., 1981: The amplification of height wave 1 in January 1979: A characteristic precondition for the major warming in February. *Mon. Wea. Rev.*, **109,** 983–989.

Labitzke, K., 1982: On the interannual variability of the middle stratosphere during the northern winters. *J. Met. Soc. Japan*., **60**, 124– 139.

Labitzke, K., 1987: Sunspots, the QBO, and the stratospheric temperatures in the North Polar Region. *Geophys. Res. Lett.*, **14**, 535–537.

Labitzke, K., and B. Naujokat, 1983: On the variability and trends of the temperature in the atmosphere, *Beitr. Phys. Atmos*. **56**, 495-507.

Labitzke, K and Von Loon, 1999: *The Stratosphere: Phenomena, History, and Relevance*. Springer-Verlag, 179 pp.

Labizke, K. and Naujokat, B, 2000: The lower Arctic stratosphere in winter since 1953. *SPARC Newsletters, http://www.atmosp.physics. utoronto.ca/SPARC/News15/15 Labitzke.html, http://www.geo. fu-berlin.de/en/met/ag/strat/produkte/northpole/index.html*, **15**, 11–14.

Labitzke. K., and Collaborators, 2002: The Berlin Stratospheric Data Series, *CD from Meteorological Institute, Free University Berlin, Berlin, Germany.*

Labitzke, K., and M. Kunze 2009: On the remarkable Arctic winter in 2008/2009. *J. Geophys. Res.,* **114**, D00I02, doi: 10.1029/2009JD012273.

Leovy, C. B., 1964: Simple models of thermally driven mesospheric circulations. *J. Atmos. Sci.,* **21**, 327-341.

Lewis, J. M., 2003: Ooishi's Observation: Viewed in the Context of Jet Stream Discovery. *Bull. Amer. Meteor. Soc.*, **84**, 357–369. doi: http://dx.doi.org/10.1175/BAMS-84-3-357.

Liberato. M. L. R., M. Castanheira, L. De la torre, C. C. Dacamara and L. Gimeno, 2007: Wave Energy Associated with the Variability of the Stratospheric Polar Vortex. *J. Atmos. Sci.*, **64,** 2683-2694.

Limpasuvan, V., D. W. J. Thompson, and D. L. Hartmann, 2004: The life cycle of the Northern Hemisphere sudden stratospheric warmings. *J. Climate.*, **17**, 2584–2596.

Limpasuvan, V., D. Wu, M. Schwartz, J. Waters, Q. Wu, and T. Killeen, 2005: The two-day wave in EOS MLS temperature and wind measurements during 2004--2005 winter. *Geophys. Res. Lett.*, **32**(17): doi: 10.1029/2005GL023396. issn: 0094-8276.

Lin, H., J. Derome, R. J. Greatbatch, K. A. Peterson, and J. Lu, 2002: Tropical links of the Arctic Oscillation. *Geophys. Res. Lett.*, Vol. 29, 1943.

Lindzen, R. S. 1981: Turbulence and stress owing to gravity wave and tidal breakdown. *J. Geophys. Res.,* **86**, 9707–9714.

Liu, H. L., and R. G. Roble 2005: Dynamical coupling of the stratosphere and mesosphere in the 2002 Southern Hemisphere major stratospheric sudden warming. *Geophys. Res. Lett.*, 32, L13804, doi:10.1029/2005GL022939.

Liu, H., E. Doornbos, M. Yamamoto, and S. Tulasi Ram 2011: Strong thermospheric cooling during the 2009 major stratosphere warming. *Geophys. Res. Lett.*, **38**, L12102, doi:10.1029/2011GL047898.

Louise. B. J., 1979: *Fundamentals of Meteorology*. Prentice-Hall, Inc., Englewood Cliffs, N.J. 07632. **321** pp.

Lowenthal, M., 1957: Abnormal mid-stratospheric temperatures. *J. Meteor.*, **14**, 476.

Lu, H., M. P. Baldwin, L. J. Gray, M. J. Jarvis 2008: Decadal-scale changes in the effect of the QBO on the northern stratospheric polar vortex. *J. Geophys. Res.*, **113,** D10114, doi:10.1029/2007JD009647.

Manney, G. L., R. W. Zurek, M. E. Gelman, A. J. Miller, and R. Nagatani,1994: The anomalous Arctic lower stratospheric polar vortex of 1992– 1993, *Geophys. Res. Lett.*, **21**, 2405– 2408.

Manney, G. L., W. A. Lahoz, L. S. Elson, L. Froidevaux, R. S. Harwooct, A. 0'Nei11, R. Swinbank, J. W. Waters, R. W. Zurek, 1994: Stratospheric warmings in the ear1y winter in the northern and southern hemispheres. *Q. J. R. Meteorol. Soc.*, JPL TRS 1992+, http://hdl.handle.net/2014/34418

Manney G. L., W. A. Lahoz, R. Swinbank, A. O'Neill, P. M. Connew and R. W. Zurek 1999: Simulation of the December 1998 stratospheric major warming; *J. Geophys. Res.*, **26(17)**, 2733-2736.

Manney, G. L., and J. L. Sabutis 2000: Development of the polar vortex in the 1999-2000 Arctic winter stratosphere. *Geophys. Res. Lett.*, **27**, 2589–2592.

Manney, G., J. Sabutis, and R. Swinbank, 2001: A unique stratospheric warming event in November 2000. *Geophys. Res. Lett.*, **28**(13): doi: 10.1029/2001GL012973. issn: 0094-8276.

Manney, G. L., K. Kruger, J. L. Sabutis, S. A. Sena, and S. Pawson, 2005: The remarkable 2003–2004 winter and other recent warm winters

in the Arctic stratosphere since the late 1990s. *J. Geophys. Res.*, 110, **14**, D04107. doi:10.1029/2004JD005367.

Manney et al. and Coauthors, 2005: Simulations of dynamics and transport during the September 2002 Antarctic major warming. *J. Atmos. Sci.*, **62**, 690–707.

Manney, G. L., M. J. Schwartz, K. Kruger, M. L. Santee, S. Pawson, J. N. Lee, W. H. Daffer, R. A. Fuller, and N. J. Livesey 2009: Aura microwave limb sounder observations of dynamics and transport during the record-breaking 2009 Arctic stratospheric major warming. *Geophys. Res. Lett.*, **36**, L12815, doi:10.1029/2009GL038586.

Marenco, F., V. Santacesaria, A. Bais, D. Balis, A. di Sarra, A. Papayannis, and C. S. Zerefos, 1997: Optical properties of tropospheric aerosols determined by lidar and spectrophotometric measurements (PAUR campaign). *Appl. Opt.*, **36,** 6875–6886.

Martius, O., L. M. Polvani, and H. C. Davies 2009: Blocking precursors to stratospheric sudden warming events, *Geophys. Res. Lett.*, **36**, L14806, doi:10.1029/2009GL038776.

Matsuno, T., 1971: A Dynamical Model of the Stratospheric Sudden Warming. *J. Atmos. Sci*., **28**, 1479–1494.doi:10.1175/15200469.

McGuirk, J. P., 1978: Planetary scale forcing of the January 1977 weather. *Science*., **199**, 293-295.

McIntyre, M. E., 1982: How well do we understand the dynamics of stratospheric warmings?, *J. Meteorol. Soc. Jpn.*, **60**, 37–65, 1982.

Miyakoda, K, R. F. Strickler, and G. D. Hembree, 1970: Numerical simulation of the breakdown of a polar-night vortex in the stratosphere. *J. Atmos. Sci.*, vol. **27**, Issue 1, pp.139-154.

Miyoshi Y. 2003: Effects of the stratospheric sudden warming on the temperature in the MLT region. *Adv. Polar Upper Atmos. Res.*, **17**. 1-12.

Mohanakumar, K. 2008: Stratosphere Troposphere Interactions -An Introduction, *Springer, New York.*

Muench, H. S. and T. R. Borden, 1962: Atlas of monthly mean stratosphere charts, 1955-1959: Part I, January-June; Part II, July-December. *Air Force Surveys in Geophysics.,* No. **141**.

Mukherjee, B. K., and Bh. V, Ramana Murty, 1972: High-level warmings over a tropical station. *Mon. Wea. Rev.*, **100** (9), 674–681.

Mukherjee B. K, K. Indira, R. S. Reddy and Bh. V. Ramana Murthy, 1985: Stratospheric/Mesospheric warmings over tropics during winter and their implications for warming campaign of 1983-84. *Indian. J. Rad. Space Phy.*,**14**, 34-37.

Mukherjee, B. K., K. Indira, R. S. Reddy, and Bh. V. Ramana Murthy, 1985: Stratwarm phenomenon at low latitudes. *Indian J Radio and Space Physics*, **14** (1985) 34.

Mukherjee, B. K., Indira, K., Dani, K. K., 1987: Perturbations in tropical middle atmosphere during winter 1984 -1985. *Meteorol. Atmos. Phys.*, **37,** 17–26.

Mukherjee, B. K., 1990: Stratwarm phenomenon at low-latitudes—Current status and future prospects. *Indian J Radio Space Phys.,* **19**, 193–201.

Mukougawa, H., and T. Horooka, 2004: Predictability of stratospheric sudden warming : A case study for 1998 / 99 winter. *Mon.Wea. Rev.*, **132**, 1764-1776.

Mukougawa, H., H. Sakai, and T. Hirooka 2005: High sensitivity to the initial condition for the prediction of stratospheric sudden warming. *Geophys. Res. Lett.*, 32, **4 PP**, L17806, doi:10.1029/ 2005GL022909.

Nakagawa, K. I., and K. Yamazaki, 2006: What kind of stratospheric sudden warming propagates to the troposphere? *Geophys. Res. Lett* 33., L04801, **4 PP**, doi:10.1029/2005GL024784.

Naujokat, B., and K. Grunow, 2003: The stratospheric arctic winter 2002/03: balloon flight planning by trajectory calculations. In: 16th

ESA symposium on european rocket and balloon programmes and related research, Sankt Gallen, Switzerland; *Ed.: Barbara Warmbein. ESA SP-530, Noordwijk: ESA Publications Division*, **421 – 425**, ISBN 92-9092-840-9.

Naujokat, B., K. Labitzke, R. Lenschow, K. Petzoldt, and R. C. Wohlfahrt, 1987: The stratospheric winter 1986/87: A major midwinter warming 35 years after they were first detected. Beilagezur Berliner Wetterkarte, SO 9/87.

Naujokat, B., K. Labitzke, R. Lenschow, K. Petzoldt, and R. C. Wohlfahrt, 1989: The stratospheric winter 1988/89: Extremely low temperatures followed by a major warming. *Beilage zur Berliner Wetterkarte*, SO 12/89.

Naujokat, B., K. Labitzke, R. Lenschow, K. Petzoldt, and R. C. Wohlfahrt, 1993: 1985/86: The fourth winter of MAP-Dynamics, a cold winter with two minor warmings and a major final warming. *Solar-Terrestrial Energy Program, Collection of Reports on the Stratospheric Circulation during the Winters 1974/5 - 1991/2. Stratospheric Research Group, Free University, Berlin. Urbana, IL: University of Illinois, 1993., p.159.*

Naujokat, B., and K. Labitzke, eds 1993: Solar-Terrestrial Energy Program: Collection of Reports on the stratospheric circulation during the winters 1974/75–1991/92. *Scientific Committee on Solar Terrestrial Physics (SCOSTEP)*, Urbana, Illinois, USA.

Naujokat, B., K. Labitzke, R. Lenschow, B. Rajewski, M. Wiesner, and R. C. Wohlfart, 1994: The stratospheric winter 1993/94: a winter with someminor warmings and an early final warming. *&i/age ZUY Berliner Wetterkarte. SO 24194.*

Newman, P. A., and E. R. Nash, 2000: Quantifying wave driving of the stratosphere. *J. Geophys. Res.*, **104,** 12485-12497.

Newman, P. A., E. Nash, and J. Rosenfield, 2001: What controls the temperature of the Arctic stratosphere during the spring? *J. Geophys. Res.*, **106**, 19999–20010.

O'Neill, A., and V. D. Pope, 1988: Simulations of linear and nonlinear disturbances in the stratosphere. *Quart. J. Roy. Meteor. Soc.*, **114,** 1063–1110.

O'Neill, A., J. R. Holton, J. A. Pyle, and J. A. Curry, 2003: Stratospheric sudden warmings. *Encyclopedia of Atmospheric Sciences,* Eds., Elsevier, 1342–1353.

Oort, A. H., and J. J. Yienger, 1996: Observed interannual variability in Hadley circulation and its connection to ENSO. *J. Climate*., **9** 2751-2767.

Palmer, T. N., 1981: Diagnostic study of a wavenumber-2 stratospheric sudden warming in a transformed Eulerian-mean formalism. *J. Atmos. Sci.*, **38**, 844–855.

Pawson, S., and B. Naujokat, 1999: The cold winters of the middle 1990's in the norther lower stratosphere, *J. Geophys. Res.*, **104**, 14,209-14,222.

Pawson, S., K. G. Labitzke, and R. Lenschow, 1993: Climatology of the Northern Hemisphere stratosphere derived from Berlin analyses. Part I. Monthly means, *Met. Abh. FU-Berlin,* Neue Folge Serie A, Band 7, Heft 3.

Peters, D. H.W, P. Vargin, A. Gabriel, N. Tsvetkova, and V. Yushkov, 2010: Tropospheric forcing of the boreal polar vortex splitting in January 2003. *Ann. Geophys.*, **28**, 2133–2148.

Petzoldt, K., 1987: Large-scale dynamics of the mean flow breakdown in the stratosphere and mesosphere during the winter 1983/84. In ESA, *Proceedings of the 8th ESA Symposium on European Rocket and Balloon Programs and Related Research p 181-185 (SEE N88-16201 08-46).*

Plumb, R. A., 1981: Forced waves in a baroclinic shear flow. Part 2: damped and undammed evolution at finite stability. J. Atmos.Sci., 38, 1856-1869.

Plumb, R. A., 2002: Stratospheric transport, *J. Meteorol. Soc. Jpn.*, **80**, 793–809.

Polvani, L. M, and D. W. Waugh, 2004: Upward wave activity flux as a precursor to extreme stratospheric events and subsequent anomalous surface weather regimes. *J. Climate*, **17**, 3548–3554.

Quiroz, R. S., 1969: The warming of the upper stratosphere in February 1966 and the associated structure of the mesosphere. *Mon. Weather Rev.*, **97**, 541-552.

Quiroz, R. S., 1971: The determination of the amplitude and altitude of stratospheric warmings from satellite-measured radiance changes. *J. Appl. Meteorol.*, **10**, 555-574.

Quiroz, R. S., A. J. Miller, and R. M. Nagatani, 1975: A comparison of observed and simulated properties of sudden stratospheric warmings. *J. Atmos. Sci.*, **32**,1723-1736.

Quiroz, R. S., 1977: The tropospheric-stratospheric polar vortex breaks down of January 1977. *Geophys. Res. Lett.*, **4**, 151-154.

Ramanathan, V., 1977: Troposphere-stratosphere feedback mechanism: Stratospheric warming and its effects on the polar energy budget and the tropospheric circulation. *J. Atmos.Sci.*, 34, 439-447.

Randel et al., 2004: The SPARC Intercomparison of Middle-Atmosphere Climatologies. *J. Climate.*, **17,** 986-1003.

Randel W. J., 1993: Global variations of zonal mean ozone during stratospheric warming events. *J. Atmos. Sci.*, **50**, 3308–3321.

Randel, W. J., B. A. Boville, 1987: Observations of a Major Stratospheric Warming during December 1984. *J. Atmos. Sci.*, **44**, 2179–2186.

Reed, R. J., J. L. Woolfe, H. Nishimoto, 1963: A spectral analysis of the energetic of the stratospheric sudden warming of Early 1957. *J. Atmos. Sci.,* **20**, 256-275.

Rosenlof, K. H., and J. R. Holton, 1993: Estimates of stratospheric residual circulation using the downward principle. *J. Geophys. Res.*, **98**, 10465–10479.

Ryoo, J. M., and H. Y. Chun, 2005: Stratospheric major sudden warmings revealed in NCEP Reanalysis Data for 41 years (1958-1999*). J. Korean. Meteorol. Soc.,* **41**, 2, 173- 190.

Scherhag, R., 1952. Die explosionsartige Stratospharenerwa ¨rmung des Spa 1951/52. Berichte des Deutschen Wetterdienstes 38, 51–63.

Scherhag, R., 1960: Stratospheric temperature changes and the associated changes in pressure distribution. *J. Meteorol.,* **17**, 575-582, 1960.

Schimanke, S., J. Körper, T. Spangehl, and U. Cubasch, 2011: Multi-decadal variability of sudden stratospheric warmings in an AOGCM. *Geophys. Res. Lett.*, 38, L01801, doi:10.1029/2010GL045756.

Schoeberl, M. R., 1978: Stratospheric warming: observation and theory. *Rev. Geophys. Space Phys.,* **16**, 521-538.

Schoeberl, M. R., and D. F. Strobel, 1978: The zonal averaged circulation of the middle atmosphere. *J. Atmos. Sci.,* **35**, 577-591.

Scott, A. F. D., 1972: Mesospheric temperatures and winds during a stratospheric warming. *Phil. Trans. Roy. Soc. London.,* **271**, 547-557.

Scott, R. K and D. G. Dritchel 2006: Vortex–vortex interactions in the winter stratosphere. *J. Atmos. Sci.*, **63**, 726-740.

Shepherd, M. G., D. L. Wu, I. N. Fedulina, S. Gurubaran, J. M. Russell, M. G. Mlynczak,G. Shepherd, 2007: Stratospheric warming effects on the tropical mesospheric temperature field. *J. Atmos. Sol. - Terr. Phy.*, **69**, 2309–2337.

Shepherd, T. G. 2007: Transport in the middle atmosphere, *J. Meteorol. Soc. Jpn.,* **85B**, 165–191.

Simmons, A. J., K. M. Willett, P. D. Jones, P. W. Thorne, and D. P. Dee, 2010: Low-frequency variations in surface atmospheric humidity, temperature and precipitation: Inferences from reanalyses and monthly gridded observational datasets. *J. Geophys. Res.*, **115**, D01110, doi:10.1029/2009JD012442.

Singer, W., P. Hoffmann, A. H. Manson, C. E. Meek, R. Schminder, D. KPurschner, G. A. Kokin, A. K. Knyazev, Yu. L. Portnyagin, N. A. Makarov, A. N. Fahrutdinova, V. V. Sidorov, G. Cevolani, H. G. Muller, E. S. Kazimirovsky, V. A Gaidukov, R. R. Clark, R. P. Chebotarev, Y. Karadjajev, 1994: The wind regime of the mesosphere and lower thermosphere during the DYANA campaign. *J. Atmos. Sol. Terr. Phys.*, **56**, 1717–1729.

Siskind, D.E., L. Coy, P. Espy., 2005: Observations of stratospheric warmings and mesospheric coolings by the TIMED SABER instruments. *Geophys. Res. Lett.*, **32**, L09804, doi:10.1029/2005GL022399.

Sivakumar, V., B. Morel, H. Bencherif, J. L. Baray, S. Baldy, A. Hauchecorne, P. B. Rao, 2004: Rayleigh lidar observation of a warm stratopause over a tropical site, Gadanki (13.51N, 79.21E). *Atmos. Chem. Phys.*, **4**, 1989–1996.

Sridharan, S. and S. Sathishkumar, 2008: Seasonal and interannual variations of gravity wave activity in the low-latitude mesosphere and lower thermosphere over Tirunelveli (8.7° N, 77.8° E). *Ann. Geophys.*, **26**, 3215-3223, doi:10.5194/angeo-26-3215.

Strong, C., and R. E. Davis 2006: Variability in the altitude of fast upper tropospheric winds over the Northern Hemisphere during winter, *J. Geophys. Res.*, **111**, D10106, doi:10.1029/2005JD006497.

Taylor B. F., and J. D. Perry, 1977: The major stratospheric warming of 1976-1977, *Nature*, **267**, 417-418.

Teweles, S., 1958: Anomalous warming of the stratosphere over North America in early 1957. *Mon. Weather Rev.*, **86**, 377-396.

Thayer, J. P and J. M. Livingston, 2008: Observations of wintertime arctic mesospheric cooling associated with baroclinic zones. *Geophys. Res. Lett.*, **35**, L18803, doi:10.1029/2008GL034955.

Third European Stratospheric Experiment on Ozone (THESEO): The Northern hemisphere stratosphere in the winter of 1998/99. www.ozone-sec.ch.cam.ac.uk/EORCU/reports/wr9798.pdf

Thompson, D. W. J., and J. M.Wallace, 1998: The Arctic Oscillation signature in the wintertime geopotential height and temperature fields. *Geophys. Res. Lett.*, **25**, 1297-1300.

Tung, K. K., and R. S. Lindzen 1979: Theory of stationary long waves. Part I: Simple theory of blocking. *Mon. Weather Rev.*, **107**, 714–734.

Uppala, S.M., Kållberg, P.W., Simmons, A.J., Andrae, U., da Costa Bechtold, V., Fiorino, M., Gibson, J.K., Haseler, J., Hernandez, A., Kelly, G.A., Li, X., Onogi, K., Saarinen, S., Sokka, N., Allan, R.P., Andersson, E., Arpe, K., Balmaseda, M.A., Beljaars, A.C.M., van de Berg, L., Bidlot, J., Bormann, N., Caires, S., Chevallier, F., Dethof, A., Dragosavac, M., Fisher, M., Fuentes, M., Hagemann, S., Hólm, E., Hoskins, B.J., Isaksen, L., Janssen, P.A.E.M., Jenne, R., McNally, A.P., Mahfouf, J.-F., Morcrette, J.-J., Rayner, N.A., Saunders, R.W., Simon, P., Sterl, A., Trenberth, K.E., Untch, A., Vasiljevic, D., Viterbo, P., and Woollen, J. 2005: The ERA-40 re-analysis. *Quart. J. R. Meteorol. Soc.*, **131**, 2961-3012.doi:10.1256/qj.04.176.

Van loon R., A. Madden., and R. L. Jenne, 1975: Oscillations in the winter stratosphere, Part 1: description. *Mon. Wea. Rev.*, **103**, 154-162.

Vineeth, C., T. K. Pant, K. K. Kumar, and S. G. Sumod., 2008: Tropical connection to the polar stratospheric sudden warming through quasi 16-day planetary wave. *Ann. Geophys.*, Volume **28**, Issue 11, pp.2007-2013.

Walterscheid, R. L., G.G. Sivjee, R. G. Roble, 2000: Mesospheric and lower thermospheric manifestations of a stratospheric warming event over Eureka, Canada, (80°N). *Geophys. Res. Lett.*, **27**, 2897–2900.

Wang, L., and W. Chen 2010: Downward Arctic Oscillation signal associated with moderate weak stratospheric polar vortex and the

cold December 2009. *Geophys. Res. Lett.*, **37**, L09707, doi:10.1029/2010GL042659.

Waugh, D. W., W. J. Randel, S. Pawson, P. A. Newman, and E. R. Nash, 1999: Persistence of the lower stratospheric polar vortices. *J. Geophys. Res.*, **104** (D22), 27 191–27 201.

Waugh, D. W., and L. M. Polvani, 2009: Stratospheric polar vortices. *Geophysical Monograph Series.*, **190**.43-57.

Weber, M., S. Dikty, J. P. Burrows, H. Garny, M. Dameris, A. Kubin, J. Abalichin, and U. Langematz 2011: The Brewer-Dobson circulation and total ozone from seasonal to decadal time scales. *Atmos. Chem. Phys. Discuss.*, **11**, 13829–13865.

Williams, E. R., 1988: Minor stratospheric warmings and their relation to the ionosphere. *Physica Scripta*. **37**, 188-192.

WMO, 1978: Abridged final report of the seventh session of the Commission for Atmospheric Sciences. *WMO Rep.*, **509**, 113 pp.

Yoshida, K., and K. Yamazaki 2011: Tropical cooling in the case of stratospheric sudden warming in January 2009: focus on the tropical tropopause layer. *Atmos. Chem. Phys. Discuss.*, **11**, 2263–2296.

Young, P., D. Thompson, K. Rosenlof, 2005: The seasonal cycle and interannual variability in stratospheric temperatures and links to the Brewer-Dobson circulation: An analysis of MSU and SSU data, 1979-2005.

Yu, L., Z. Zhang, M. Zhou, S. Zhong, D. Lenschow, H. Hsu, H. Wu, and B. Sun, 2010: Validation of ECMWF and NCEP–NCAR reanalysis data in Antarctica. *Adv. Atmos. Sci.*, **27**(5), 1151–1168, doi:10.1007/s00376-010-9140-1.

Yulaeva, E., J. R. Holton and J. M. Wallace, 1994: On the cause of the annual cycle in tropical lower-stratospheric temperatures. *J. Atmos. Sci.*, **51**, 169-174.

Zhou, S., A. J. Miller, J. Wand, and J. K. Angell, 2002: Downward-propagation temperature anomalies in the preconditioned polar stratosphere. *J. Climate.*, **15**, 781-792.

Zhou, T. B., and C. B. Fu, 2009: Intercomparison of the summertime subtropical high from the ERA-40 and NCEP/NCAR reanalysis over East Eurasia and the western North Pacific. *Adv. Atmos. Sci.*, **26**, Issue 1, pp 119-131.

Zurek, R. W., G. L. Manney, A. J. Miller, M. Gelman and R. Nagatani, 1996: Interannual variability of north polar vortex in the lower stratosphere using UARS mission. *Geophys. Res. Lett.*, **23**(3), 289–292, doi:10.1029/95GL03336.